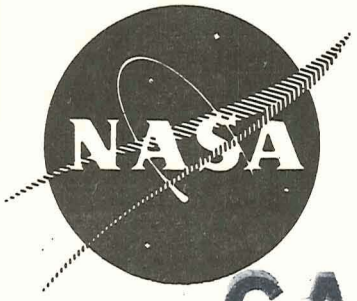

NASA CR-72879
R-8758

ANALYSIS OF THE WAVE MOTION IN BAFFLED COMBUSTION CHAMBERS

by

C. L. Oberg, W. H. Evers and T. L. Wong

ROCKETDYNE, A DIVISION OF NORTH AMERICAN ROCKWELL CORPORATION

prepared for

NATIONAL AERONAUTICS AND SPACE ADMINISTRATION

NASA Lewis Research Center
Contract No. NAS3-11226
Richard J. Priem, Project Manager

1. Report No.	2. Government Accession No.	3. Recipient's Catalog No.
NASA CR-72879		

4. Title and Subtitle	5. Report Date
ANALYSIS OF THE WAVE MOTION IN BAFFLED COMBUSTION CHAMBERS	October 1971
	6. Performing Organization Code

7. Author(s)	8. Performing Organization Report No.
C. L. Oberg, W. H. Evers, T. L. Wong	R-8758
	10. Work Unit No.

9. Performing Organization Name and Address	11. Contract or Grant No.
Rocketdyne, a Division of North American Rockwell Corporation Canoga Park, California 91304	NAS3-11226
	13. Type of Report and Period Covered
12. Sponsoring Agency Name and Address	Contractor Report
National Aeronautics and Space Administration Washington, D.C. 20546	14. Sponsoring Agency Code

15. Supplementary Notes

Technical Officer, Richard J. Priem, Chemical Rockets Division, NASA Lewis Research Center, Cleveland, Ohio

16. Abstract

Analytical methods have been developed to predict the wave motion in baffled combustion chambers. Principally, the method involves solution of the wave equation through use of an iterative/variational method. Calculated results are in good agreement with available data from bench scale acoustic models. Convergence of series expressions which occur in the analysis and of the iteration scheme was demonstrated numerically. Calculated results with gain/loss end-wall boundary conditions do not agree with observed engine stability, which indicates that other gain/loss representations must be used. The principal contribution from this study to aid the design of baffles is the ability to accurately predict instability frequencies and oscillatory pressure and velocity distributions for baffled chambers.

17. Key Words (Suggested by Author(s))	18. Distribution Statement
Combustion Instability Acoustics Baffles	Unclassified - unlimited

19. Security Classif. (of this report)	20. Security Classif. (of this page)	21. No. of Pages	22. Price*
Unclassified	Unclassified	127	$3.00

* For sale by the National Technical Information Service, Springfield, Virginia 22151

FOREWORD

The research program described herein was sponsored by the National Aeronautics and Space Administration, Lewis Research Center, Cleveland, Ohio, 44135, under contract NAS3-11226. The study was conducted during the 12-month ending December 31, 1970. Initial effort under this contract began May 22, 1968. NASA Project Manager was Dr. R. J. Priem. The Rocketdyne program manager was Mr. T. A. Coultas and Dr. C. L. Oberg was project engineer.

This report has been assigned the Rocketdyne report No. R- 8758.

ABSTRACT

Analytical methods have been developed to predict the wave motion in baffled combustion chambers. Principally, the method involves solution of the wave equation through use of an iterative/variational method. Calculated results are in good agreement with available data from bench scale acoustic models. Convergence of series expressions which occur in the analysis and of the iteration scheme was demonstrated numerically. Calculated results with gain/loss end-wall boundary conditions do not agree with observed engine stability, which indicates that other gain/loss representations must be used. The principal contribution from this study to aid the design of baffles is the ability to accurately predict instability frequencies and oscillatory pressure and velocity distributions for baffled chambers.

CONTENTS

ILLUSTRATIONS

TABLES

NOMENCLATURE*

c	=	sound velocity, in./sec
$G(\vec{r}\|\vec{r}_o)$	=	Green's function
k	=	ω/c, $inch^{-1}$
k_q	=	$(k^2 - q^2\pi^2/w^2)^{1/2}$, $inch^{-1}$
k_m	=	$(k^2 - m^2\pi^2/W^2)^{1/2}$, $inch^{-1}$
ℓ	=	baffle length, inches
L	=	main chamber length, inches
L_T	=	$(\ell + L)$, total chamber length, inches
m	=	main chamber summation index, positive integral values
M_o	=	steady flow Mach number
n	=	baffle compartment summation index, positive integral values
$\vec{N}$	=	unit normal vector directed outward
p	=	pressure, lb_f/in^2
q	=	summation index, positive integral values
$\vec{r}$	=	position vector, inches
r	=	radial coordinate, inches
R	=	chamber radius, inches
S	=	surface area, sq in.
w	=	width of baffle compartment, inches
W	=	width of main chamber, inches
x	=	longitudinal position coordinate, inches

*A separate table of nomenclature is included in appendices C and D.

y = transverse position coordinate, inches

y_I = specific acoustic admittance of injector end (dimensionless)

y_N = specific acoustic admittance of nozzle end (dimensionless)

z = axial coordinate, inches

α = damping coefficient, imaginary part of complex angular frequency, seconds^{-1}

ϵ_ν = 1 if $\nu = 0$, 2 if $\nu \neq 0$

μ = baffle compartment index, positive integral values

ξ = normal pressure gradient, $lb_f/in.^3$

ρ = time averaged gas density, $lb_m/in.^3$

ϕ = $\omega W/c$ or $\omega R/c$

ω = angular frequency, radians/sec

SUBSCRIPTS

a = refers to main chamber

b = refers to baffle compartments

r = refers to radial summation

s = refers to interface plane

T = refers to total length or area

θ = refers to angular summation

μ = refers to μ^{th} baffle compartment

0 = refers to source coordinates for Green's functions

SUPERSCRIPTS

s = refers to source surface (interface)

$\wedge$ = denotes maximum value retained in summation

SUMMARY

Analytical methods have been developed to predict the wave motion in baffled combustion chambers. These methods may be usefully applied to aid the design of injector face baffles.

An analytical method has been developed by employing variational and iterational techniques to solve the wave equation for baffled chambers. For this purpose the wave equation and boundary conditions were converted to an integral equation which was solved by these approximate means. The analytical method has been applied to both two-dimensional and cylindrical chambers with no steady flow and with relatively simple baffle configurations. Results from this analysis provide a good estimate of the instability frequencies and oscillatory pressure and velocity distributions in similar combustion chambers. Application of the analysis to more complicated baffle configurations appears straight-forward. The analysis was partially extended to include uniform steady flow in the chamber, but no numerical results were obtained. Nonetheless, no substantial difficulties associated with this extension were found.

Analytical results for closed chambers were found to be in excellent agreement with available data from bench-scale acoustic models. In addition, convergence of the several series-type expressions which appear in the analysis and, also, of the iteration scheme was investigated. Detailed calculations were used to demonstrate satisfactory convergence of the several series and of the iteration scheme.

Stability calculations were made for a number of chamber/baffle configurations with gain/loss end-wall boundary conditions. Admittance-type boundary conditions were used with signs chosen to represent a loss at the nozzle end and a gain at the injection end of the chamber. Results from each of the cases analyzed showed that, as long as the injector had a gain-type admittance, the predicted stability of the chamber was degraded by the presence of baffles. Because this result is obviously incompatible with observed engine stability, this simple representation of gains and losses must be inadequate. This failure to properly predict observed stability trends may be due to effects of velocity-coupled combustion driving or of wake-type drag losses on the baffles, neither of which are included in the current analytical formulation.

The principal contribution from this study to aid the design of baffles is the ability to accurately predict instability frequencies and oscillatory pressure and velocity distributions in baffled chambers.

INTRODUCTION

The intent of this report is to describe recently developed analytical methods and results which may be used to aid the design and development of injector face baffles. These results and methods have been obtained from an analytical study to investigate the stabilizing effects of baffles on acoustic modes of combustion instability. Many of the analytical details and supporting studies obtained from this investigation will be described only briefly so that emphasis may be placed on information useful for baffle design and development.

Injector face baffles are often required to prevent acoustic modes of combustion instability in rocket engines. These baffles are currently designed on a largely empirical basis. Some attempts have been made to systematize available experimental results (for example, see Ref. 1); other attempts have been made to use the Priem-type instability model to guide baffle design (Ref. 2). These approaches still provide only rough design guidelines. Analytical models are now available which will predict the stabilizing effects of baffles and, thereby, provide a theoretical basis for baffle design.

The acoustic modes of instability for unbaffled engines are currently approximated by the corresponding modes of a similarly shaped closed acoustic cavity, e.g., a cylinder. Employing methods described herein, the acoustic modes of closed but baffled chambers can also be calculated and used for similar purposes.

Calculation of the acoustic modes of closed baffled chambers was only an interim goal of the program on which this report is based. Nonetheless, this capability

can be used to aid baffle development by providing approximate frequencies, and oscillatory pressure and velocity distributions for the instability modes that can occur in the baffled engine. Thus, the general acoustic mode characteristics can be understood even though stability of the engine cannot be predicted. This analysis shows that baffled chambers may exhibit well-defined acoustic modes similar to the corresponding modes of unbaffled chambers. This conclusion is supported by available data from bench-scale acoustic models and hot firings. Thus, the normal acoustic modes are not eliminated by the introduction of baffles, they are only disguised.

ANALYTICAL APPROACH

The analytical approach being used has been generally described in Ref. 3. Without steady flow the analysis concerns approximate solution of the wave equation, which simply represents a composite of the linearized fluid dynamic equations obtained through the assumption of small variations from the mean (time average) value. With uniform steady flow, additional terms arise so that an inhomogeneous wave equation is obtained but, nevertheless, the general approach remains unchanged.

Solution of the wave equation for a baffled chamber is complicated by the fact that the standard separation-of-variables technique cannot be used because of the boundary shape. For similar problems, Morse (Ref. 4, pg. 1039) suggests the use of an integral formulation which may be subsequently solved by approximate means. This suggestion has been followed in this study.

The wave equation and boundary conditions were rewritten as an integral equation which, in turn, was solved by a combined variational and iterational method.

This approach was found to work very well. The approach has been applied to both two-dimensional and cylindrical baffled chambers and has been extended to include uniform steady flow in the two-dimensional case. Further, the effects of combustion driving and nozzle losses have been simulated to some extent through incorporation of gain/loss-type boundary conditions.

Integral Formulation

The wave equation and accompanying boundary conditions were converted to an integral equation through the use of Green's functions, as described by Morse (Ref. 5, pg. 321). The same conversion can be accomplished for this case without the introduction of Green's functions if a properly formulated sum of separated-type solutions is used (described in Appendix A). Nonetheless, the use of Green's functions greatly facilitates the analysis and allows it to be done more systematically.

The Helmholtz equation (which is the wave equation for a harmonic time dependence), i.e.,

$$\nabla^2 p + k^2 p = 0 \tag{1}$$

may be rewritten as

$$p(\vec{r}) = \int_S G(\vec{r}|\vec{r}_o)\, \vec{N} \cdot \vec{\nabla}_o p(\vec{r}_o) dS_o \tag{2}$$

where $G(\vec{r}|\vec{r}_o)$ is a Green's function, which satisfies either the same boundary conditions as the pressure (p), or a zero-gradient boundary condition. In

addition, Green's function satisfies the differential equation

$$\nabla^2 G + k^2 G = -\delta(\vec{r}-\vec{r}_o) \tag{3}$$

where $\delta(\vec{r}-\vec{r}_o)$ is a Dirac delta function. Expressions for the Green's function may be obtained in several ways, such as described by Morse (Ref. 4, pp 791 to 834).

The integral expression for pressure is used with separate Green's functions written for each baffle compartment and also for the main chamber. Each of these Green's functions is zero outside of the compartment to which it applies. However, the oscillatory pressure and normal component of velocity must be continuous across the conceptual interface between each region. Therefore, at this interface,

$$p_a(\vec{r}_s) = \int_S G_a(\vec{r}_s|\vec{r}_o)\xi(\vec{r}_o)dS_o = -\int_S G_{b\mu}(\vec{r}_s|\vec{r}_o)\xi(\vec{r}_o)dS_o = p_{b\mu}(\vec{r}_s) \tag{4}$$

where $G_a(\vec{r}|\vec{r}_o)$ is the Green's function for the main chamber, $G_{b\mu}(\vec{r}|\vec{r}_o)$ is the Green's function for the μ^{th} baffle compartment, and, to simplify the notation,

$$\xi(\vec{r}_o^s) = \vec{N}\cdot\vec{\nabla}_o\, p_a(\vec{r}_o^s) = -\vec{N}\cdot\vec{\nabla}_o\, p_b(\vec{r}_o^s) \tag{5}$$

In addition, the normal pressure gradient, ξ, must satisfy the integral equation

$$\begin{aligned}\xi(\vec{r}_o^s) &= \int \vec{N}\cdot\vec{\nabla}_o\, G_a(\vec{r}_s|\vec{r}_o^s)\xi(\vec{r}_o^s)dS \\ &= -\int \vec{N}\cdot\vec{\nabla}_o\, G_b(\vec{r}_s|\vec{r}_o^s)\xi(\vec{r}_o^s)dS\end{aligned} \tag{6}$$

Equation 6 was obtained directly from Eq. 2 by differentiation.

Simultaneous solution of Eq. 4 and 6, or their equivalents, to give the allowed frequencies of oscillation and the normal pressure gradient is the pivotal portion of the analysis. Both the Green's functions and ξ depend on frequency. With this information, the oscillatory pressure and velocity at any point in the chamber may be calculated from the integral expression for pressure, Eq. 2, by integration. The velocity components may be obtained from the gradient of the pressure. A variational-iterational technique has been developed to solve Eq. 4 and 6.

This approximate solution technique results from a direct combination of a variational technique, which allows the "best" form of an approximate solution to be selected, and an iteration technique, which allows an initially selected approximate solution to be systematically improved (also see Ref. 3). The variational procedure results in replacement of Eq. 4 by a characteristic equation; the procedure used is described by Morse and Ingard (Ref. 5, pg. 680). Employing the variational function developed by them, with a slight generalization for multiple compartments, a characteristic equation was obtained.

$$\int_{S_t} \xi \int_{S_t} G_a(\vec{r}|\vec{r}_o)\xi dS_o dS + \int_{S_t} \xi \int_{S_\mu} G_{b\mu}(\vec{r}|\vec{r}_o)\xi dS_o dS = 0 \qquad (7)$$

Where an approximate normal velocity of the form $u = A\xi$, has been used, the value of the amplitude (A) being optimized by the method. Thus, at this level of approximation, by assuming a reasonable estimate for the normal gradient, ξ, the frequency may be calculated from Eq. 7. Employing the

integral expression for pressure (Eq. 2) Eq. 7 may be rewritten as

$$\int_S \xi (p_a - p_b) dS = 0 \qquad (8)$$

If the exact expressions for ξ is obtained, then Eq. 8 is satisfied identically because $p_a = p_b$. However, as it has been used, the variational procedure does not indicate how to estimate ξ; rather, it indicates that the best estimate of the allowed frequencies corresponding to a particular estimate of ξ is obtained by satisfying Eq. 8. The iteration procedure is used to obtain an arbitrarily good estimate of ξ. Nonetheless, continuity of pressure at the interface is satisfied only in the average sense defined by Eq. 8. The iteration procedure has been set up so that an initial estimate of ξ may be improved with iterations such that in the limit $p_a = p_b$.

The iteration procedure consists of assuming a pressure distribution for p_b, calculating the corresponding ξ and then p_a from that ξ (by employing the integral expression for pressure). A new estimate is obtained for p_b by equating it to the newly calculated p_a. All of this is possible because the expressions for p_a, p_b and ξ are expressed as series of orthogonal functions.

This procedure leads to series-type algebraic expressions for the characteristic equation and the pressures. These are easily solved by numerical means. By such means, convergence of the iteration scheme has been demonstrated, i.e., p_a does indeed approach p_b with iterations. However, other variations of this scheme did not converge, as will be discussed subsequently.

Gain/Loss-Type Boundary Conditions

Nonzero, admittance-type boundary conditions can be added at each end of the chamber without difficulty. By defining Green's functions, which satisfy the same boundary conditions at the closed ends of the chamber as those satisfied by the pressure, the foregoing equations may be used without change.

Uniform Steady Flow

If a uniform steady flow is assumed to exist in the chamber, the analysis must be modified to some extend. The linearized fluid dynamic equations for small amplitude oscillations may be combined to give an inhomogeneous wave equation.

$$\nabla^2 p + k^2 p - 2jkM_o \frac{\partial p}{\partial z} + M_o^2 \frac{\partial^2 p}{\partial z^2} = 0 \qquad (9)$$

This equation with the boundary conditions can be converted to an integral equation as before and a parallel analysis may be applied. During the course of the program, the characteristic equation and iteration equations were developed but no numerical results have been obtained.

ANALYTICAL RESULTS

These analytical methods have been used to investigate the oscillatory characteristics of both two-dimensional and cylindrical baffled chambers with either rigid end-walls or gain/loss end-wall boundary conditions. Further, the convergence properties of the iteration scheme and of the several series expressions which arise in the analysis have been carefully examined. Finally, the analysis has been extended to include the influence of uniform steady flow but no numerical results have been obtained.

The utility of these methods are dependent upon the convergence properties of the expressions. To be useful, acceptable convergence must occur with reasonable computing requirements since the equations are solved numerically. Generally, the convergence properties were found to be good and the computing requirements (computing time or storage) were not considered excessive for any case. These factors will be discussed more completely later in this report.

Rigid Walled Chambers

The oscillatory characteristics of several baffled chambers with rigid walls (no gains or losses) and no steady flow were examined in a series of calculations. A number of calculations were made for two dimensional chambers containing one or more zero-width baffles of equal length and spacing. A number of calculations were also made for cylindrical chambers containing three radially directed zero-width baffles of equal length and spacing. Results from the latter calculations are probably of the greatest practical interest.

These calculations were done for the chamber configurations shown in Fig. 1 and 2. These also serve to indicate the dimensional notation used in the analyses. The relatively complicated expressions used to make these calculations are given in Appendices C and D along with listings of the corresponding computer programs. The calculations were restricted to the first transverse and the first tangential modes.

Typical pressure and velocity profiles for the two-dimensional case are shown in Fig. 3. The calculations clearly indicate a discontinuity (singularity) in the axial component of velocity at the baffle tip. In the physical situation, this discontinuity would be replaced by a steep gradient region. Clearly a strong flow around the baffle tip is indicated. Also shown is the degree to which a pressure match has been achieved with the indicated ten iterations. Note that the pressure distributions are roughly similar to the sinusoidal distribution obtained without a baffle. The pressure amplitude was greatest at the injector plane and diminished with length, as shown in Fig. 4.

Typical pressure and velocity distribution for the cylindrical case are shown in Fig. 5 and 6. Again, a discontinuity in the axial component of velocity at the baffle tip is indicated. The oscillatory character of this velocity distribution on either side of the baffle would probably be diminished if a greater number of terms in the series were retained, i.e. a more nearly monotonic distribution is expected. Note that the pressure match is reasonably good.

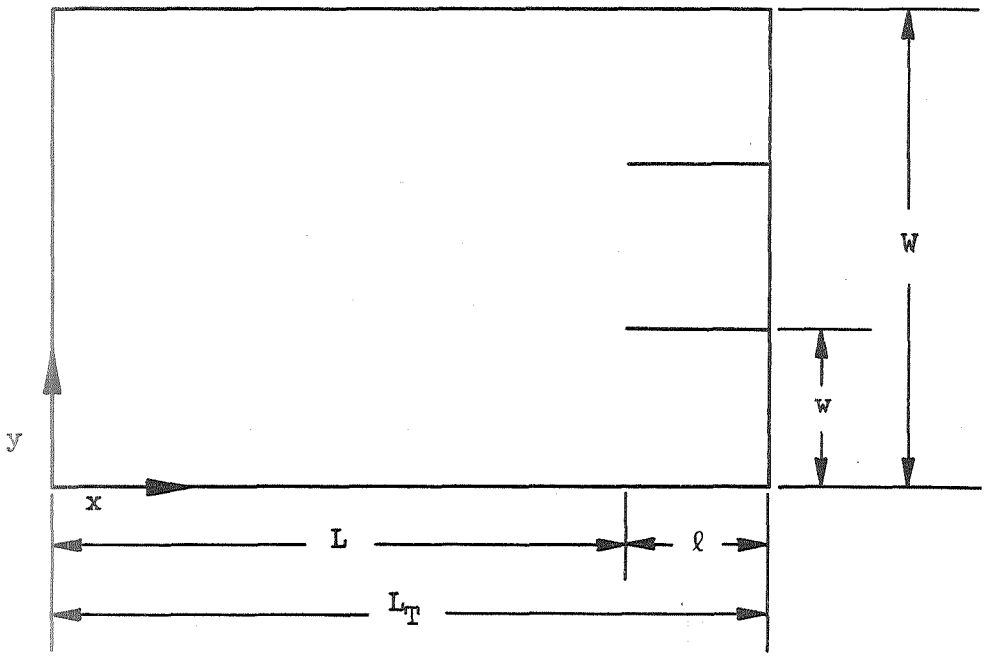

Figure 1. Configuration and Notation Used in Two-Dimensional Chamber Analysis

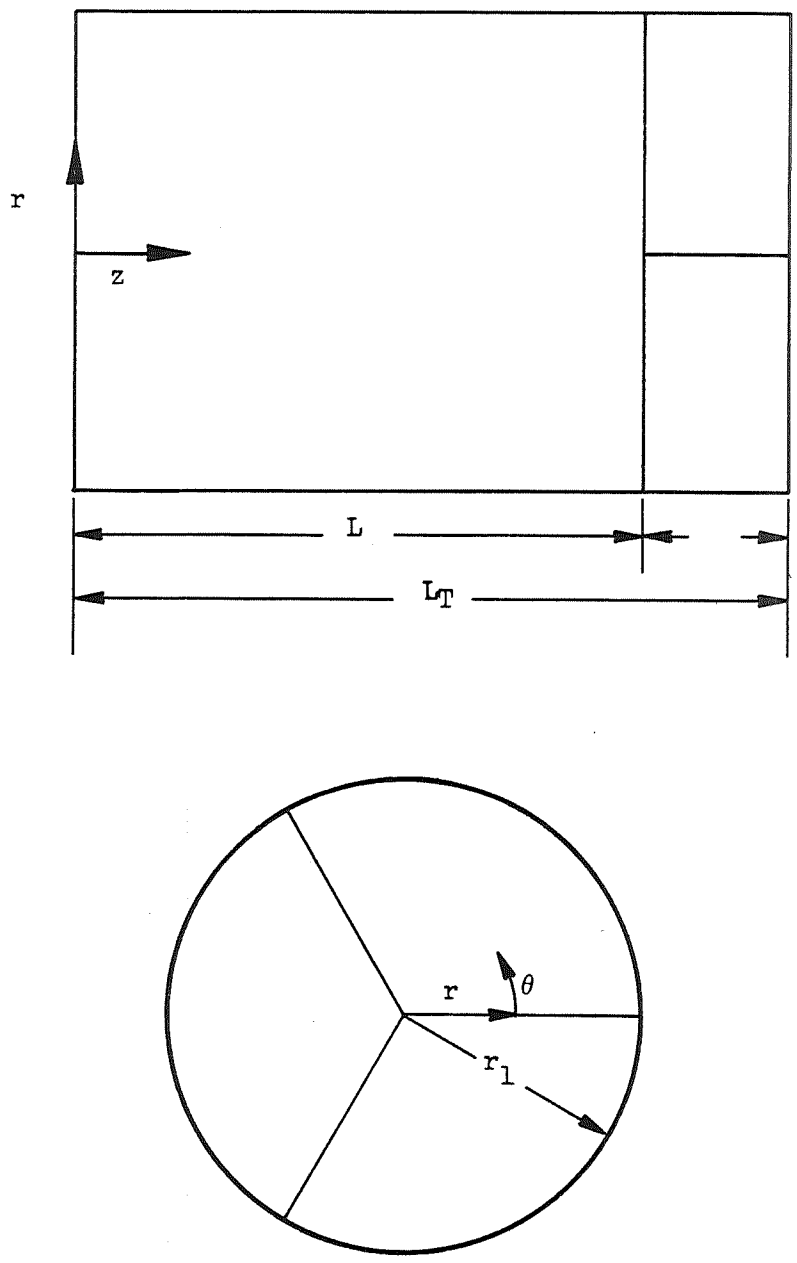

Figure 2. Configuration and Notation Used in Cylindrical Chamber Analysis

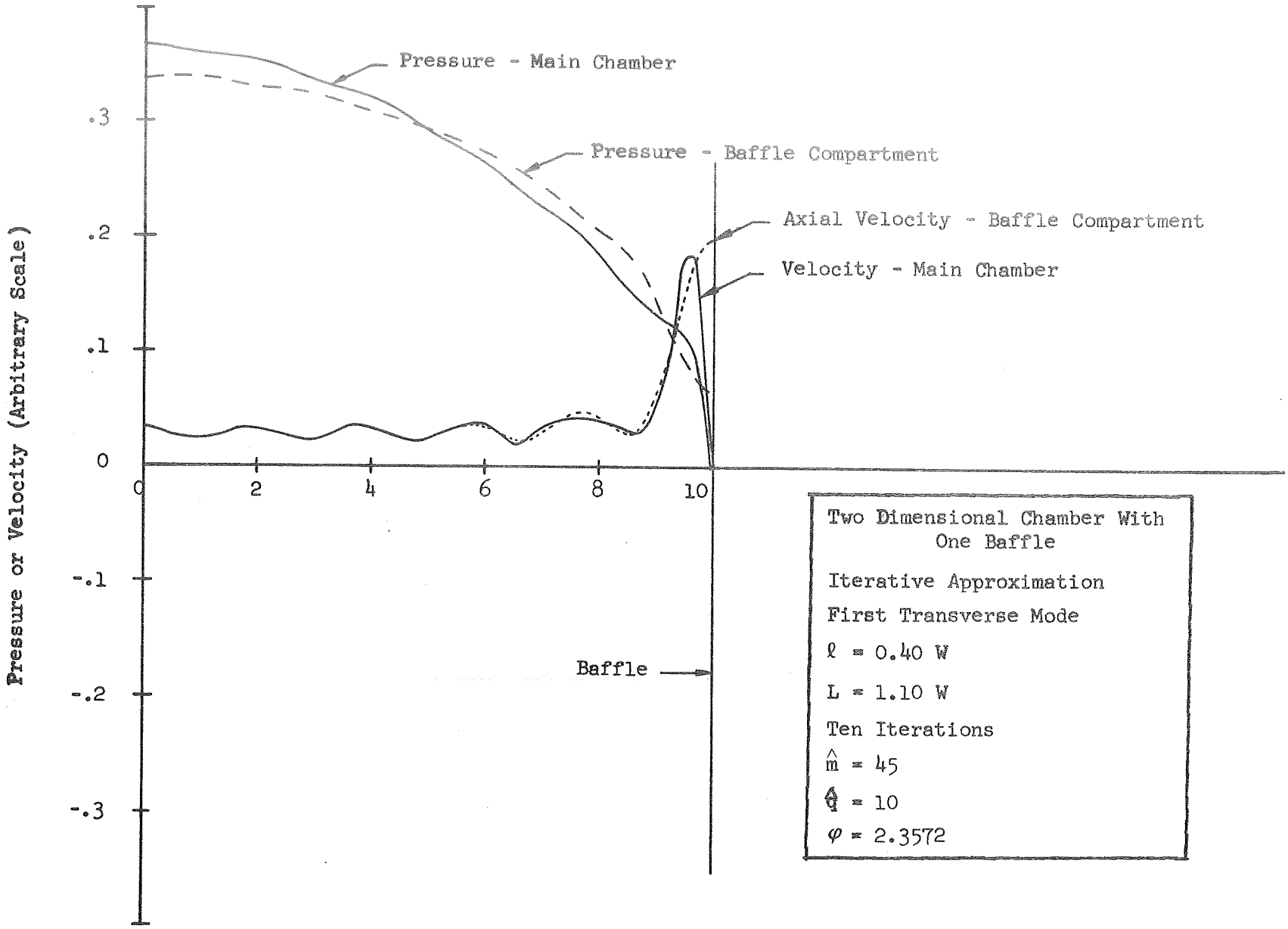

Figure 3. Transverse Profiles at the Interface

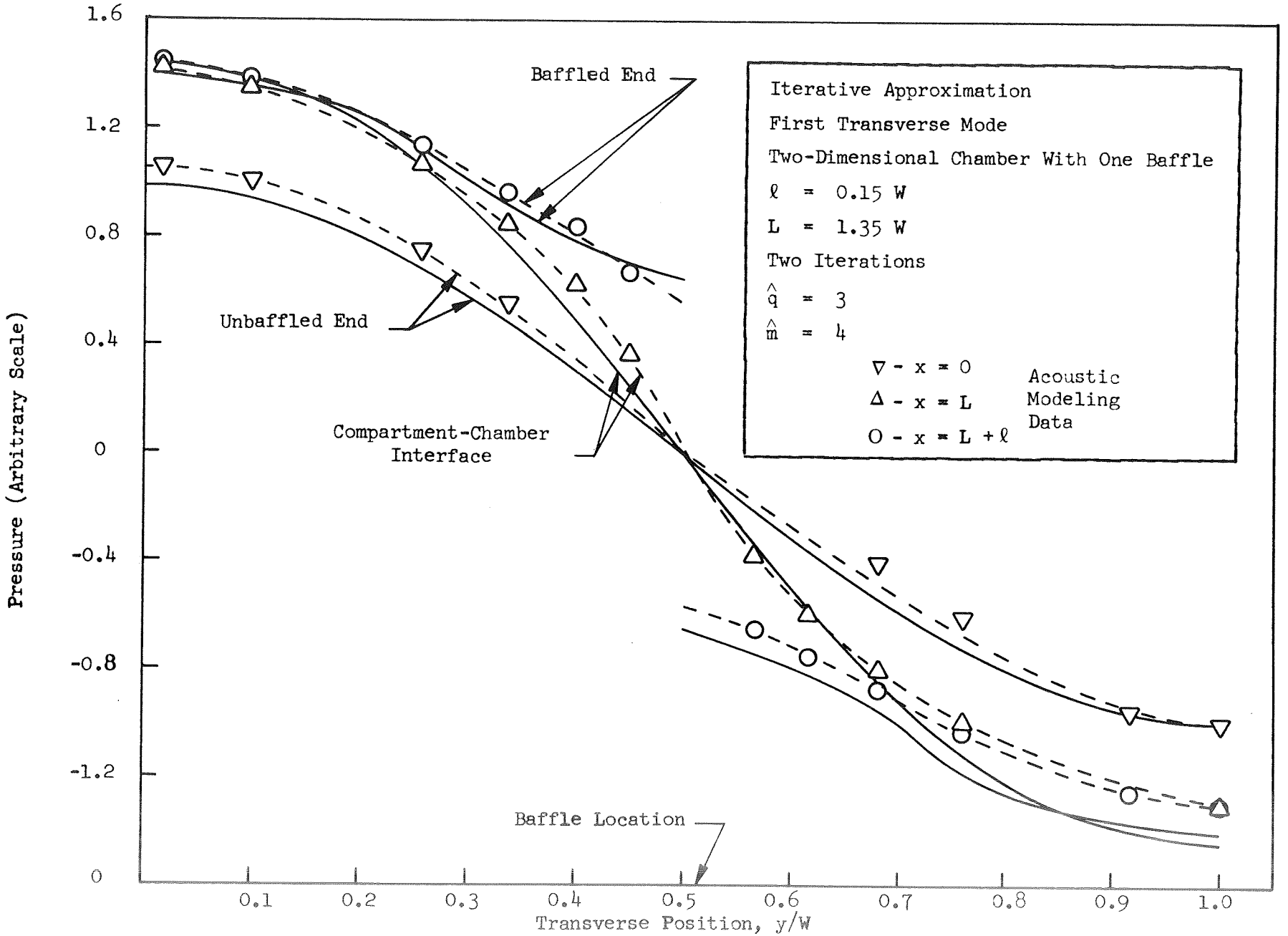

Figure 4. Comparison Between Measured and Predicted Pressure Distributions for Baffled Chamber

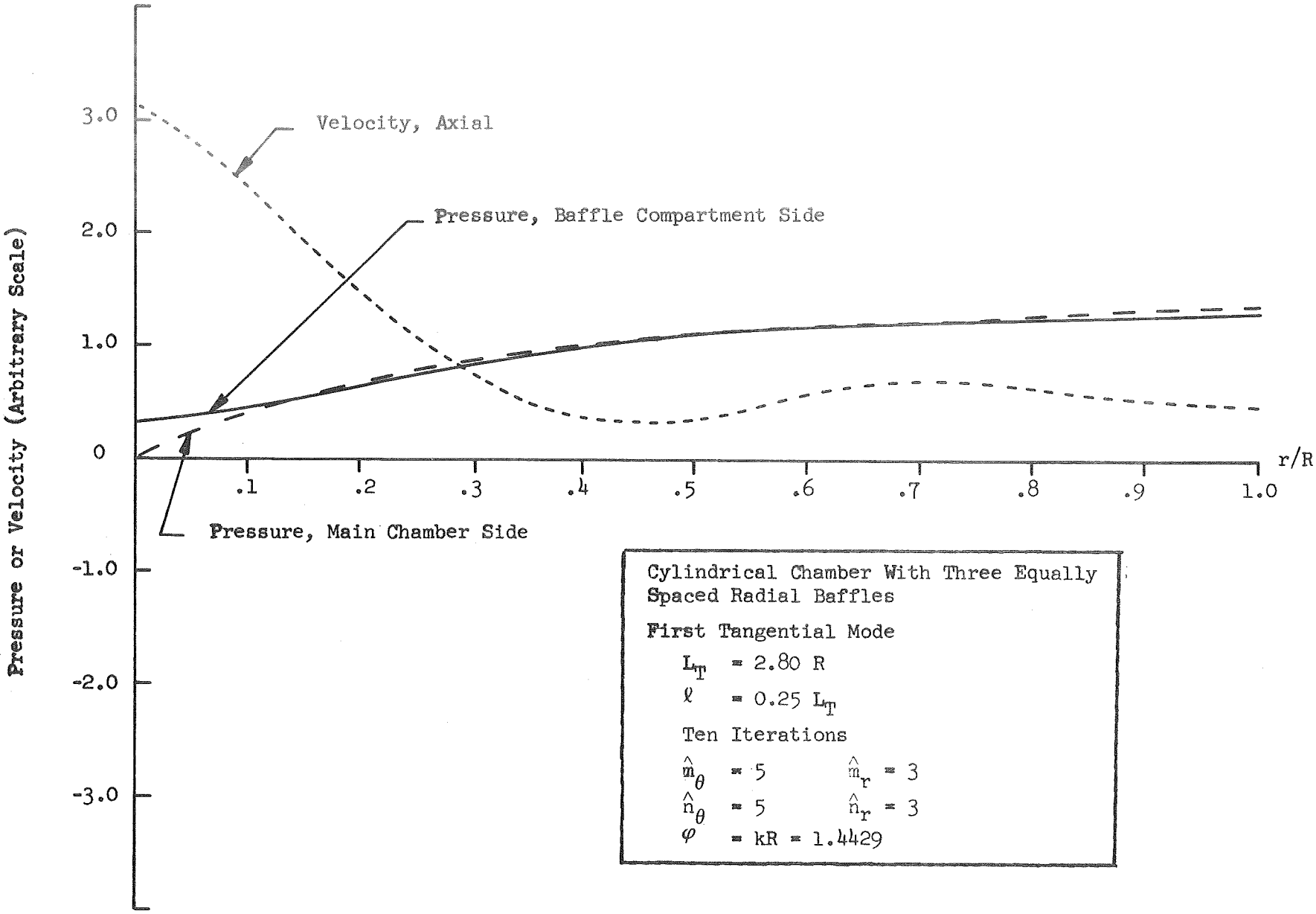

Figure 5. Interface Pressure and Velocity Profiles in Radial Direction (θ = 0+)

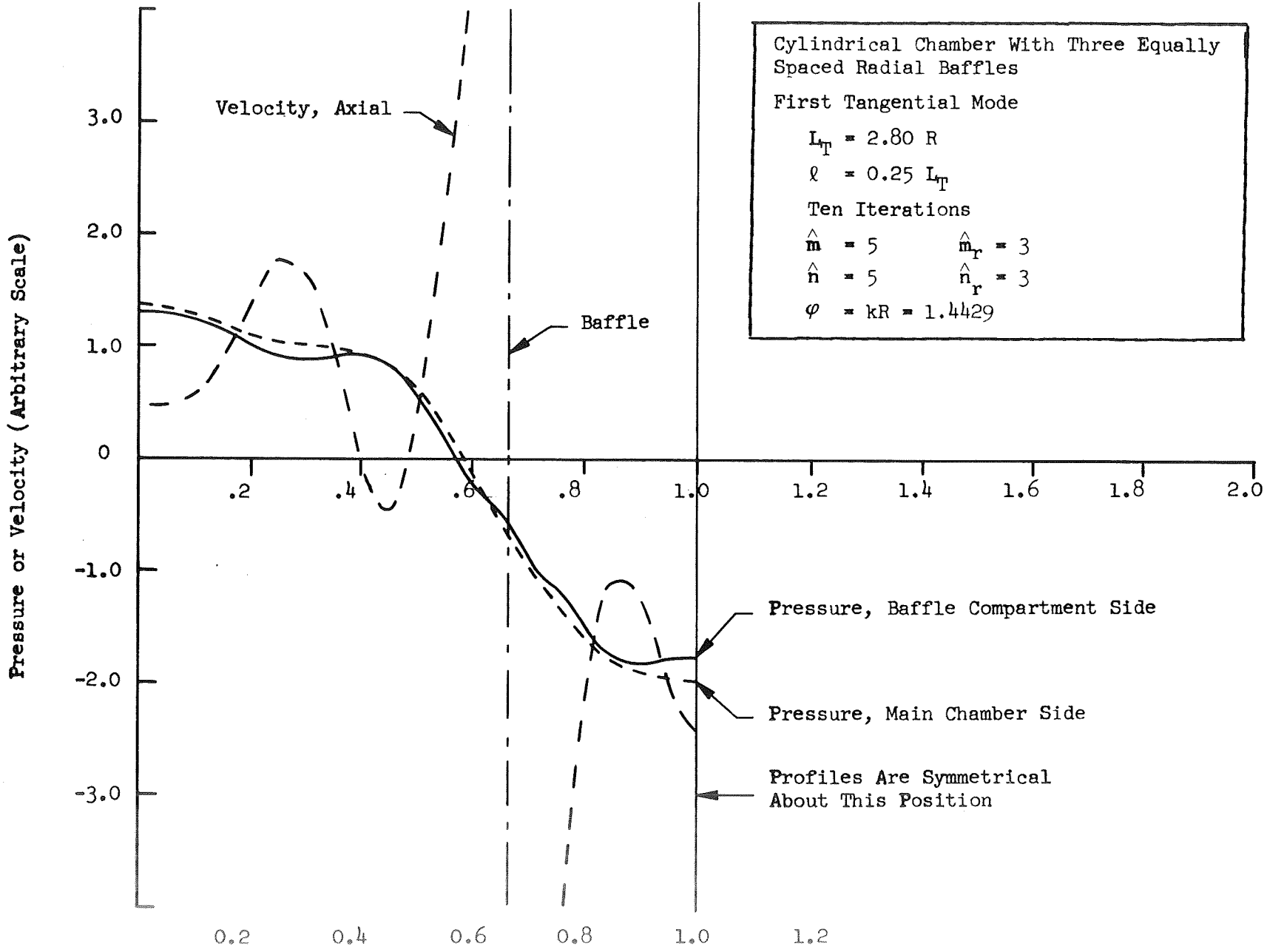

Figure 6. Interface Pressure and Velocity Profiles in Angular Direction (r/R = 1.0)

The calculated frequencies were found to be depressed from the unbaffled values as the baffle-length/chamber-length ratio was increased or as the chamber-width (radius)/chamber-length ratio was increased. These effects are illustrated by the frequency results shown in Tables 1 and 2 and in Fig. 7.

It should be noted that solution of the characteristic equation to obtain the frequencies (the roots or zeros of this equation) yields more than one frequency in the range of interest. This effect is illustrated in Fig. 8 which shows the variation of the characteristic equation with frequency. Two roots or allowed frequencies are shown, only one of which corresponds to the first transverse mode. The second root, usually the lower one, is discarded because it corresponds to a poor pressure match at the interface. This discarded root may represent a poor estimate of a physically realizable frequency or may simply be an extraneous root.

The multiple roots arise simply because there are different combinations of series coefficients (these are frequency dependent) which will satisfy the characteristic equation. Generally, this effect has not been troublesome because once the appropriate root is located its variation can be followed when various parameters are changed. The criteria for selecting the roots to be utilized should always be the degree of pressure match.

By and large, all of the foregoing discussion has concerned calculations with the normal gradient, ξ, represented as a series of compartment eigenfunctions. Other calculations have been made with ξ expressed as a series of the main chamber eigenfunctions and, also, with alternating expressions. None of the latter calculations produced results as good as those described, a poor pressure

TABLE 1. CALCULATED EIGENVALUES FOR TWO-DIMENSIONAL CHAMBERS WITH ZERO ADMITTANCE BOUNDARY CONDITIONS*

Objectives	L_T/W	ℓ/L_T	$\frac{\omega W}{c}$
Effect of ℓ/L_T	1.5	0.1	3.05217
	1.5	0.2667	2.3742
	1.5	0.4333	1.76541
	1.5	0.5667	1.44435
Effect of L_T/W	1.0	0.25	2.783564
	1.5	0.25	2.451465
	2.0	0.25	2.103642
Effect of No. of Baffles			
1 - Baffle	1.5	0.2667	2.3742
4 - Baffles	1.5	0.2667	2.24889

*$\hat{q}$ = 10; $\hat{m}$ = 15; 10 iterations

TABLE 2. CALCULATED EIGENVALUES FOR CYLINDRICAL CHAMBERS WITH ZERO ADMITTANCE BOUNDARY CONDITIONS*

Objectives	L_T/R	ℓ/L_T	$\frac{\omega W}{c}$
Effect of ℓ/L_T	2.8	0.00	1.84118
	2.8	0.10	1.80062
	2.8	0.25	1.44294
	2.8	0.50	0.90381
Effect of L_T/R	1.0	0.25	1.76668
	2.8	0.25	1.44294
	5.0	0.25	0.96102

*$\hat{m}_\theta$ = 5, $\hat{n}_\theta$ = 5, $\hat{m}_r$ = 3, $\hat{n}_r$ = 3; 10 iterations

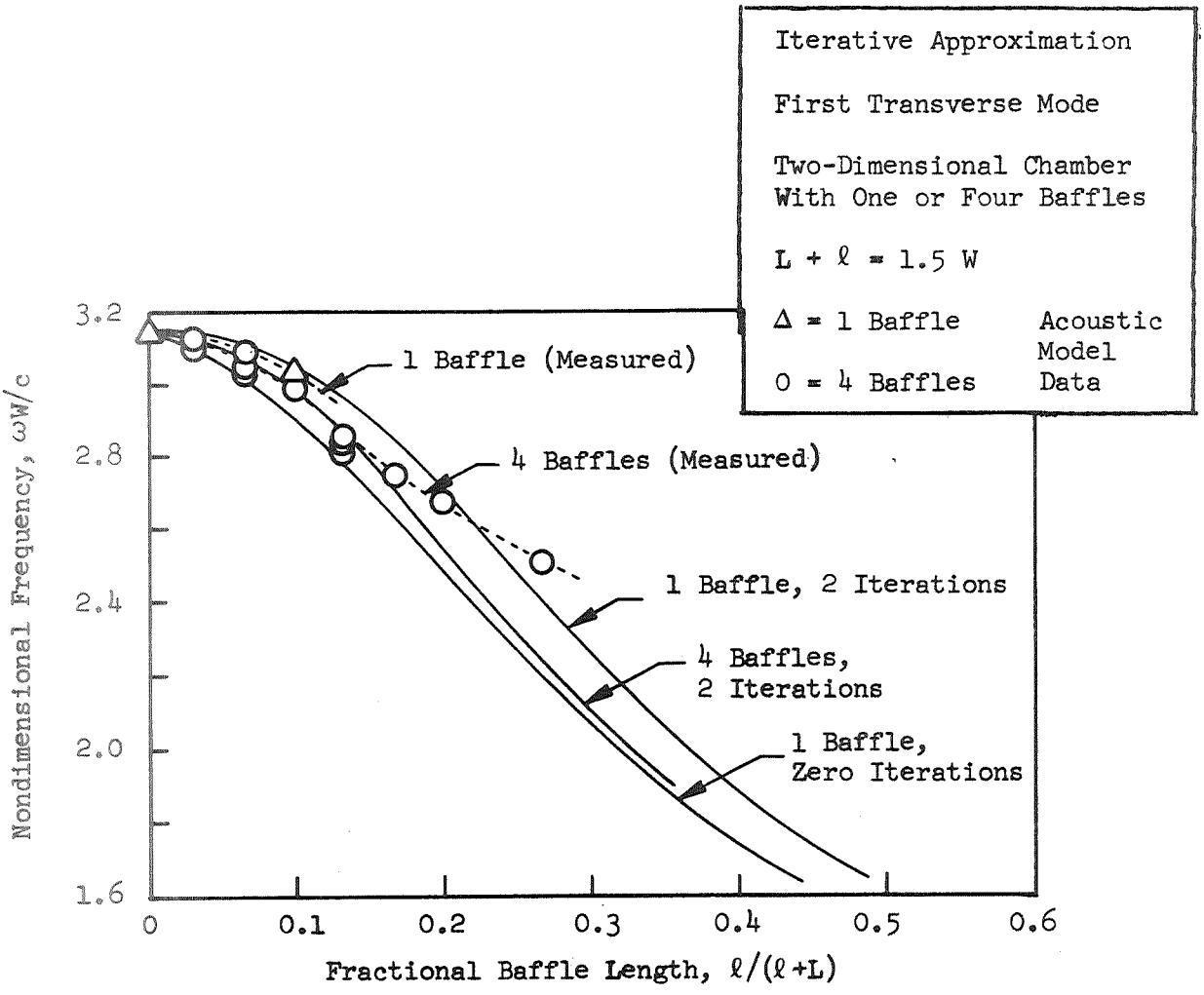

Figure 7. **Predicted Frequency Dependence on Baffle Length From the Iterative Approximation**

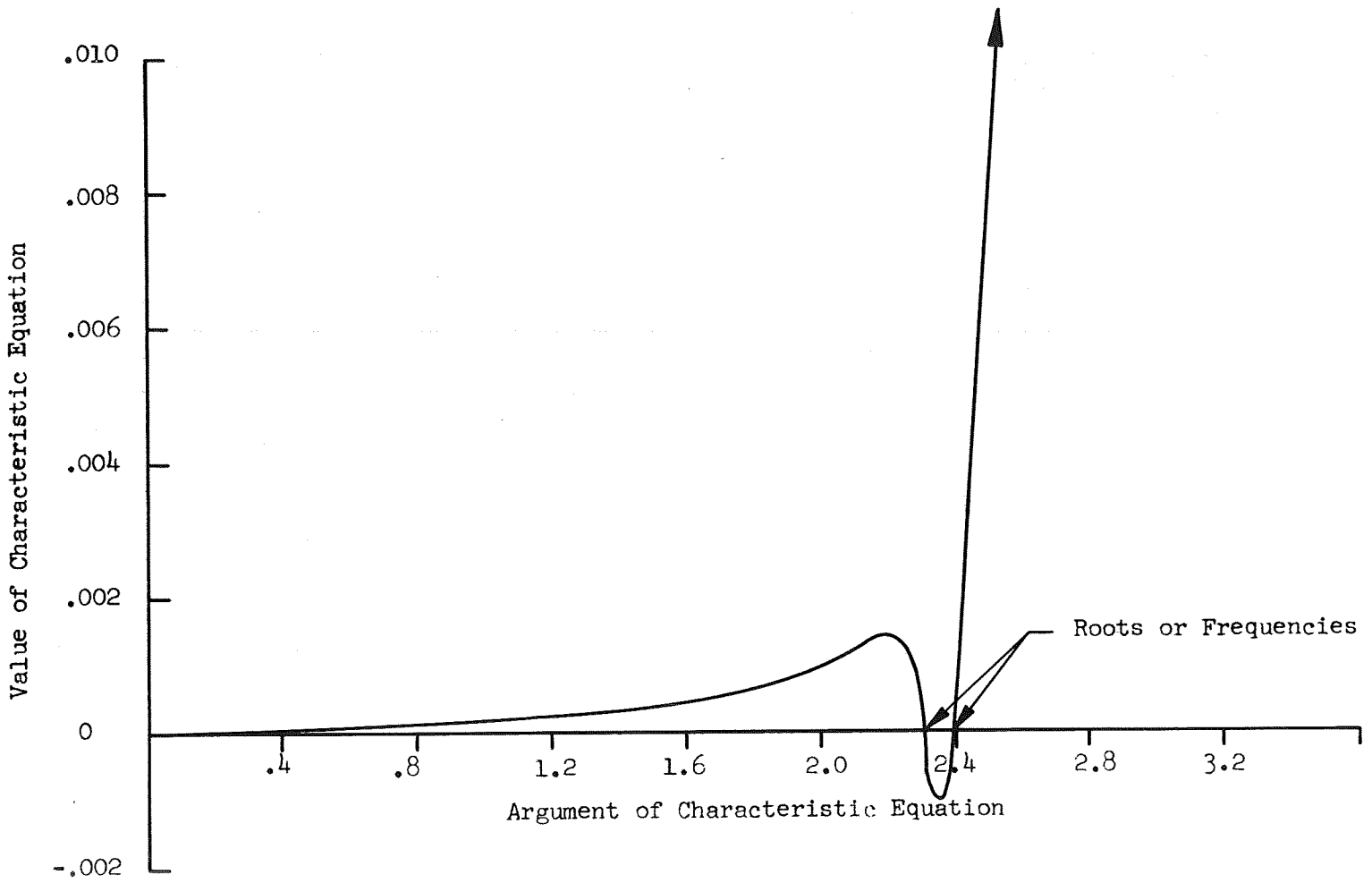

Figure 8. Plot of Characteristic Equation for Typical Two-Dimensional Case

match being obtained. This difference in results stems from the velocity singularity that occurs at the baffle tip, as shown in Fig. 3. The compartment series can readily describe this singularity because a separate expression is used for each compartment and it need not be continuous between compartments. The main chamber series, on the other hand, must be continuous at the baffle tip. Consequently, many more terms are required in the main chamber series than in the compartment series to approximate the velocity singularity. It is entirely possible that, if a sufficient number of terms is retained in the main chamber formulation, comparable pressure matches could be obtained, but no clear indication of this has been observed. Thus, it may also fail.

Convergence

A number of calculations were made to investigate the convergence properties of the analytical method. Generally this investigation was directed toward the two-dimensional rigid walled chamber. The results are believed generally applicable to the cylindrical case as well.

Two kinds of convergence considerations are required, because the set of equations developed to describe the baffled chamber contains several infinite series as well as an iterated approximation. The infinite series arise from the series representations for the oscillatory pressure and velocity in the main chamber and separate but similar representations for the baffle compartments. These series arise irrespective of the iterated approximation. Therefore, independent of whether or not the iteration scheme converges, a sufficient number of terms must be retained in each of the infinite series to adequately

approximate the entire series. Thus, for a two-dimensional chamber convergence is required of the series in m and q (series indices for the main chamber and compartment expansions, respectively). Once the required numbers of terms ($\hat{m}$ and $\hat{q}$) were determined, the question of iterative convergence could be investigated.

Generally it was found that relatively small numbers of iterations and terms (i.e. terms retained in the various series expressions) were required before the calculated oscillatory frequencies ceased to change as more terms and iterations were added. Somewhat larger numbers of terms and iterations were required before the calculated pressure distributions ceased to change. The calculated velocity distributions, especially near the baffle tips, required the largest numbers of terms and iterations.

Initially convergence was investigated by examining the variation of the pressure profile on the compartment side of the chamber/compartment interface as the number of terms in q was increased but with fixed numbers of terms in m and iterations. When this profile became insensitive to further increase, convergence of the series in q was considered to be achieved. A similar procedure was then used to determine the required number of terms in m, this time with the number of terms in q fixed at the level required for convergence of that series. Finally, with an adequate number of terms in m and q, the number of iterations was increased.

For a single baffle in a two-dimensional chamber with a baffle-length-to-chamber-length ratio of 0.1 and a chamber length-to-width ratio of 1.5, results from the indicated set of convergence calculations is shown in Fig. 9a

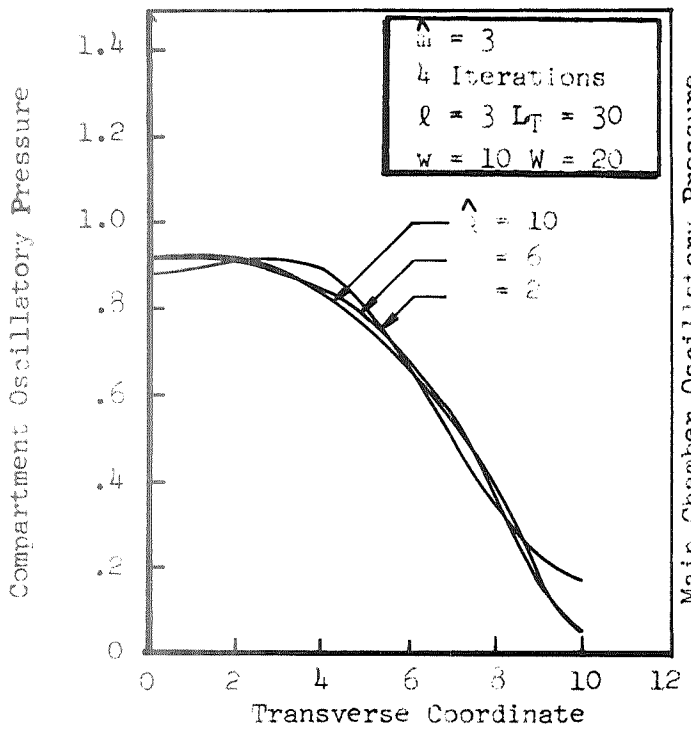

Figure 9a. Compartment Pressure Variarion With q

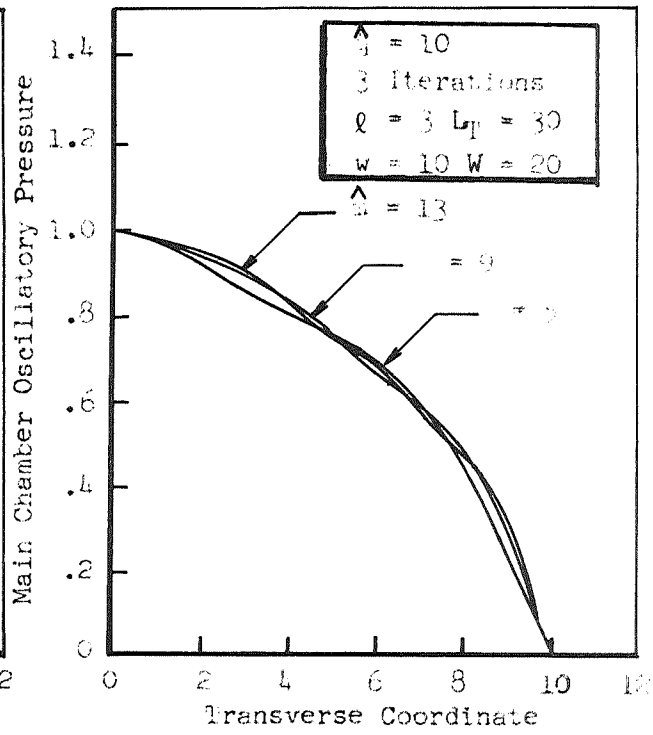

Figure 9b. Chamber Pressure Variation With m

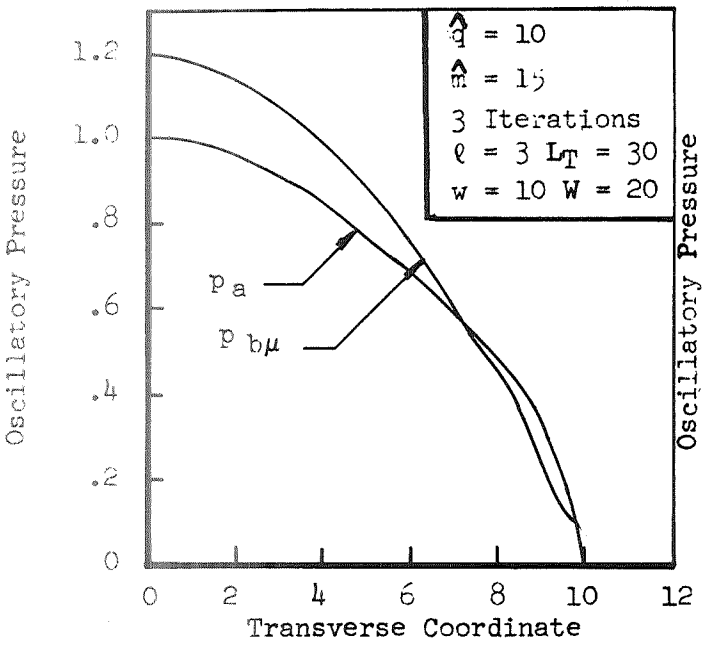

Figure 9c. Comparative Compartment and Chamber Pressure Profiles

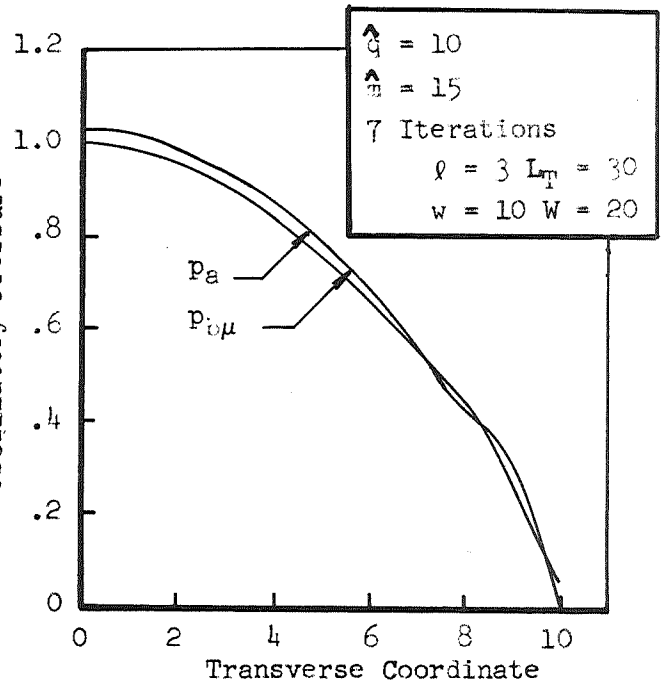

Figure 9d. Comparative Compartment and Chamber Pressure Profiles

through 9d. In Fig. 9a compartment-side pressure profiles are shown for various $\hat{q}$, i.e., number of terms in q. Corresponding calculations are shown in Fig. 9b where the number of terms in m was varied. Clearly convergence is occurring and approximately 10 terms in q and 15 terms in m are adequate for this case. It should be noted that for the first transverse mode all of the even order terms in m are zero, which is required for proper symmetry of the pressure profile.

Figures 9c and 9d show comparative pressure profiles on each side of the chamber/compartment interface for various numbers of iterations. Again, it is clear that convergence is occurring. Error calculations show that the error decreases in a monotonic fashion. Errors are even smaller with more than one baffle.

Somewhat larger numbers of terms are required to describe the velocity profile near the baffle tip. In Fig. 10 are shown calculated profiles from the truncated series with $\hat{q} = 10$ and $\hat{m} = 15$. Clearly, the series for the main chamber velocity is not adequately approximated with 15 terms. However, Fig. 3 demonstrates that an excellent velocity match is achieved if $\hat{m}$ is increased to $\hat{m} = 45$. Figures 11 and 12 show calculated results for 10 and 20 iterations, respectively, and with $\hat{q} = 23$ and $\hat{m} = 45$. The velocity agreement would improve if the ratio of $\hat{m}$ to $\hat{q}$ was increased.

Adequate convergence was considered to have been demonstrated by these calculations. Additional convergence considerations are described in Appendix B.

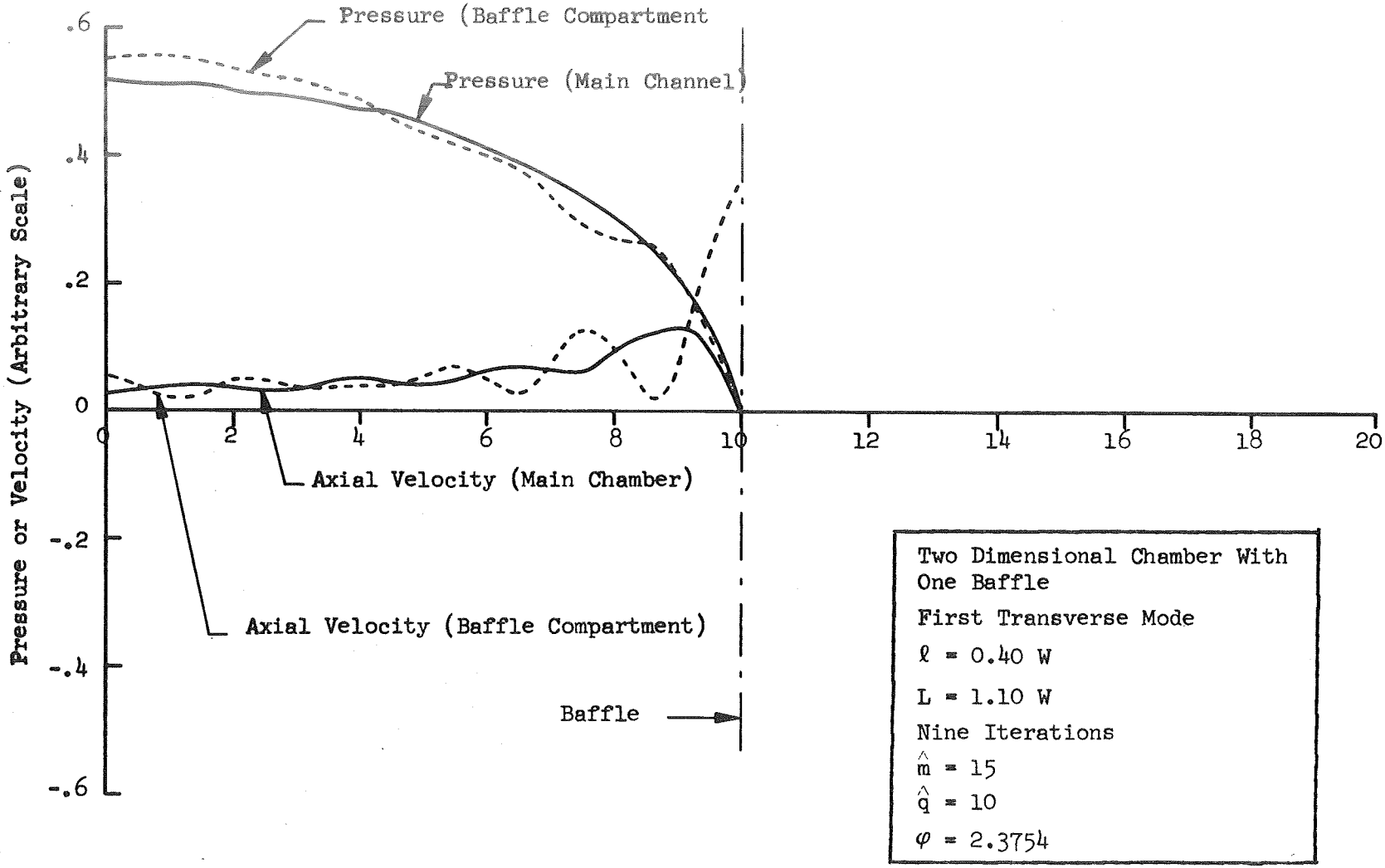

Figure 10. Calculated Pressure and Axial Velocity at Interface in Two-Dimensional Chamber

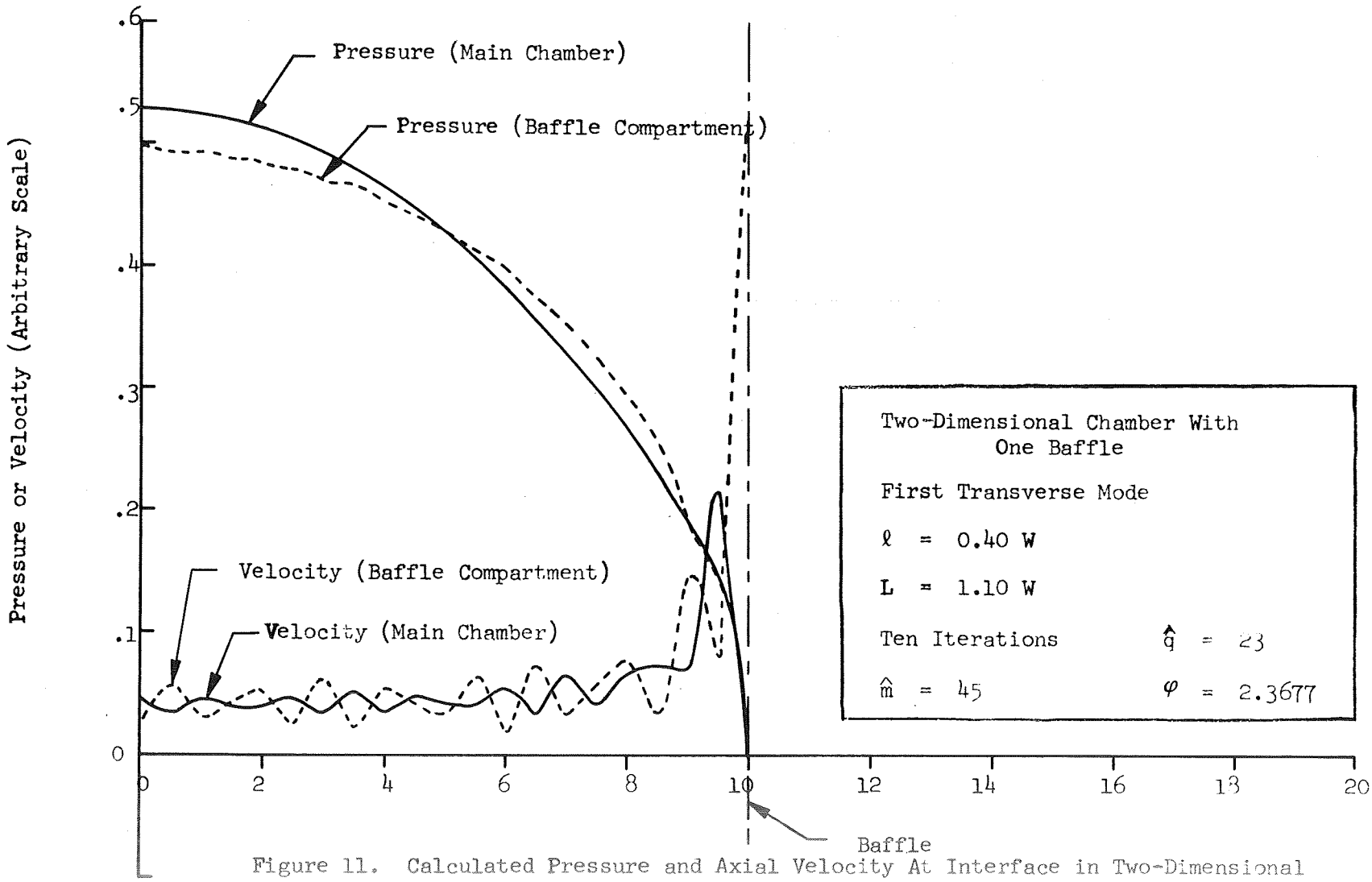

Figure 11. Calculated Pressure and Axial Velocity At Interface in Two-Dimensional Chamber

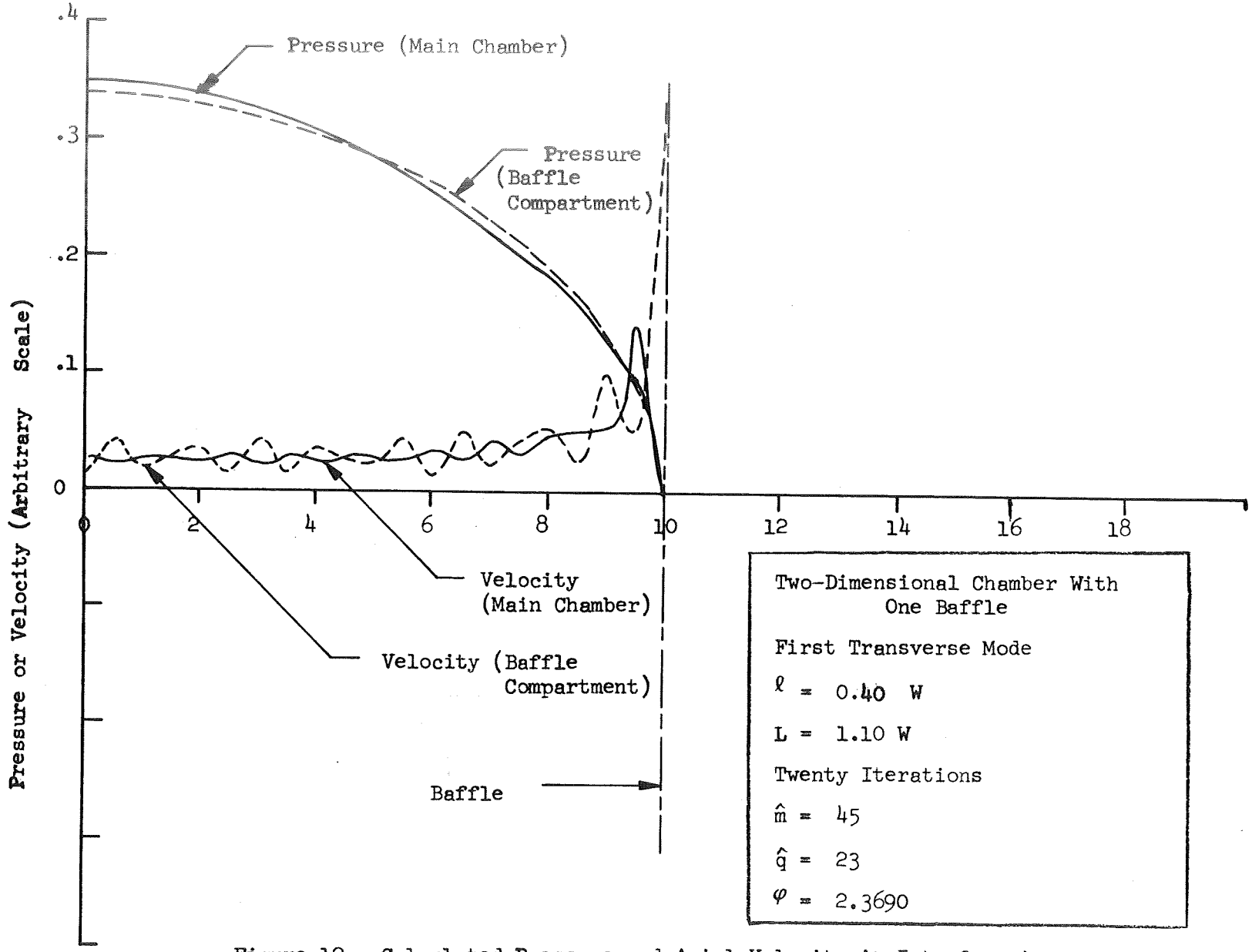

Figure 12. Calculated Pressure and Axial Velocity At Interface in Two-Dimensional Chamber

Gain/Loss Boundary Conditions

The effects of pressure-coupled combustion driving and nozzle losses were partially simulated by employing nonzero acoustic admittance values at each end of the chamber. A gain-type condition was imposed at the injector end and a loss-type condition at the nozzle end.

The boundary condition was written in terms of a specific acoustic admittance:

$$y = \rho c \frac{\vec{N} \cdot \vec{u}}{p}$$

with y_I being the injector admittance and y_N being the nozzle admittance.

With such boundary conditions, the characteristic equation becomes complex and solution of it yields complex frequencies or eigenvalues. The real part of that eigenvalue corresponds to the angular frequency of oscillation; the imaginary part corresponds to an exponential growth or decay coefficient. Thus, whether stability or instability is predicted depends on the sign of this imaginary part of the eigenvalue.

A series of calculations were made for both two-dimensional and cylindrical chambers. The results are shown in Tables 3 and 4. In every case, the baffles were found to degrade stability (as long as the real part of y_I was negative) rather than improve it as found in practice. This implies that the stability model is inadequate, possibly because velocity (transverse) coupling with the combustion is more important than the pressure sensitive case that was simulated. Another possible explanation is that the baffles contribute nonlinear losses due to wake effects which were not included in this analysis.

TABLE 3. DAMPING CALCULATIONS FOR THE NONZERO ADMITTANCE CASES*

Objectives	Number of Baffles	W/L_T	ℓ/L_T	y_N	y_I	$\frac{\omega W}{c}$	$\frac{\alpha W}{c}$
Effect of number of baffles	1	1.0	0.25	0.06	-0.06	2.722	-0.0773
	2	1.0	0.25	0.06	-0.06	2.706	-0.0527
	3	1.0	0.25	0.06	-0.06	2.654	-0.0557
Effect of baffle length	3	1.0	0.10	0.06	-0.06	3.059	-0.0153
	3	1.0	0.25	0.06	-0.06	2.654	-0.0557
	3	1.0	0.50	0.06	-0.06	1.925	-0.0599
Effect of injector admittance	3	1.0	0.25	0.06	-0.20	2.680	-0.2170
	3	1.0	0.25	0.06	-0.06	2.654	-0.0557
	3	1.0	0.25	0.06	-0.02	2.652	-0.0106
Effect of nozzle admittance	3	1.0	0.25	0.2	-0.06	2.665	-0.0305
	3	1.0	0.25	0.06	-0.06	2.654	-0.0557
	3	1.0	0.25	0.02	-0.06	2.653	-0.0634
Effect of chamber width-to-length	3	2.0	0.25	0.06	-0.06	2.896	-0.0176
	3	1.0	0.25	0.06	-0.06	2.654	-0.0557
	3	0.50	0.25	0.06	-0.06	1.996	-0.0702

*All calculations were made with 15 terms in m, 10 terms in q, and 9 iterations.

TABLE 4. CALCULATED EIGENVALUES FOR CYLINDRICAL CHAMBERS WITH FINITE ADMITTANCE BOUNDARY CONDITIONS*

Objectives	L_T/R	ℓ/L_T	y_N	y_I	$\frac{\omega r_w}{c}$	$\frac{\alpha r_w}{c}$
Effect of ℓ/L_T	2.8	0.10	0.06	-0.06	1.80472	-0.01665
	2.8	0.25	0.06	-0.06	1.44383	-0.04459
	2.8	0.50	0.06	-0.06	0.90390	-0.03392
Effect of L_T/R	1.0	0.25	0.06	-0.06	1.77020	-0.00729
	2.8	0.25	0.06	-0.06	1.44383	-0.04459
	5.0	0.25	0.06	-0.06	0.98895	-0.03405
Effect of End Admittance	2.8	0.25	0.00	0.00	1.44294	---
	2.8	0.25	0.06	-0.06	1.44383	-0.04459
	2.8	0.25	0.20	-0.20	1.45344	-0.15259

*$m_\theta = 5$, n_θ, $m_r = 3$, $n_r = 3$; 10 iterations

The results from stability limit calculations made for the two-dimensional case with gain/loss boundary conditions were similar to those reported previously in Ref. 3; no region was found in which a beneficial effect of baffles was indicated.

Computing Time Requirements

The utility of the foregoing analytical methods depends in part on the computing requirements in terms of computing time and storage. Therefore, it is of interest to determine these requirements for a "typical" case. Unfortunately, a typical case is very difficult to specify because of the variability in the numbers of terms and iterations that may be deemed necessary. Moreover, occasionally considerable difficulty is encountered in finding the roots of the characteristic equation. Projecting the requirements of another computer system is even more difficult. Nonetheless, an attempt has been made to estimate the computing time requirements.

All calculations have been made on a G.E. Model 440 time sharing computer system. For "typical" cases the rough maximum requirements are shown below.

	Two-dimensional	Cylindrical
Rigid wall case	< 150 sec or < $0.42	< 450 sec or < $1.25
Nonzero admittance case	< 900 sec or < $2.50	< 1500 sec or < $4.20

The dollar figures shown are based on a nominal rate of $10 per hour of computing time. The salary of the engineer operating the computer is not included.

If these same cases were to run on an IBM-360 Model 65 computer in a batch processing rather than time sharing mode, the computing times would be 1/2 (very roughly) of the times shown above. This estimate includes an allowance for requiring more trial cases because of the inability to interact directly with the computer. The computer logic being used has, of course, been selected for a time sharing mode. Therefore, some improvements are possible for use with a batch processing computer.

Clearly the computing costs are well within an acceptable range.

CONCLUSIONS

A satisfactory analytical method (variational-iterational technique) has been developed to analyze the wave motion in baffled combustion chambers. This method may be used to accurately predict the instability frequencies and the oscillatory pressure and velocity distributions in baffled chambers. A number of relatively simple configurations have been analyzed thus far and application of the method to other baffle configurations appears straightforward, although the details of the analysis are complicated.

Stability calculations have been made for a number of chamber/baffle configurations with gain/loss end-wall boundary conditions, which were used to simulate

combustion gains and chamber losses. In each case analyzed (with gain type admittance at the injector end), the predicted stability of the chamber was degraded by the introduction of baffles. Because this result is in direct conflict with observed engine stability, this simple analytical representation of chamber gains and losses must be inadequate. This failure to properly predict observed stability trends may be due to velocity-coupled combustion driving effects or to wake-type drag losses on the baffles, neither of which are included in the current analytical formulation.

Nevertheless, the ability to predict instability frequencies, and oscillatory velocity and pressure distributions in baffled chambers may be used to advantage for the design of baffles.

REFERENCES

1. McBride, J. M.: "Blade Arrangement and Blade Design," ICRPG Reference Book on Liquid Propellant Rocket Combustion Instability, Sections 8.2.2 and 8.2.3, 1969 (to be published).

2. R-7868, by L. P. Combs, C. L. Oberg, T. A. Coultas, and W. H. Evers, Jr., Liquid Propellant Rocket Engine Combustion Stabilization Devices, Rocketdyne, a Division of North American Rockwell Corporation, Canoga Park, California, May 1969 (not yet approved for distribution).

3. Oberg, C. L., T. L. Wong, and R. A. Schmeltzer: Analysis of the Acoustic Behavior of Baffled Combustion Chambers, NASA CR-72625, R-8076, Rocketdyne, a Division of North American Rockwell Corporation, Canoga Park, California, January 1970.

4. Morse, P. M. and H. Feshbach: Methods of Theoretical Physics, McGraw-Hill Book Co., Inc., New York, 1953.

5. Morse, P. M. and K. U. Ingard: Theoretical Acoustics, McGraw-Hill Book Co., Inc., New York, 1968.

APPENDIX A

ALTERNATE DERIVATION OF INTEGRAL EQUATION

The integral equation for pressure can be derived from the wave equation by employing a sum of separated solutions rather than starting with a Green's function. Essentially this approach is an alternate derivation or definition of the surface Green's function. The method is described for the two-dimensional case but the cylindrical closely parallels it.

A two-dimensional chamber is considered with rigid walls on three sides but an arbitrary boundary condition at $x = L$. The separation of variables technique is used without applying the boundary condition at $x = L$. The separated solutions may be written as

$$f_m(x,y) = \cos \frac{m\pi y}{W} \cos k_m x \tag{A-1}$$

where $k_m = (k^2 - m^2\pi^2/w^2)^{1/2}$. Note that only one index, m, appears. Because the individual separated solutions cannot satisfy the arbitrary boundary condition at $x = L$, a sum of these solutions is tried, i.e.,

$$p = \sum_m a_m \cos \frac{m\pi y}{W} \cos k_m x \tag{A-2}$$

where a_m is an unspecified coefficient. The pressure gradient at $x = L$ may be obtained by differentiating Eq. A-2,

$$\left.\frac{\partial p}{\partial x}\right|_{x = L} = - \sum_m a_m k_m \sin k_m L \cos \frac{m\pi y}{W} \tag{A-3}$$

The coefficients may be obtained in terms of this gradient from orthogonality,

$$A_m = \frac{-\int_0^W \left.\frac{\partial p}{\partial x}\right|_{x=L} \cos \frac{m\pi y_o}{W} \, dy_o}{\frac{W}{\epsilon_m} k_m \sin k_m L} \qquad \text{(A-4)}$$

where

$$\frac{W}{\epsilon_m} = \int_o^W \cos^2 \frac{m\pi y_o}{W} \, dy_o$$

$$\epsilon_m = \begin{cases} 1 & m = 0 \\ 2 & m \neq 0 \end{cases}$$

Thus, the pressure at any point in the chamber may be expressed in terms of the gradient at $x = L$, i.e., Eq. A-2 becomes

$$p = -\sum_m \frac{\epsilon_m}{W} \frac{\cos k_m x \cos \frac{m\pi y}{W} \int_0^W \left.\frac{\partial p}{\partial x}\right|_{x=L} \cos \frac{m\pi y_o}{W} \, dy_o}{k_m \sin k_m L} \qquad \text{(A-5)}$$

By noting that the integration in Eq. A-5 is over the variable y_o and that a series may be integrated term by term, Eq. A-5 may be written as

$$p = \int \left.\frac{\partial p}{\partial x}\right|_{x=L} G \, dy_o \qquad \text{(A-6)}$$

where, by definition,

$$G = - \sum_{m} \frac{\epsilon_m}{W} \frac{\cos k_m X \cos \frac{m\pi y}{W} \cos \frac{m\pi y_o}{W}}{k_m \sin k_m L} \qquad (A\text{-}7)$$

Equations A-6 and A-7 are identical with those obtained by starting with a Green's function (see Ref. 3 or Appendix C).

APPENDIX B

ADDITIONAL CONVERGENCE CONSIDERATIONS

It is important to define the degree to which a continuous oscillatory velocity distribution is obtained with the analytical method being used. This question relates closely to convergence of the series representations for pressures and velocities, but not (directly, at least) to convergence of the iteration scheme. In general, each of these series should be regarded as being of infinite extent but are approximated by truncated series for numerical purposes.

The analysis is such that if the normal gradient distribution at the chamber/compartment interface (ξ) and the frequency (or k) are given, then the pressures and pressure gradients (or velocities) can be subsequently calculated for any point in the chamber or compartment from the integral expressions. For example, the axial gradient of pressure in the main chamber may be written (for the two-dimensional case) as

$$\frac{\partial p_a}{\partial x} = \sum \frac{\epsilon_m}{W} \frac{\sin k_m x}{\sin k_m L} \cos \frac{m\pi y}{W} \int \xi \cos \frac{m\pi y_o}{W} \, dy_o \qquad \text{(B-1)}$$

If $x = L$, this expression is simply a Fourier series expansion for ξ. A similar result is obtained for the baffle compartments, i.e.,

$$\frac{\partial p_o}{\partial x} = \sum \frac{\epsilon_q}{w} \frac{\sin k_q (L_t - x)}{\sin k_q \ell} \cos \frac{q\pi (y - \mu w)}{w} \int \xi \cos \frac{q\pi (y_o - \mu w)}{w} \, dy_o \qquad \text{(B-2)}$$

Again, for $x = L$, the expression becomes a Fourier series expression for ξ.

Because for $x = L$ each of these expressions is a Fourier series for the same thing, then the normal component of velocity is continuous, at least if the series converge. Any deviation from continuous character must arise from truncation of the series for the calculations. This conclusion is valid for any level of iteration or approximation for ξ (and the solution); however, the pressure is not continuous unless the exact solution is obtained.

The variational-iterational technique is the means being used to calculate approximations for ξ and k. With the compartment approximation, the Fourier series for ξ in terms of the compartment-side eigenfunctions is used, which may be denoted as ξ_b. The eigenvalue (frequency), in turn, is calculated from the characteristic equation,

$$\int \xi_b (p_a - p_b)\, dS = 0 \qquad \text{(B-3)}$$

The iteration is used to generate approximate expressions for ξ_b, $p_a(L)$, and $p_b(L)$; the iteration is set up so that $p_a(L)$ and $p_b(L)$ approach the same distribution.

Thus, for numerical purposes a sufficient number of terms must be retained in the series expressions for ξ_b, p_b, and p_a to adequately approximate each of these infinite series. Note that the numbers of terms required to approximate the series expressions for $\partial p_a/\partial x$ and $\partial p_b/\partial x$ are likely to be different from the number required for p_a and p_b expressions, because the gradients vary more rapidly with position than the pressures.

One further factor is worth noting. The series expressions for $\partial p_a/\partial x$ and $\partial p_b/\partial x$ (Eq. B-1 and B-2) suggest that fewer terms are required for positions on either side of the interface. The coefficients are reduced by the ratio of sine terms which approaches $e^{m\pi(x-L)/W}$ for $x < L$ and large m or $e^{q\pi(L_t-x)/w}$ for $x > L$ and large q.

APPENDIX C

TWO-DIMENSIONAL BAFFLED CHAMBERS

This appendix details the equations, logic and computer programs which were developed to described two-dimensional baffled thrust chambers with non-zero end-wall admittance boundary conditions. The rigid wall case is obtained by simply equating these admittance values to zero.

Also included in this Appendix is a listing of the main computer program and the auxiliary programs used for generating pressure and velocity distributions and input files. Finally, a sample calculation is included for a rigid end-wall chamber containing a single baffle.

To simplify the computer operations, the mathematical notation used here and in Appendix D is different from that used in the main text. A separate table of nomenclature for these appendices is included at the end of Appendix D, which also shows the relationships between the nomenclature used in the text and in the appendices.

GENERAL EQUATIONS

The general characteristic equation derived from the variational method for the two-dimensional baffled chamber shown in Fig. 1 is

$$\int_{y_o}^{y_{\bar{\mu}}} \left(p^{(o)} - p^{(\mu)}\right) \frac{\partial p^{(\mu)}}{\partial x} \, dy = 0 \quad \text{at } x = x_1 \tag{C-1}$$

It may be observed that this is simply an equation for conservation of the energy flux across the interface between the main chamber and the baffle compartments for the rigid-wall case. Corresponding to any pressure gradient at the interface,the pressures in the different regions are given by the integral equation corresponding to the wave equation, i.e.,

$$p^{(\mu)}(x,y) = -\int_{y_\mu}^{y_{\mu+1}} G^{(\mu)}(x, y|x_1, y') \frac{\partial p^{(\mu)}}{\partial x'}(x_1,y')\, dy' \qquad \text{(C-2a)}$$

$$p^{(0)}(x,y) = +\int_{y_0}^{y_\mu} G^{(0)}(x, y|x_1, y') \frac{\partial p^{(\mu)}}{\partial x'}(x_1,y')\, dy' \qquad \text{(C-2b)}$$

where $G^{(\mu)}$ and $G^{(0)}$ are the Green's functions in the μ^{th} baffle compartment and the main chamber respectively. The pressures obtained from Eq. C-2a and C-2b are not equal at the interface unless the pressure gradient at the interface used for the integration corresponds to the exact solution of the wave equation and the appropriate boundary conditions.

Because the exact solution is unknown at the outset, an initial form for this pressure gradient is assumed and an iteration scheme is used to improve the accuracy of the initial form. This iteration scheme proceeds as follows. First, some form is assumed for the pressure gradient at the interface:

$$\frac{\partial p^{(\mu)(\ell)}(x_1,y)}{\partial x} \qquad \text{(C-3)}$$

Then the above integral equations are used to obtain $p^{(\mu)(\ell)}(x,y)$ and $p^{(0)(\ell)}(x,y)$ directly. Since, for the exact solution, the pressures must match identically at the interface $(x = x_1)$, a new approximation for the baffle compartment pressure profile at the interface is obtained by equating the pressures:

$$p^{(\mu)(\ell+1)}(x_1,y) = p^{(0)(\ell)}(x_1,y) \tag{C-4}$$

A new pressure gradient is then obtained by differentiating the corresponding integral equation and the iteration sequence is complete. The iteration may be repeated as many times as desired.

Assumptions and Definitions

The assumptions and definitions used to obtain the above algebraic forms of the characteristic and iteration equations are presented here for reference.

The ℓ^{th} approximation to the pressure profile on either side of the interface is assumed to be represented by an eigenfunction expansion, i.e.,

$$p^{(\mu)(\ell)} \equiv \sum_{n_y=1} b_{n_y}^{(\mu)(\ell)} \psi_{n_y}^{(\mu)}(y) \tag{C-5a}$$

$$p^{(0)(\ell)} \equiv \sum_{m_y=1} a_{m_y}^{(0)(\ell)} \psi_{m_y}^{(0)}(y) \tag{C-5b}$$

where the orthonormal eigenfunctions are

$$\psi_{n_y}^{(\mu)}(y) \equiv \cos\left[\alpha_{y,n_y}^{(\mu)}(y-y_\mu)\right] \Big/ \sqrt{\epsilon_{n_y}^{(\mu)}} \tag{C-6a}$$

$$\psi_{m_y}^{(0)}(y) \equiv \cos\left[\alpha_{y,m_y}^{(0)}(y-y_o)\right] \Big/ \sqrt{\epsilon_{m_y}^{(0)}} \tag{C-6b}$$

the corresponding eigenvalues are;

$$\alpha^{(\mu)}_{y,n_y} \equiv \frac{(n_y-1)\pi}{(y_{\mu+1}-y_\mu)} \tag{C-7a}$$

$$\alpha^{(0)}_{y,m_y} \equiv \frac{2(m_y-1)\pi}{(y_{\bar{\mu}}-y_o)} \tag{C-7b}$$

and:

$$\epsilon^{(\mu)}_{n_y} \equiv (1+\delta_{n_y,1})(y_{\mu+1}-y_\mu)/2 \tag{C-8a}$$

$$\epsilon^{(0)}_{m_y} \equiv (1+\delta_{m_y,1})(y_{\bar{\mu}}-y_o)/2 \tag{C-8b}$$

The Kronecker delta is defined by:

$$\delta_{m,n} \equiv \begin{cases} 1 & m = n \\ 0 & m \neq n \end{cases} \tag{C-9}$$

Integrals of products of the eigenfunctions are then:

$$\int_{y_\mu}^{y_{\mu+1}} \psi^{(\mu)}_{n_y}(y)\ \psi^{(\mu)}_{n'_y}(y)\,dy = \delta_{n_y,n'_y} \tag{C-10a}$$

$$\int_{y_o}^{y_{\bar{\mu}}} \psi^{(0)}_{m_y}(y)\ \psi^{(0)}_{m'_y}(y)\,dy = \delta_{m_y,m'_y} \tag{C-10b}$$

$$I^{(0\ \mu)}_{(m_y\ n_y)} \equiv \int_{y_\mu}^{y_{\mu+1}} \psi^{(0)}_{m_y}(y)\ \psi^{(\mu)}_{n_y}(y)\,dy \tag{C-11}$$

The Green's function for each region has been represented by an eigenfunction expansion also,

$$G^{(\mu)}(\vec{r}|\vec{r}') \equiv -\sum_{n_y=1} \psi^{(\mu)}_{n_y}(y)\ \psi^{(\mu)}_{n_y}(y') F^{(\mu)}_{n_y}(x|x') \tag{C-12a}$$

$$G^{(0)}(\vec{r}|\vec{r}') \equiv -\sum_{m_y=1} \psi^{(0)}_{m_y}(y)\ \psi^{(0)}_{m_y}(y)\ F^{(0)}_{m_y}(x|x') \tag{C-12b}$$

where

$$F^{(\mu)}_{n_y}(x|x') \equiv \begin{cases} \dfrac{\cos\left[\alpha^{(\mu)}_{x,n_y}(x-x_1)\right]\cos\left[\alpha^{(\mu)}_{x,n_y}(x_2-x') + \delta^{(\mu)}_{R\,x,n_y}\right]}{\alpha^{(\mu)}_{x,n_y}\,\Omega^{(\mu)}_{n_y}} & x<x' \\ \dfrac{\cos\left[\alpha^{(\mu)}_{x,n_y}(x'-x_1)\right]\cos\left[\alpha^{(\mu)}_{x,n_y}(x_2-x) + \delta^{(\mu)}_{R\,x,n_y}\right]}{\alpha^{(\mu)}_{x,n_y}\Omega^{(\mu)}_{n_y}} & x>x' \end{cases} \tag{C-13a}$$

$$F^{(0)}_{m_y}(x|x') \equiv \begin{cases} \dfrac{\cos\left[\alpha^{(0)}_{x,m_y}(x-x_o) + \delta^{(0)}_{L\,x,m_y}\right]\cos\left[\alpha^{(0)}_{x,m_y}(x_1-x')\right]}{\alpha^{(0)}_{x,m_y}\,\Omega^{(0)}_{m_y}} & x<x' \\ \dfrac{\cos\left[\alpha^{(0)}_{x,m_y}(x'-x_o) + \delta^{(0)}_{L\,x,m_y}\right]\cos\left[\alpha^{(0)}_{x,m_y}(x_1-x)\right]}{\alpha^{(0)}_{x,m_y}\,\Omega^{(0)}_{m_y}} & x>x' \end{cases} \tag{C-13b}$$

in which

$$\alpha^{(\mu)}_{x,n_y} \equiv \sqrt{k^2 - (\alpha^{(\mu)}_{y,n_y})^2} \qquad \text{(C-14a)}$$

$$\alpha^{(0)}_{x,m_y} \equiv \sqrt{k^2 - (\alpha^{(0)}_{y,m_y})^2} \qquad \text{(C-14b)}$$

and the finite admittance boundary conditions give:

$$\delta^{(\mu)}_{R\,x,n_y} \equiv \tan^{-1}\left(ik\beta_{x_2} \Big/ \alpha^{(\mu)}_{x,n_y} \right) \qquad \text{(C-15a)}$$

$$\delta^{(0)}_{L\,x,m_y} \equiv \tan^{-1}\left(ik\beta_{x_0} \Big/ \alpha^{(0)}_{x,m_y} \right) \qquad \text{(C-15b)}$$

Finally

$$\Gamma^{(\mu)}_{R\,n_y}(x) \equiv + \alpha^{(\mu)}_{x,n_y} \frac{\sin\left[\alpha^{(\mu)}_{x,n_y}(x_2-x) + \delta^{(\mu)}_{R\,x,n_y}\right]}{\cos\left[\alpha^{(\mu)}_{x,n_y}(x_2-x_1) + \delta^{(\mu)}_{R\,x,n_y}\right]} \qquad \text{(C-16a)}$$

$$\Gamma^{(0)}_{L\,m_y}(x) \equiv - \alpha^{(0)}_{x,m_y} \frac{\sin\left[\alpha^{(0)}_{x,m_y}(x-x_o) + \delta^{(0)}_{L\,x,m_y}\right]}{\cos\left[\alpha^{(0)}_{x,m_y}(x_1-x_o) + \delta^{(0)}_{L\,x,m_y}\right]} \qquad \text{(C-16b)}$$

and

$$B^{(0)(\ell)}_{m_y} \equiv \sum_{\mu=1}^{\bar{\mu}} \left\{ \sum_{n_y=1} (b^{(\mu)(\ell)}_{n_y}\ \Gamma^{(\mu)}_{R\,n_y}(x_1)\ \mathbf{I}^{(0)(\mu)}_{(m_y)(n_y)} \right\} \qquad \text{(C-17)}$$

Final Equations

When series expressions are used to represent the interface pressure profiles in both the main chamber and the baffle compartments, the iteration scheme proceeds as follows:

$$p^{(\mu)(\ell)}(x_1,y) = \sum_{n_y=1} b^{(\mu)(\ell)}_{n_y} \psi^{(\mu)}_{n_y}(y) \qquad \text{(C-18a)}$$

$$\frac{\partial p}{\partial x}^{(\mu)(\ell)}(x_1,y) = \sum_{n_y=1} \left(b_{n_y}^{(\mu)(\ell)} \Pi^{(\mu)}_{R\,n_y}(x_1) \right) \psi^{(\mu)}_{n_y}(y) \qquad \text{(C-18b)}$$

$$p^{(0)(\ell)}(x_1,y) = \sum_{m_y=1} \frac{B^{(0)(\ell)}_{m_y}}{\Pi^{(0)}_{L\,m_y}(X_1)} \psi^{(0)}_{m_y}(y)$$

$$\equiv \sum_{m_y=1} a^{(0)(\ell)}_{m_y} \psi^{(0)}_{m_y}(y) \qquad \text{(C-18c)}$$

$$\frac{\partial p}{\partial X}^{(0)(\ell)}(x_1,y) = \sum_{m_y=1} B^{(0)}_{m_y} \psi^{(0)}_{m_y}(y)$$

$$\equiv \sum_{m_y=1} \left(a^{(0)(\ell)}_{m_y} \Pi^{(0)}_{L\,m_y}(x_1) \right) \psi^{(0)}_{m_y}(y) \qquad \text{(C-18d)}$$

$$p^{(\mu)(\ell+1)}(x_1,y) \equiv \sum_{n_y=1} b_{n_y}^{(\mu)(\ell+1)} \psi_{n_y}^{(\mu)}(y)$$

$$= \sum_{n_y=1} \left(\sum_{m_y=1} a_{m_y}^{(0)(\ell)} I_{(n_y)}^{(0)\,m_y} \right) \psi_{n_y}^{(0)}(y) \qquad \text{(C-18e)}$$

With the same series expression representations, the general characteristic equation reduces to an algebraic equation which can be solved numerically, i.e.,

$$\sum_{m_y=1} \left(\left[a_{m_y}^{(0)(\ell)} \right]^2 \Gamma_{L\,m_y}^{(0)}(x_1) \right) - \sum_{\mu=1}^{\bar{\mu}} \left\{ \sum_{n_y=1} \left[b_{n_y}^{(\mu)(\ell)} \right]^2 \Gamma_{R\,n_y}^{(\mu)}(x_1) \right\} = 0 \qquad \text{(C-19)}$$

COMPUTER PROGRAMS

The computer programs used to solve for the fundamental acoustic modes of the two-dimensional baffled chamber with gain/loss end-wall boundary conditions are described in this section. The computer logic is illustrated by the flow chart shown in Fig. 13. All programs are written in GE-400 Series Fortran* using complex arithmetic. The individual programs, functions and relation to equations and lines in the program are detailed below.

B2D444 - Main Program (See Flowchart C-1)

This program is used to obtain the frequency and damping coefficient (eigenvalue) as well as the series expansion coefficients for the interface pressures and axial velocities for a particular two-dimensional baffled chamber with gain/loss end-wall boundary conditions. Complex quantities are noted. A full sample calculation is given at the end of this Appendix.

a. Input 1: Line 1240
   MUBAR = $\bar{\mu}$ = No. of baffle compartments
   YO = y_o
   YMUBAR= $y_{\bar{\mu}}$

b. Perform y Integration: Lines 1340-1760: Eq. C-11
   FINTTM(MUD,MYOD,NYUD) = $I_{\binom{m_y}{n_y}}^{\binom{0}{\mu}}$

c. Input 2: Line 1790
   XO = x_0
   Xl = x_1
   X2 = x_2
   BETAOP = $\beta_{x_{0+}}$ (Complex)
   BETA2L = $\beta_{x_{2-}}$ (Complex)

*CPB-1473, GE-400 Series Time-Sharing FORTRAN manual, General Electric Company, Information Systems Division, 13430 North Black Canyon Highway, Phoenix, Arizona, 1970.

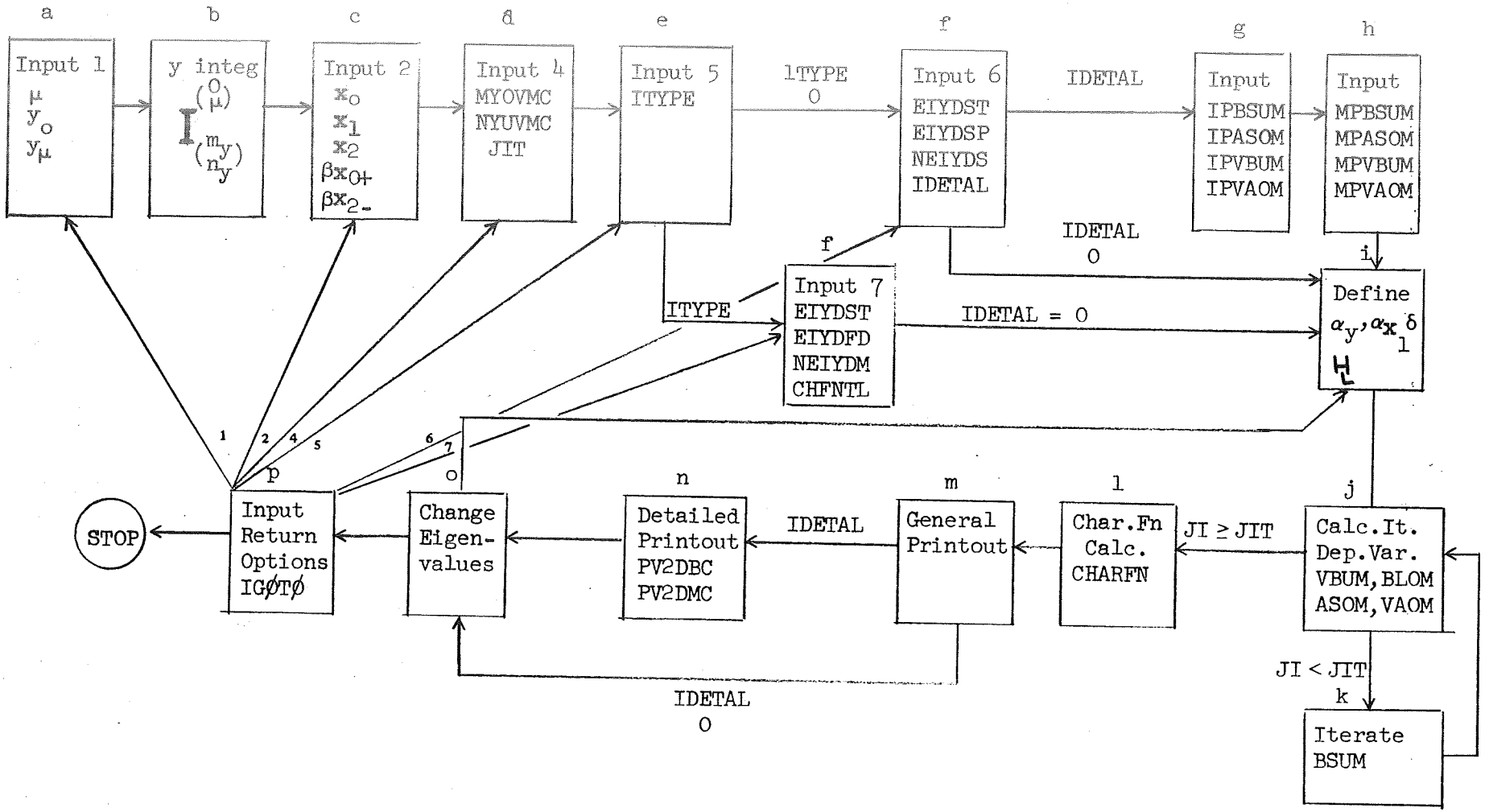

Figure 13. Flow Chart for Program to Analyze Two-Dimensional Baffled Chambers The Accompanying Description of the Computer Programs is Keyed to This Flowchart Through the Letters a...k.

d. Input 4: Line 1830

MYOVMC = No. of antisymmetric terms retained in main chamber series
NYUVMC = No. terms retained in baffle compartment series
JIT = No. iterations performed

e. Input 5: Line 1880

ITYPE = { 0 for step calculation of characteristic function
1 for root finding calculation of characteristic function

f. Input 6: Line 1910: (ITYPE = 0)

EIYDST = $k(y_{\bar{\mu}}-y_o)$ Initial guess (Complex)
EIYDSP = $k(y_{\bar{\mu}}-y_o)$ Increment (Complex)
NEIYDS = No. of calculations
IDETAL = { 0 for simple printout of characteristic function
1 for detailed printout of series expansion coefficients and pressure/axial velocity profiles

g. Input: Line 1950: (ITYPE = 0)(IDETAL = 1)

IPBSUM, IPASOM, IPVBUM, IPVAOM = 0 for no print, 1 for printout of

BSUM(MUD,NYUD) = $b_{n_y}^{(\mu)(\ell)}$
ASOM(MYOD) = $a_{m_y}^{(o)(\ell)}$
VBUM(MUD,NYUD) = $b_{n_y}^{(\mu)(\ell)} H_{n_y}^{(\mu)}(x_1)$
VAOM(MYOD) = $a_{m_y}^{(o)(\ell)} H_{m_y}^{(o)}(x_1)$

h. Input: Line No.: (ITYPE =0)(IDETAL = 1)

MPBSUM, MPASOM, MPVBUM, MPVAOM = 0 for no print, 1 for print of

$p^{(\mu)(\ell)}(x_1,y)$
$p^{(o)(\ell)}(x_1,y)$
$\partial p^{(\mu)(\ell)}(x_1,y)/\partial x$
$\partial p^{(o)(\ell)}(x_1,y)/\partial x$

f'. Input 7: Line 2000: (ITYPE = 1)

EIYDST = $k(y_{\bar{\mu}}-y_o)$ Initial guess (Complex)
EIYDFD = $k(y_{\bar{\mu}}-y_o)$ Finite difference (Complex)
NEIYDM = No. of Calculations
CHFNTL = Tolerance on characteristic function final value

i. Definition: Lines 2150-2730: Eqns. C-7a,b; C-14a,b; C-15a,b; C16a,b

JI	$= 0$	
AYOM(MYOD)	$\equiv \alpha^{(0)}_{y,m_y}$	
AXOV	$\equiv \alpha^{(0)}_{x,m_y}$	(Complex)
DELLOV	$\equiv \delta^{(0)}_{L x,m_y}$	(Complex)
HLOM(MYOD)	$\equiv H^{(0)}_{Lm_y}(x_1)$	(Complex)
BSUM(MUD,NYUD)	$\equiv b^{(\mu)(0)}_{n_y}$	(Complex)
AYUM(NYUD)	$\equiv \alpha^{(\mu)}_{y,n_y}$	(Complex)
AXUV	$\equiv \alpha^{(\mu)}_{x,n_y}$	
DELRUV	$\equiv \delta^{(\mu)}_{R x,n_y}$	(Complex)
HRUM(NYUD)	$\equiv H^{(\mu)}_{Rn_y}(x_1)$	(Complex)

j. Calculate Iteration Dependent Variables: Lines 2760-2950; Eqns. C-17, C-18

VBUM(MUD,NYUD)	$\equiv b^{(\mu)(\ell)}_{n_y} H^{(\mu)}_{Rn_y}(x_1)$	(Complex)
BLOM(MYOD)	$\equiv B^{(0)(\ell)}_{m_y}$	(Complex)
ASOM(MYOD)	$\equiv a^{(0)(\ell)}_{m_y}$	(Complex)
VAOM(MYOD)	$\equiv a^{(0)(\ell)}_{m_y} H^{(0)}_{Lm_y}(x_1)$	(Complex)

k. Perform Iteration: Lines 2960-3110: Eqn. C-18e

JI = JI +1

BSUM(MUD,NYUD) $\equiv b^{(\mu)(\ell+1)}_{n_y}$

l. Calculate Characteristic Function: Lines 3140-3320: Eq. C-19

$$\text{SUM1} = \sum_{m_y=1} \left(\left[a_{m_y}^{(0)(\ell)} \right]^2 H_{m_y}^{(0)} (x_1) \right) \qquad \text{(Complex)}$$

$$\text{SUM2} = \sum_{\mu=1}^{\bar{\mu}} \left\{ \sum_{n_y=1} \left(\left[b_{n_y}^{(\mu)(\ell)} \right] H_{n_y}^{(\mu)} (x_1) \right) \right. \qquad \text{(Complex)}$$

CHARFN = SUM1 - SUM2 (Complex)

m. General Printout: Line 3360

EIGNYD = $k(y_{\bar{\mu}} - y_o)$ (Complex)
SUM1 (Complex)
CHARFN (Complex)
SUM2 (Complex)

n. Detailed Printout: Lines 3390 - 3610
(According to Inputs g,h)
Calls PV2DBC, PV2DMC for pressure/axial velocity profiles

o. Increment Eigenvalue: Lines 3630 - 3950
ITYPE = 0 → EIGNYD = EIGNYD + ELYDSP (Complex)
ITYPE = 1 → EIGNYD = EIGNYD - $\dfrac{\text{CHAREN}}{\frac{d(\text{CHARFN})}{d(\text{EIGNYD})}}$ (Complex)

p. Return to Options: Lines 3970-4010

Input 1	IGØTO = 1
" 2	2
" 4	4
" 5	5
" 6	6
" 7	7

Subroutines

PV2DBC - Baffle Compartment Interface Pressure/Axial Velocity Profiles

This program takes coefficients of pressure/axial velocity series expressions and generates the appropriate profiles at the interface on the baffle compartment side.

a. Input: Line 5000 (Variable List)
   NYPNT = No. of equally spaced y points for printout
   IMUD = Compartment at which printout should stop
   (NYPNT = 0 for return to main program)

b. Printout: Line 5420: Eqn. C-5a
   Value of pressure or velocity at y location
   y Location
   Compartment number

PV2DMC - Main Chamber Interface Pressure/Axial Velocity Profiles

This program takes coefficients of pressure velocity series expressions and generates the appropriate profiles at the interface on the main chamber side.

a. Input: Line 6000 (Variable List)
   NYPNT = No. of equally spaced y points for printout
   YSTØP = y position at which printout should stop
   (NYPNT = 0 for return to main program)

b. Printout: Line 6320: Eq. C-5b
   Value of pressure or velocity at y location
   y location

B2D444

```
0100C TW0-DIMENSI0NAL BAFFLED CHAMBER MAIN PR0GRAM
1000 DIMENSI0N FINTTM(4,24,24)
1010&  ,AYOM(24),AYUM(24)
1020&  ,HLOM(24),HRUM(24)
1030&  ,ASOM(24),VAOM(24),BSUM(4,24),VBUM(4,24),BLOM(24)
1040 C0MM0N MUBAR,YD,YDU,AYOM,AYUM,PI
1050 C0MPLEX BETAOP,BETA2L,EIYDST,EIYDSP,EIYDFD,EIGNYD,EIYDOR,EYDOR2
1060&  ,AXOV,ARGO,RTARGO,DELLOV,CTANO,AXUV,ARGU,RTARGU,DELRUV,CTANU
1070&  ,HLOM,HLOV,HRUM,HRUV
1080&  ,ASOM,ASOV,ALUM,ALUV,VAOM,BSUM,BSUV,BLOM,BLOV,VBUM
1090&  ,TM,SERSUM,SUM1,SUM2,CHARFN,CHARFO,CHARFL,CHARFU
1100&  ,CHARFL,CHARFU,RTARGO,RTARGU
1110  11 F0RMAT(//"TW0-DIMENSI0NAL BAFFLED CHAMBER")
1120  12 F0RMAT(//T2,"MUBAR=",I2/
1130&  T4,"Y0=",F5.2,T17,"YMUBAR=",F5.2,T34,"X0=",F5.2,T47,"X1=",F5.2,
1140&  T60,"X2=",F5.2/
1150&  T11,"BETAOP=",2F5.2,T31,"BETA2L=",2F5.2)
1160  14 F0RMAT(/T2,"TRANSVERSE M0DE NUMBER",I3)
1170  16 F0RMAT(/T2,"MYOVMC=",I2/T2,"NYUVMC=",I2//T2,"JIT=",I2)
1180  18 F0RMAT(T16,"EIGNYD",T52,"SUM1"/T16,"CHARFN",T52,"SUM2")
1190  19 F0RMAT(T10,1PE16.10,",",1PE17.10)
1200  20 F0RMAT(2(1PE16.10,",",1PE16.10," :",1PE16.10,",",1PE16.10/))
1210 PI=3.1415926536
1220C MUBAR IS THE NUMBER 0F C0MPARTMENTS
1230  1001 PRINT," 1 INPUT:MUBAR,Y0,YMUBAR"
1240 INPUT,MUBAR,Y0,YMUBAR
1250 IF(MUBAR.LT.5)  G0 T0 10015
1260 PRINT,↑,"MUBAR MUST BE LESS THAN 5--TRY AGAIN"
1270 G0 T0 1001
1280  10015 C0NTINUE
1290 FMUBAR=FL0AT(MUBAR)
1300 YD=YMUBAR-Y0
1310 YD2=YD**2
1320 YDU=YD/FMUBAR
1330C
1340C Y INTEGRAL CALCULATI0N
1350C
1360 MYOINT=24
1370 NYUINT=24
1380 D0 910 MUD=1,MUBAR
1390 FINTTM(MUD,1,1)=1.0/SQRT(FMUBAR)
1400 D0 901 NYUD=2,NYUINT
1410 FINTTM(MUD,1,NYUD)=0.0
1420  901 C0NTINUE
1430 FMUD=FL0AT(MUD)
1440 YUL0=YDU*(FMUD-1.0)
1450 YUP1L0=YDU*FMUD
1460 D0 904 MYOD=2,MYOINT
1470 FMYOD=FL0AT(MYOD)
1480     FMYOD=2.0*(FMYOD-1.0)
```

B2D444 CØNTINUED

```
1490 ALYOV=(FMYOD-1.0)*PI/YD
1500 ARGUU=ALYOV*YULO
1510 ARGUP1=ALYOV*YUP1LO
1520 C=(SQRT(2.0*FMUBAR))/(ALYOV*YD)
1530 FVALUE=C*(SIN(ARGUP1)-SIN(ARGUU))
1540 IF((ABS(FVALUE)).LT.(1.0E-6))  FVALUE=0.0
1550 FINTTM(MUD,MYOD,1)=FVALUE
1560  DØ 903 NYUD=2,NYUINT
1570  FNYUD=FLØAT(NYUD)
1580  ALYUV=(FNYUD-1.0)*PI/YDU
1590  ALYDIF=ABS(ALYOV-ALYUV)
1600  IF(ALYDIF.LT.(1.0E-6))  GØ TØ 902
1610  C=(ALYOV/(ALYOV**2-ALYUV**2))*SQRT(FMUBAR)*2.0/YD
1620  AC=(FNYUD-1.0)*PI
1630 FVALUE=C*(CØS(AC)*SIN(ARGUP1)-SIN(ARGUU))
1640 IF((ABS(FVALUE)).LT.(1.0E-6))  FVALUE=0.0
1650 FINTTM(MUD,MYOD,NYUD)=FVALUE
1660  GØ TØ 903
1670  902 CØNTINUE
1680  C=1.0/SQRT(FMUBAR)
1690 FVALUE=C*CØS(ARGUU)
1700 IF((ABS(FVALUE)).LT.(1.0E-6))  FVALUE=0.0
1710 FINTTM(MUD,MYOD,NYUD)=FVALUE
1720  903 CØNTINUE
1730 904 CØNTINUE
1740 910 CØNTINUE
1750C
1760C END Y INTEGRAL CALCULATIØN
1770C
1780 1002 PRINT,'' 2 INPUT:X0,X1,X2,BETAOP,BETA2L''
1790 INPUT,X0,X1,X2,BETAOP,BETA2L
1800 1003 CØNTINUE
1810 NMØDE=1
1820 1004 PRINT,'' 4 INPUT:MYOVMC,NYUVMC,JIT''
1830 INPUT,MYOVMC,NYUVMC,JIT
1840 IF((MYOVMC.LE.MYOINT).AND.(NYUVMC.LE.NYUINT))  GØ TØ 1005
1850 PRINT,↑,''MYOVMC & NYUVMC MUST BE LESS THAN 25--TRY AGAIN''
1860 GØ TØ 1004
1870 1005 PRINT,'' 5 INPUT:ITYPE''
1880 INPUT,ITYPE
1890 IDETAL=0
1900 IF(ITYPE)  9999,1006,1007
1910 1006 PRINT,'' 6 INPUT:EIYDST,EIYDSP,NEIYDS,IDETAL''
1920 INPUT,EIYDST,EIYDSP,NEIYDS,IDETAL
1930 IF(IDETAL.NE.1)  GØ TØ 1008
1940 PRINT,''   INPUT:IPBSUM,IPASOM,IPVBUM,IPVAOM''
1950 INPUT,IPBSUM,IPASOM,IPVBUM,IPVAOM
1960 PRINT,''   INPUT:MPBSUM,MPASOM,MPVBUM,MPVAOM''
1970 INPUT,MPBSUM,MPASOM,MPVBUM,MPVAOM
1980 GØ TØ 1008
```

B2D444 CØNTINUED

```
1990  1007 PRINT,"  7 INPUT:EIYDST,EIYDFD,NEIYDM,CHFNTL"
2000  INPUT,EIYDST,EIYDFD,NEIYDM,CHFNTL
2010  1008 CØNTINUE
2020C
2030C PRINT INPUT
2040C
2050  PRINT 11
2060  PRINT 12,MUBAR,YO,YMUBAR,XO,X1,X2,BETAOP,BETA2L
2070  PRINT 14,NMØDE
2080  PRINT 16,MYOVMC,NYUVMC,JIT
2090  PRINT 18
2100  NEIYDD=0
2110  NCNTRL=-2
2120  EIGNYD=EIYDST
2130  1 CØNTINUE
2140C
2150C DEFINITIØNS
2160C
2170  JI=0
2180  EIYDOR=EIGNYD/YD
2190  EYDOR2=EIYDOR**2
2200  AYOM(1)=0.0
2210  AYUM(1)=0.0
2220     DØ 30 MYOD=2,MYOVMC
2230  FMYOD=FLØAT(MYOD)
2240     FMYOD=2.0*(FMYOD-1.0)
2250  AYOV=(FMYOD-1.0)*PI/YD
2260  AYOM(MYOD)=AYOV
2270  AYOV2=AYOV**2
2280  RTARGO=EYDOR2-AYOV2
2290  AXOV=CSQRT(RTARGO)
2300  ARGO=AXOV*(X1-XO)
2310  DELLOV=(0.0,1.0)*EIYDOR*BETAOP/AXOV
2320  CTANO=CSIN(ARGO)/CCØS(ARGO)
2330  HLOV=-AXOV*(CTANO+DELLOV)/(1.0-DELLOV*CTANO)
2340  HLOM(MYOD)=HLOV
2350  30 CØNTINUE
2360  HLOM(1)=0.0
2370  DØ 32 MUD=1,MUBAR
2380  DØ 31 NYUD=1,NYUVMC
2390  BSUM(MUD,NYUD)=0.0
2400  31 CØNTINUE
2410  32 CØNTINUE
2420  IF(MUBAR.NE.1)  GØ TØ 33
2430  BSUM(1,2)=1.0
2440  GØ TØ 39
2450  33 IF(MUBAR.NE.2)  GØ TØ 34
2460  BSUM(1,1)=+1.0
2470  BSUM(2,1)=-1.0
2480  GØ TØ 39
```

B2D444 CONTINUED

```
2490  34 IF(MUBAR.NE.3)  GO TO 35
2500 BSUM(1,1)=+1.0
2510 BSUM(2,1)= 0.0
2520 BSUM(3,1)=-1.0
2530 GO TO 39
2540  35 IF(MUBAR.NE.4)  GO TO 36
2550 BSUM(1,1)=+1.0
2560 BSUM(2,1)=+0.5
2570 BSUM(3,1)=-0.5
2580 BSUM(4,1)=-1.0
2590  36 CONTINUE
2600  39 CONTINUE
2610 DO 40 NYUD=1,NYUVMC
2620 FNYUD=FLOAT(NYUD)
2630 AYUV=(FNYUD-1.0)*PI/YDU
2640 AYUM(NYUD)=AYUV
2650 AYUV2=AYUV**2
2660 RTARGU=EYDOR2-AYUV2
2670 AXUV=CSQRT(RTARGU)
2680 ARGU=AXUV*(X2-X1)
2690 DELRUV=(0.0,1.0)*EIYDOR*BETA2L/AXUV
2700 CTANU=CSIN(ARGU)/CCOS(ARGU)
2710 HRUV=AXUV*(CTANU+DELRUV)/(1.0-DELRUV*CTANU)
2720 HRUM(NYUD)=HRUV
2730  40 CONTINUE
2740  45 CONTINUE
2750C
2760C BLOM CALCULATION
2770C
2780     DO 90 MYOD=2,MYOVMC
2790 SERSUM=0.0
2800 DO 80 MUD=1,MUBAR
2810 DO 60 NYUD=1,NYUVMC
2820 TM=BSUM(MUD,NYUD)*HRUM(NYUD)
2830 VBUM(MUD,NYUD)=TM
2840 TM=TM*FINTTM(MUD,MYOD,NYUD)
2850 SERSUM=SERSUM+TM
2860  60 CONTINUE
2870  80 CONTINUE
2880 BLOM(MYOD)=SERSUM
2890 VAOM(MYOD)=SERSUM
2900 ASOM(MYOD)=SERSUM/HLOM(MYOD)
2910  90 CONTINUE
2920 BLOM(1)=0.0
2930 VAOM(1)=0.0
2940 ASOM(1)=0.0
2950 IF(JI.EQ.JIT)  GO TO 150
2960 JI=JI+1
2970C
2980C ITERATION EQUATION CALCULATION
```

B2D444 CØNTINUED

```
2990C
3000 DØ 140 MUD=1,MUBAR
3010 DØ 120 NYUD=1,NYUVMC
3020 SERSUM=0.0
3030    DØ 110 MYOD=2,MYOVMC
3040 TM=ASOM(MYOD)
3050 TM=TM*FINTTM(MUD,MYOD,NYUD)
3060 SERSUM=SERSUM+TM
3070 110 CØNTINUE
3080 BSUM(MUD,NYUD)=SERSUM
3090 120 CØNTINUE
3100 140 CØNTINUE
3110 GØ TØ 45
3120 150 CØNTINUE
3130C
3140C CHARACTERISTIC EQUATIØN CALCULATIØN
3150C
3160 SERSUM=0.0
3170    DØ 170 MYOD=2,MYOVMC
3180 ASOV=ASOM(MYOD)
3190 TM=(ASOV**2)*HLOM(MYOD)
3200 SERSUM=SERSUM+TM
3210 170 CØNTINUE
3220 SUM1=SERSUM
3230 SERSUM=0.0
3240 DØ 200 MUD=1,MUBAR
3250 DØ 190 NYUD=1,NYUVMC
3260 BSUV=BSUM(MUD,NYUD)
3270 TM=(BSUV**2)*HRUM(NYUD)
3280 SERSUM=SERSUM+TM
3290 190 CØNTINUE
3300 200 CØNTINUE
3310 SUM2=SERSUM
3320 CHARFN=SUM1-SUM2
3330C
3340C GENERAL PRINTØUT
3350C
3360 IF(NCNTRL.EQ.-2)  PRINT 20,EIGNYD,SUM1,CHARFN,SUM2
3370 IF(IDETAL.NE.1)  GØ TØ 260
3380C
3390C DETAILED PRINTØUT--BSUM,ASOM,VBUM,VAOM
3400C
3410 IF((IPBSUM+MPBSUM).NE.0)  PRINT,↑2,"BSUM",↑
3420 IF(IPBSUM.NE.1)  GØ TØ 241
3430 PRINT 19,((BSUM(MD,NY),MD=1,MUBAR),NY=1,NYUVMC)
3440 241 CØNTINUE
3450 IF(MPBSUM.EQ.1)  CALL PV2DBC(BSUM,NYUVMC)
3460 IF((IPASOM+MPASOM).NE.0)  PRINT,↑2,"ASOM",↑
3470 IF(IPASOM.NE.1)  GØ TØ 243
3480 PRINT 19,(ASOM(MY),MY=1,MYOVMC)
```

B2D444 CØNTINUED

```
3490 243 CØNTINUE
3500 IF(MPASOM.EQ.1)  CALL PV2DMC(ASOM,MYOVMC)
3510 IF((IPVBUM+MPVBUM).NE.0)  PRINT,↑2,"VBUM",↑
3520 IF(IPVBUM.NE.1)  GØ TØ 245
3530 PRINT 19,((VBUM(MD,NY),MD=1,MUBAR),NY=1,NYUVMC)
3540 245 CØNTINUE
3550 IF(MPVBUM.EQ.1)  CALL PV2DBC(VBUM,NYUVMC)
3560 IF((IPVAOM+MPVAOM).NE.0)  PRINT,↑2,"VAOM",↑
3570 IF(IPVAOM.NE.1)  GØ TØ 247
3580 PRINT 19,(VAOM(MY),MY=1,MYOVMC)
3590 247 CØNTINUE
3600 IF(MPVAOM.EQ.1)  CALL PV2DMC(VAOM,MYOVMC)
3610 260 CØNTINUE
3620C
3630C CHANGE EIGNYD--STEP CHANGE ØR RØØT FINDER
3640C
3650 NEIYDD=NEIYDD+1
3660 IF(ITYPE.EQ.1)  GØ TØ 300
3670 EIGNYD=EIGNYD+EIYDSP
3680 IF(NEIYDD.LT.NEIYDS)  GØ TØ 1
3690 GØ TØ 1009
3700 300 CØNTINUE
3710 EIYDFR=EIYDFD
3720 EIYDFI=-(0.0,1.0)*EIYDFD
3730 IF(ABS(EIYDFR).GT.(1.0E-10))  GØ TØ 301
3740 CHARFI=-(0.0,1.0)*CHARFN
3750 CHARFN=+(0.0,1.0)*CHARFI
3760 GØ TØ 302
3770 301 CØNTINUE
3780 IF(ABS(EIYDFI).GT.(1.0E-10))  GØ TØ 302
3790 CHARFR=CHARFN
3800 CHARFN=CHARFR
3810 302 CØNTINUE
3820 NCNTRL=NCNTRL+1
3830 IF(NCNTRL)  310,320,330
3840 310 CHARFØ=CHARFN
3850 IF((CABS(CHARFØ).LT.CHFNTL).ØR.(NEIYDD.GT.NEIYDM))  GØ TØ 1009
3860 EIGNYD=EIGNYD-EIYDFD/2.0
3870 GØ TØ 1
3880 320 CHARFL=CHARFN
3890 EIGNYD=EIGNYD+EIYDFD
3900 GØ TØ 1
3910 330 CHARFU=CHARFN
3920 EIGNYD=EIGNYD-EIYDFD/2.0-CHARFØ*EIYDFD/(CHARFU-CHARFL)
3930 NCNTRL=-2
3940 GØ TØ 1
3950 1009 PRINT,↑2,↑2
3960C
3970C WHERE TØ GØ?
3980C
```

B2D444 CØNTINUED

```
3990 PRINT,"   INPUT:IGØTØ"
4000 INPUT,IGØTØ
4010 GØ TØ (1001,1002,1003,1004,1005,1006,1007,1008,9999),IGØTØ
4020 9999 STØP
4030 END
```

PV2DBC

```
5000 SUBR0UTINE PV2DBC(C0EF,NYUVMC)
5010 DIMENSI0N C0EF(4,24),AY0M(24),AYUM(24),EPSM(24),PVVAL(50),YVAL(50)
5020& ,MUDM(50)
5030 C0MM0N MUBAR,YD,YDU,AY0M,AYUM,PI
5040 C0MPLEX C0EF
5050 15 F0RMAT(/5X,"Y-VARIATI0N")
5060 10 F0RMAT(2X,1P2E17.10,I10)
5070 YDU02=YDU/2.0
5080 D0 100 NYUD=2,NYUVMC
5090 EPSM(NYUD)=SQRT(YDU02)
5100 100 C0NTINUE
5110 EPSM(1)=SQRT(YDU)
5120 1 C0NTINUE
5130 PRINT,↑2," INPUT:NYPNT,IMUD",↑*
5140 INPUT,NYPNT,IMUD
5150 IF(NYPNT.EQ.0)  RETURN
5160 YINC=YD/NYPNT
5170 NYPNT1=NYPNT+1
5180 YDUSVE=YDU
5190 YDU=YDU+1.0E-6
5200 YP0S=0.0
5210 D0 500 NYD=1,NYPNT1
5220 IF((YP0S.GE.(0.0)).AND.(YP0S.LE.YDU))  MUD=1
5230 IF((YP0S.GT.YDU).AND.(YP0S.LE.(2.0*YDU)))  MUD=2
5240 IF((YP0S.GT.(2.0*YDU)).AND.(YP0S.LE.(3.0*YDU)))  MUD=3
5250 IF((YP0S.GT.(3.0*YDU)).AND.(YP0S.LE.(4.0*YDU)))  MUD=4
5260 MUDM(NYD)=MUD
5270 FMUD=FL0AT(MUD)
5280 SUM=0.0
5290 D0 400 NYUD=1,NYUVMC
5300 TM=(C0S(AYUM(NYUD)*(YP0S-(FMUD-1.0)*YDU)))/EPSM(NYUD)
5310 SUM=SUM+TM*C0EF(MUD,NYUD)
5320 400 C0NTINUE
5330 PVVAL(NYD)=SUM
5340 YVAL(NYD)=YP0S
5350 YP0S=YP0S+YINC
5360 NYMAX=NYD
5370 IF(MUD.EQ.IMUD)  G0 T0 600
5380 500 C0NTINUE
5390 600 C0NTINUE
5400 YDU=YDUSVE
5410 PRINT 15
5420 PRINT 10,(PVVAL(NYD),YVAL(NYD),MUDM(NYD),NYD=1,NYMAX)
5430 G0 T0 1
5440 END
```

PV2DMC

```
6000 SUBR0UTINE PV2DMC(C0EF,MY0VMC)
6010 DIMENSI0N C0EF(24),AY0M(24),AYUM(24),EPSM(24),PVVAL(50),YVAL(50)
6020 C0MM0N MUBAR,YD,YDU,AY0M,AYUM,PI
6030 C0MPLEX C0EF
6040 15 F0RMAT(/5X,"Y-VARIATI0N")
6050 10 F0RMAT(2X,1P2E17.10)
6060 YD02=YD/2.0
6070 D0 100 MY0D=1,MY0VMC
6080 EPSM(MY0D)=SQRT(YD02)
6090 100 C0NTINUE
6100 EPSM(1)=SQRT(YD)
6110 1 C0NTINUE
6120 PRINT,↑2,"                          INPUT:NYPNT,YST0P",↑*
6130 INPUT,NYPNT,YST0P
6140 IF(NYPNT.EQ.0)  RETURN
6150 YINC=YD/NYPNT
6160 NYPNT1=NYPNT+1
6170 YP0S=0.0
6180 D0 500 NYD=1,NYPNT1
6190 SUM=0.0
6200 D0 400 MY0D=1,MY0VMC
6210 TM=(C0S(AY0M(MY0D)*YP0S))/EPSM(MY0D)
6220 SUM=SUM+TM*C0EF(MY0D)
6230 400 C0NTINUE
6240 PVVAL(NYD)=SUM
6250 YVAL(NYD)=YP0S
6260 YP0S=YP0S+YINC
6270 NYMAX=NYD
6280 IF(YP0S.GT.YST0P)  G0 T0 600
6290 500 C0NTINUE
6300 600 C0NTINUE
6310 PRINT 15
6320 PRINT 10,(PVVAL(NYD),YVAL(NYD),NYD=1,NYMAX)
6330 G0 T0 1
6340 END
```

```
B2D444     20:49  NAR  JAN. 12,1971


 1 INPUT:MUBAR,YO,YMUBAR
 ?2,0.0,20.0

 2 INPUT:X0,X1,X2,BETAOP,BETA2L
 ?0.0,22.0,30.0,0.0,0.0,0.0,0.0

 4 INPUT:MYOVMC,NYUVMC,JIT
 ?9,11,9

 5 INPUT:ITYPE
 ?0

 6 INPUT:EIYDST,EIYDSP,NEIYDS,IDETAL
 ?2.10,0.00,0.10,0.00,5,0


TWO-DIMENSIONAL BAFFLED CHAMBER


 MUBAR= 2
   YO= 0.00      YMUBAR=20.00      X0= 0.00      X1=22.00      X2=30.00
          BETAOP= 0.00 0.00    BETA2L= 0.00 0.00

 TRANSVERSE MODE NUMBER  1

 MYOVMC= 9
 NYUVMC=11

 JIT= 9
                EIGNYD                                   SUM1
                CHARFN                                   SUM2
 2.100000000E+00, 0.000000000E+00 : 6.538184205E-04,-2.027816548E-15
 1.332115098E-03,-7.933974209E-15 :-6.782966779E-04, 5.906157662E-15

 2.200000000E+00, 0.000000000E+00 : 9.940097568E-04, 8.873427550E-14
 1.507850295E-03,-4.960516071E-14 :-5.138405381E-04, 1.383394362E-13

 2.300000000E+00, 0.000000000E+00 : 1.622256384E-02, 6.630450630E-12
-9.606727823E-04,-8.554863378E-13 : 1.718323662E-02, 7.485936967E-12

 2.400000000E+00, 0.000000000E+00 : 1.173579350E+00, 4.920248138E-10
 5.936791142E-02, 4.881326962E-11 : 1.114211438E+00, 4.432115441E-10

 2.500000000E+00, 0.000000000E+00 : 1.033172516E+02, 4.197352154E-08
 2.526114527E+01, 1.194714700E-08 : 7.805610635E+01, 3.002637454E-08



   INPUT:IGOTO
 ?5
```

typical run

a. find region of root

```
 5 INPUT:ITYPE
 ?1

 7 INPUT:EIYDST,EIYDFD,NEIYDM,CHFNTL
 ?2.40,0.00,1.0E-5,0.00,20,1.0E-6
```

b. find root precisely

```
TWØ-DIMENSIØNAL BAFFLED CHAMBER


 MUBAR= 2
   YØ= 0.00      YMUBAR=20.00      XØ= 0.00      X1=22.00      X2=30.00
          BETAØP= 0.00 0.00    BETA2L= 0.00 0.00

 TRANSVERSE MØDE NUMBER  1

 MYOVMC= 9
 NYUVMC=11

 JIT= 9
                EIGNYD                                        SUM1
                CHARFN                                        SUM2
 2.400000000E+00, 0.000000000E+00 : 1.173579351E+00, 4.920248144E-10
 5.936791161E-02, 4.881326972E-11 : 1.114211440E+00, 4.432115447E-10

 2.388201239E+00, 0.000000000E+00 : 6.999842057E-01, 2.944444864E-10
 1.833588810E-02, 2.204684692E-11 : 6.816483176E-01, 2.723976395E-10

 2.380035851E+00, 0.000000000E+00 : 4.901332498E-01, 2.066040718E-10
 4.618831696E-03, 1.191939794E-11 : 4.855144181E-01, 1.946846739E-10

 2.376193064E+00, 0.000000000E+00 : 4.146003601E-01, 1.749232594E-10
 6.675558889E-04, 8.659428914E-12 : 4.139328042E-01, 1.662638305E-10

 2.375424204E+00, 0.000000000E+00 : 4.009582986E-01, 1.691969568E-10
 2.223936644E-05, 8.097440466E-12 : 4.009360593E-01, 1.610995163E-10

 2.375396778E+00, 0.000000000E+00 : 4.004801120E-01, 1.689962101E-10
 2.728484105E-08, 8.077901597E-12 : 4.004800847E-01, 1.609183085E-10




   INPUT:IGØTØ
 ?5
```

```
 5 INPUT:ITYPE
?0

 6 INPUT:EIYDST,EIYDSP,NEIYDS,IDETAL
?2.375396778,0.00,0.00,0.00,1,1

   INPUT:IPBSUM,IPASOM,IPVBUM,IPVAOM
?1,1,0,0

   INPUT:MPBSUM,MPASOM,MPVBUM,MPVAOM
?1,1,0,0


TWØ-DIMENSIØNAL BAFFLED CHAMBER


 MUBAR= 2
   YØ= 0.00      YMUBAR=20.00      XØ= 0.00      X1=22.00      X2=30.00
          BETAØP= 0.00 0.00    BETA2L= 0.00 0.00

 TRANSVERSE MØDE NUMBER  1

 MYOVMC= 9
 NYUVMC=11

 JIT= 9
                EIGNYD                                    SUM1
                CHARFN                                    SUM2
2.375396778E+00, 0.000000000E+00 : 4.004801153E-01, 1.689962115E-10
2.743217919E-08, 8.077901728E-12 : 4.004800879E-01, 1.609183098E-10
```

c. check pressure match

BSUM

1.277951188E+00,	2.514920637E-10
-1.277951188E+00,	-2.514920637E-10
4.081312083E-01,	7.583562193E-11
4.081312083E-01,	7.583562194E-11
-1.156411098E-01,	-2.504733347E-11
1.156411098E-01,	2.504733348E-11
6.061904496E-02,	1.385767124E-11
6.061904497E-02,	1.385767124E-11
-4.094246570E-02,	-9.344819151E-12
4.094246571E-02,	9.344819153E-12
3.196590077E-02,	7.077730648E-12
3.196590078E-02,	7.077730649E-12
-2.782020370E-02,	-5.859892587E-12
2.782020371E-02,	5.859892588E-12
2.725257004E-02,	5.348733180E-12
2.725257005E-02,	5.348733182E-12
-3.578051283E-02,	-6.240244326E-12
3.578051283E-02,	6.240244326E-12
2.044916720E-02,	3.727408854E-12
2.044916720E-02,	3.727408854E-12
-1.491370772E-02,	-2.759161578E-12
1.491370772E-02,	2.759161578E-12

INPUT:NYPNT,IMUD ?40,2

Y-VARIATIØN	y	compartment
5.442445646E-01	0.000000000E+00	1
5.493694995E-01	5.000000000E-01	1
5.537478926E-01	1.000000000E+00	1
5.447328838E-01	1.500000000E+00	1
5.300293430E-01	2.000000000E+00	1
5.213012483E-01	2.500000000E+00	1
5.142940501E-01	3.000000000E+00	1
5.012466743E-01	3.500000000E+00	1
4.844678147E-01	4.000000000E+00	1
4.653907526E-01	4.500000000E+00	1
4.406395530E-01	5.000000000E+00	1
4.163369593E-01	5.500000000E+00	1
4.010044394E-01	6.000000000E+00	1
3.813387165E-01	6.500000000E+00	1
3.388607584E-01	7.000000000E+00	1
2.915630414E-01	7.500000000E+00	1
2.727839578E-01	8.000000000E+00	1
2.635908060E-01	8.500000000E+00	1
2.064240570E-01	9.000000000E+00	1
1.063659120E-01	9.500000000E+00	1
5.372469061E-02	1.000000000E+01	1
-1.063657243E-01	1.050000000E+01	2

$p^{(\mu)(\ell)}(x_1, y)$

INPUT:NYPNT,IMUD ?0,0

ASOM

```
 0.000000000E+00,  0.000000000E+00
 1.831161819E+00,  4.100003583E-10
-2.940898642E-01, -5.471580740E-11
 1.257997906E-01,  2.459738929E-11
-6.966633611E-02, -1.465313026E-11
 4.431154790E-02,  1.001758054E-11
-3.072577357E-02, -7.451021271E-12
 2.261126912E-02,  5.882380959E-12
-1.739102532E-02, -4.872570233E-12
```

INPUT:NYPNT,YSTØP ?40,10.5

Y-VARIATIØN	y
5.097627726E-01	0.000000000E+00
5.107949396E-01	5.000000000E-01
5.115545910E-01	1.000000000E+00
5.082151431E-01	1.500000000E+00
5.007195133E-01	2.000000000E+00
4.929538260E-01	2.500000000E+00
4.874320315E-01	3.000000000E+00
4.816005292E-01	3.500000000E+00
4.710032229E-01	4.000000000E+00
4.553786531E-01	4.500000000E+00
4.393472389E-01	5.000000000E+00
4.260958345E-01	5.500000000E+00
4.121359943E-01	6.000000000E+00
3.908134006E-01	6.500000000E+00
3.610550300E-01	7.000000000E+00
3.296526929E-01	7.500000000E+00
3.018264907E-01	8.000000000E+00
2.697747091E-01	8.500000000E+00
2.142618485E-01	9.000000000E+00
1.215439983E-01	9.500000000E+00
2.231841144E-11	1.000000000E+01
-1.215439982E-01	1.050000000E+01

$p^{(0)(l)}(x_1, y)$

INPUT:NYPNT,YSTØP ?0,0.

INPUT:IGØTØ
?S

RUNNING TIME: 93.9 SECS I/Ø TIME : 22.5 SECS

APPENDIX D

THREE DIMENSIONAL BAFFLED CHAMBERS

This Appendix details the equations, logic and computer programs which were developed to describe three-dimensional baffled thrust chambers with non-zero end-wall admittance boundary conditions. The rigid wall case is obtained by simply equating these admittance values to zero.

Also included in this Appendix is a listing of the main computer program and the auxiliary programs used for generating pressure and velocity distribution programs used for generating input files. The necessary Bessel function sub-routines are also included. Finally, a sample calculation is included for a rigid end-wall chamber containing a three-bladed baffle.

To simplify the computer operations, the mathematical notation used here and in Appendix C is different from that used in the main text. A separate table of nomenclature for Appendices C and D is included at the end of this Appendix, which also shows the relationships between the nomenclature used in the text and in the appendices.

This Appendix is written so that it may be used independently of Appendix C and is therefore somewhat redundant.

General Equations

The general characteristic equation derived from the variational method for the three-dimensional baffled chamber shown in Fig. 2 is

$$\int_0^{2\pi}\int_0^{r_1} (p^{(0)}-p^{(\mu)}) \frac{\partial p^{(\mu)}}{\partial z} \, r dr d\theta = 0 \quad \text{at} \quad z = z_1 \tag{D-1}$$

Again it may be noted that this is simply an equation for conservation of the energy flux across the interface between the main chamber and the baffle compartments for the rigid-wall case. Corresponding to any pressure gradient at the interface, the pressures in the different regions are given by the integral equations, i.e.,

$$p^{(\mu)}(r,\theta,z) = -\int_{\theta_\mu}^{\theta_{\mu+1}}\int_0^{r_1} G^{(\mu)}(r,\theta,z|r',\theta',z_1) \frac{\partial p^{(\mu)}}{\partial z'}(r',\theta',z_1) r'dr'd\theta' \tag{D-2a}$$

$$p^{(0)}(r,\theta,z) = +\int_0^{2\pi}\int_0^{r_1} G^{(0)}(r,\theta,z|r',\theta',z_1) \frac{\partial p^{(\mu)}}{\partial z'}(r',\theta',z_1) r'dr'd\theta' \tag{D-2b}$$

where $G^{(\mu)}$ and $G^{(0)}$ are the Green's functions in the μ^{th} baffle compartment and the main chamber, respectively. The pressures obtained from Eq. D-2a and D-2b are not equal at the interface unless the pressure gradient at the interface used in these equations corresponds to the exact solution of the wave equation and the appropriate boundary conditions.

Because the exact solution is unknown at the outset, an initial form for this pressure gradient is assumed and an iteration scheme is then used to improve the accuracy of the initial form. This iteration scheme proceeds as follows.

First, some form is assumed for the pressure gradient at the interface:

$$\frac{\partial p^{(\mu)(\ell)}(r,\theta,z_1)}{\partial z}$$

Then the above integral equations are used to obtain $p^{(\mu)(\ell)}(r,\theta,z)$ and $p^{(0)(\ell)}(r,\theta,z)$ directly. Since, for the exact solution, the pressures must match identically at the interface ($z = z_1$), a new approximation for the baffle compartment pressure profile at the interface is obtained by equating the pressures:

$$p^{(\mu)(\ell+1)}(r,\theta,z_1) = p^{(0)(\ell)}(r,\theta,z_1) \qquad \text{(D-4)}$$

A new pressure gradient is then obtained by differentiating the corresponding integral equation and the iteration sequence is complete. The iteration may be repeated as many times as desired.

Assumptions and Definitions

The assumptions and definitions used to obtain the algebraic forms of the iteration and characteristic equations are presented here for reference. The ℓ^{th} approximation to the pressure profile on either side of the interface (at the interface) is assumed to be represented by an eigenfunction expansion, i.e.,

$$p^{(\mu)(\ell)}(r,\theta,z_1) \equiv \sum_{n_\theta=1} \sum_{n_r=1} b^{(\mu)(\ell)}_{n_\theta,n_r} \psi^{(\mu)}_{n_\theta,n_r}(r,\theta) \qquad \text{(D-5a)}$$

$$p^{(0)(\ell)}(r,\theta,z_1) \equiv \sum_{m_\theta=1} \sum_{m_r=1} a^{(0)(\ell)}_{m_\theta,m_r} \psi^{(0)}_{m_\theta,m_r}(r,\theta) \qquad \text{(D-5b)}$$

where the orthonormal eigenfunctions are

$$\psi^{(\mu)}_{n_\theta,n_r}(r,\theta) = J^{(\mu)}_{\alpha_\theta,n_\theta}(\alpha^{(\mu)}_{r,n_\theta,n_r} r)\cos(\alpha^{(\mu)}_{\theta,n_\theta}\theta)/[\Lambda^{(\mu)}_{n_\theta,n_r}\epsilon^{(\mu)}_{n_\theta}]^{\frac{1}{2}} \tag{D-6a}$$

$$\psi^{(0)}_{m_\theta,m_r}(r,\theta) = J^{(0)}_{\alpha_\theta,m_\theta}(\alpha^{(0)}_{r,m_\theta,m_r} r)\cos(\alpha^{(0)}_{\theta,m_\theta}\theta)/[\Lambda^{(0)}_{m_\theta,m_r}\epsilon^{(0)}_{m_\theta}]^{\frac{1}{2}} \tag{D-6b}$$

the corresponding eigenvalues are

$$\alpha^{(\mu)}_{\theta,n_\theta} \equiv \frac{(n_\theta-1)\pi}{(\theta_{\mu+1}-\theta_\mu)} = \frac{\mu}{2}(n_\theta-1) \tag{D-7a}$$

$$\alpha_{\theta,m_\theta} \equiv (m_\theta-1) \tag{D-7b}$$

$$\alpha_{r,n_\theta,n_r} \equiv n_r^{th} \text{ root of } dJ^{(\mu)}_{\alpha_\theta,n_\theta}(\alpha^{(\mu)}_{r,n_\theta,n_r} r_1)/dr = 0 \tag{D-7c}$$

$$\alpha_{r,m_\theta,m_r} \equiv m_r^{th} \text{ root of } dJ^{(0)}_{\alpha_\theta,m_\theta}(\alpha^{(0)}_{r,m_\theta,m_r} r_1)/dr = 0 \tag{D-7d}$$

and

$$\Lambda^{(\mu)}_{n_\theta,n_r} = \left\{\frac{r_1^2}{2}\left[1 - \frac{(\alpha^{(\mu)}_{\theta,n_\theta})^2}{(\alpha^{(\mu)}_{r,n_\theta,n_r} r_1)^2}\right]\left[J^{(\mu)}_{\alpha_{\theta,n_\theta}}(\alpha^{(\mu)}_{r,n_\theta,n_r} r_1)\right]^2\right\} \tag{D-8c}$$

$$\Lambda^{(0)}_{m_\theta,m_r} = \left\{\frac{r_1^2}{2}\left[1 - \frac{(\alpha^{(0)}_{\theta,m_\theta})^2}{(\alpha^{(0)}_{r,m_\theta,m_r} r_1)^2}\right]\left[J^{(0)}_{\alpha_{\theta,m_\theta}}(\alpha^{(0)}_{r,m_\theta,m_r} r_1)\right]^2\right\} \tag{D-8d}$$

$$\epsilon^{(\mu)}_n = \begin{cases} 2\pi/\mu & n_\theta = 1 \\ \pi/\mu & n_\theta > 1 \end{cases} = (1 + \delta_{n_\theta,1})\,\pi/\mu \tag{D-8a}$$

$$\epsilon^{(0)}_m = \begin{cases} 2\pi & m_\theta = 1 \\ \pi & m_\theta > 1 \end{cases} = (1 + \delta_{m_\theta,1})\pi \tag{D-8b}$$

The Kronecker delta is defined by

$$\delta_{m,n} \equiv \begin{cases} 1 & m = n \\ 0 & m \neq n \end{cases} \tag{D-9}$$

Integrals of products of the orthonormal eigenfunctions are then

$$\int_{\theta_\mu}^{\theta_{\mu+1}} \int_{0}^{r_1} \psi^{(\mu)}_{n_\theta, n_r}(r,\theta)\psi^{(\mu)}_{n'_\theta, n'_r}(r,\theta) r dr d\theta = \delta_{n_\theta, n'_\theta}\delta_{n_r, n'_r} \tag{D-10a}$$

$$\int_{0}^{2\pi} \int_{0}^{r_1} \psi^{(0)}_{m_\theta, m_r}(r,\theta)\psi^{(0)}_{m'_\theta, m'_r}(r,\theta) r dr d\theta = \delta_{m_\theta, m'_\theta}\delta_{m_r, m'_r} \tag{D-10b}$$

$$I^{(0)}_{(\mu)}\begin{pmatrix} m_\theta, m_r \\ n_\theta, n_r \end{pmatrix} \equiv \int_{\theta_\mu}^{\theta_{\mu+1}} \int_{0}^{r_1} \psi^{(0)}_{m_\theta, m_r}(r,\theta)\psi^{(\mu)}_{n_\theta, n_r}(r,\theta) r dr d\theta \tag{D-11}$$

The Green's function for each region has been represented by an eigenfunction expansion also,

$$G^{(\mu)}(\vec{r}|\vec{r}') \equiv - \sum_{n_\theta=1} \sum_{n_r=1} \psi^{(\mu)}_{n_\theta, n_r}(r,\theta)\psi^{(\mu)}_{n_\theta, n_r}(r', \theta')F^{(\mu)}_{n_\theta, n_r}(z|z') \tag{D-12a}$$

$$G^{(0)}(\vec{r}|\vec{r}') \equiv + \sum_{m_\theta=1} \sum_{m_r=1} \psi^{(0)}_{m_\theta, m_r}(r,\theta)\psi^{(\mu)}_{m_\theta, m_r}(r',\theta')F^{(0)}_{m_\theta, m_r}(z|z') \tag{D-12b}$$

where

$$F^{(\mu)}_{n_\theta,n_r}(z|z') \equiv \begin{cases} \dfrac{\cos\left[\alpha^{(\mu)}_{z,n_\theta,n_r}(z-z_1)\right]\cos\left[\alpha^{(\mu)}_{z,n_\theta,n_r}(z_2-z') + \delta^{(\mu)}_{Rz,n_\theta,n_r}\right]}{\alpha^{(\mu)}_{z,n_\theta,n_r}\Omega^{(\mu)}_{n_\theta,n_r}} & z < z' \\ \dfrac{\cos\left[\alpha^{(\mu)}_{z,n_\theta,n_r}(z'-z_1)\right]\cos\left[\alpha^{(\mu)}_{z,n_\theta,n_r}(z_2-z) + \delta^{(\mu)}_{Rz,n_\theta,n_r}\right]}{\alpha^{(\mu)}_{z,n_\theta,n_r}\Omega^{(\mu)}_{n_\theta,n_r}} & z > z' \end{cases} \qquad \text{(D-13a)}$$

$$F^{(0)}_{m_\theta,m_r}(z|z') \equiv \begin{cases} \dfrac{\cos\left[\alpha^{(0)}_{z,m_\theta,m_r}(z-z_o) + \delta^{(0)}_{Lz,m_\theta,m_r}\right]\cos\left[\alpha^{(0)}_{z,m_\theta,m_r}(z_1-z')\right]}{\alpha^{(0)}_{z,m_\theta,m_r}\Omega^{(0)}_{m_\theta,m_r}} & z < z' \\ \dfrac{\cos\left[\alpha^{(0)}_{z,m_\theta,m_r}(z'-z_o) + \delta^{(0)}_{Lz,m_\theta,m_r}\right]\cos\left[\alpha^{(0)}_{z,m_\theta,m_r}(z_1-z)\right]}{\alpha^{(0)}_{z,m_\theta,m_r}\Omega^{(0)}_{m_\theta,m_r}} & z > z' \end{cases} \qquad \text{(D-13b)}$$

in which

$$\alpha^{(\mu)}_{z,n_\theta,n_r} \equiv \sqrt{k^2 - (\alpha^{(\mu)}_{r,n_\theta,n_r})^2} \qquad \text{(D-14a)}$$

$$\alpha^{(0)}_{z,m_\theta,m_r} \equiv \sqrt{k^2 - (\alpha^{(0)}_{r,m_\theta,m_r})^2} \qquad \text{(D-14b)}$$

$$\Omega^{(\mu)}_{n_\theta,n_r} \equiv \sin\left[\alpha^{(\mu)}_{z,n_\theta,n_r}(z_2-z_1) + \delta^{(\mu)}_{Rz,n_\theta,n_r}\right] \qquad \text{(D-14c)}$$

$$\Omega^{(0)}_{m_\theta,m_r} \equiv \sin\left[\alpha^{(0)}_{z,m_\theta,m_r}(z_1-z_o) + \delta^{(0)}_{Lz,m_\theta,m_r}\right] \qquad \text{(D-14d)}$$

and the finite admittance boundary conditions give

$$\delta^{(\mu)}_{Rz,n_\theta,n_r} \equiv \tan^{-1}(ik\beta_{z_{2-}}/\alpha^{(\mu)}_{z,n_\theta,n_r}) \qquad \text{(D-15a)}$$

$$\delta^{(0)}_{Lz,m_\theta,m_r} \equiv \tan^{-1}(ik\beta_{z_{o+}}/\alpha^{(0)}_{z,m_\theta,m_r}) \qquad \text{(D-15b)}$$

Finally,

$$\vdash\!\!\dashv^{(\mu)}_{R_{n_\theta,n_r}}(z) \equiv + \alpha^{(\mu)}_{z,n_\theta,n_r} \frac{\sin\left[\alpha^{(\mu)}_{z,n_\theta,n_r}(z_2-z) + \delta^{(\mu)}_{Rz,n_\theta,n_r}\right]}{\cos\left[\alpha^{(\mu)}_{z,n_\theta,n_r}(z_2-z_1) + \delta^{(\mu)}_{Rz,n_\theta,n_r}\right]} \tag{D-16a}$$

$$\vdash\!\!\dashv^{(0)}_{L_{m_\theta,m_r}}(z) \equiv - \alpha^{(0)}_{z,m_\theta,m_r} \frac{\sin\left[\alpha^{(0)}_{z,m_\theta,m_r}(z-z_o) + \delta^{(0)}_{Lz,m_\theta,m_r}\right]}{\cos\left[\alpha^{(0)}_{z,m_\theta,m_r}(z_1-z_o) + \delta^{(0)}_{Lz,m_\theta,m_r}\right]} \tag{D-16b}$$

$$B^{(0)(\ell)}_{m_\theta,m_r} \equiv \sum_{\mu=1}^{\bar{\mu}} \left\{ \sum_{n_\theta=1} \sum_{n_r=1} \left(b^{(\mu)(\ell)}_{n_\theta,n_r} \vdash\!\!\dashv^{(\mu)}_{R_{n_\theta,n_r}}(z_1)\right) I^{0\,(\mu)}_{(n_\theta,n_r)(m_\theta,m_r)} \right\} \tag{D-17}$$

Final Equations

When series expressions are used to represent the interface pressure profiles in both the main chamber and the baffle compartments, the iteration scheme proceeds as follows:

$$p^{(\mu)(\ell)}(r,\theta,z_1) \equiv \sum_{n_\theta=1} \sum_{n_r=1} b^{(\mu)(\ell)}_{n_\theta,n_r} \psi^{(\mu)}_{n_\theta,n_r}(r,\theta) \tag{D-18a}$$

$$\frac{\partial p^{(\mu)(\ell)}}{\partial z}(r,\theta,z_1) \equiv \sum_{n_\theta=1} \sum_{n_r=1} \left(b^{(\mu)(\ell)}_{n_\theta,n_r} \vdash\!\!\dashv^{(\mu)}_{R_{n_\theta,n_r}}(z_1)\right) \psi^{(\mu)}_{n_\theta,n_r}(r,\theta) \tag{D-18b}$$

$$p^{(0)(\ell)}(r,\theta,z_1) \equiv \sum_{m_\theta=1} \sum_{m_r=1} \frac{B^{(0)(\ell)}_{m_\theta,m_r}}{\vdash\!\!\dashv^{(0)}_{L_{m_\theta,m_r}}(z_1)} \psi^{(0)}_{m_\theta,m_r}(r,\theta) \equiv \sum_{m_\theta=1} \sum_{m_r=1} a^{(0)(\ell)}_{m_\theta,m_r} \psi^{(0)}_{m_\theta,m_r}(r,\theta) \tag{D-18c}$$

$$\frac{\partial p^{(0)(\ell)}}{\partial z}(r,\theta,z_1) \equiv \sum_{m_\theta=1} \sum_{m_r=1} B^{(0)(\ell)}_{m_\theta,m_r} \psi^{(0)}_{m_\theta,m_r}(r,\theta) \equiv \sum_{m_\theta=1} \sum_{m_r=1} \left(a^{(0)(\ell)}_{m_\theta,m_r} \vdash\!\dashv^{(0)}_{m_\theta,m_r}(z_1)\right) \psi^{(0)}_{m_\theta,m_r}(r,\theta) \tag{D-18d}$$

$$p^{(\mu)(\ell+1)}(r,\theta,z_1) \equiv \sum_{n_\theta=1} \sum_{n_r=1} b^{(\mu)(\ell+1)}_{n_\theta,n_r} \psi^{(\mu)}_{n_\theta,n_r}(r,\theta) \equiv \sum_{n_\theta=1} \sum_{n_r=1} \left(\sum_{m_\theta=1} \sum_{m_r=1} a^{(0)(\ell)}_{m_\theta,m_r} I^{(0)}_{\substack{(m_\theta,m_r)\\(n_\theta,n_r)}} \right) \psi^{(\mu)}_{n_\theta,n_r}(r,\theta) \tag{D-18e}$$

With the same series expression representations, the general characteristic equation reduces to an algebraic equation (which can be solved numerically)

$$\sum_{m_\theta=1} \sum_{m_r=1} \left(\left[a^{(0)(\ell)}_{m_\theta,m_r} \right]^2 \vdash\!\dashv^{(0)}_{m_\theta,m_r}(z_1) \right) - \sum_{\mu=1} \left\{ \sum_{n_\theta=1} \sum_{n_r=1} \left(\left[b^{(\mu)(\ell)}_{n_\theta,n_r} \right]^2 \vdash\!\dashv^{(\mu)}_{n_\theta,n_r}(z_1) \right) \right\} = 0 \tag{D-19}$$

COMPUTER PROGRAMS

The computer programs used to solve for the fundamental acoustic modes of a three-dimensional baffled chamber with gain/loss end-wall boundary conditions (see Figure 2) are described in this section. All programs are written in GE-400 Series Fortran* using complex arithmetic. The function of the component programs, the programs themselves, and the relationship between the functions, the equations and the lines in the program are detailed below. The computer logic is illustrated by the flow chart shown in Fig. 14.

*CPB-1473, GE-400 Series Time-Sharing FORTRAN manual, General Electric Company, Information Systems Division, 13430 North Black Canyon Highway, Phoenix, Arizona, 1970.

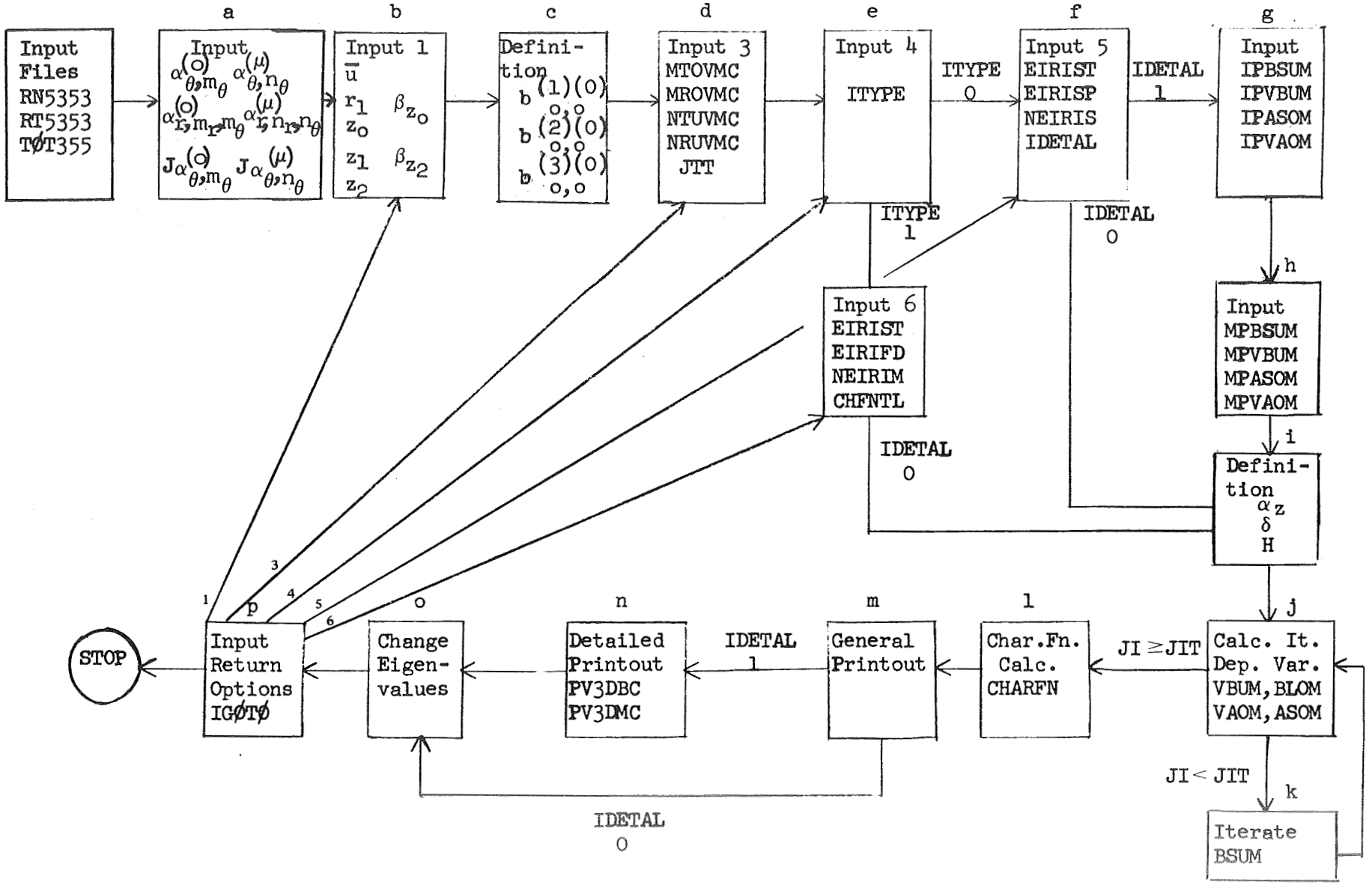

Figure 14. Flowchart for Program to Analyze Cylindrical Baffled Chambers. The Accompanying Description of the Computer Programs is Keyed to This Flowchart Through the Letters a...k.

RN5353 - INPUT FILE

This file lists data for input both to the r integration program and to the main program.

a. Specification of Numbers of Terms: Line 0100

$\text{MTOVMX} \equiv (m_\theta)_{max} = 5$
$\text{MROVMX} \equiv (m_r)_{max} = 3$
$\text{NTUVMX} \equiv (n_\theta)_{max} = 5$
$\text{NRUVMX} \equiv (n_r)_{max} = 3$

b. Specification of Integration Parameters: Line 0200.

MINGRL = 80
$\text{EPSSER} = 10^{-25}$
IPRDET = 0

c. Specification of Zeros of J' and Values of J: Lines 1010-2053

$\text{ATOM}(1) \equiv \alpha^{(0)}_{\theta,1} = 0.00$

$\text{AROM}(1,1) \equiv (\alpha^{(0)}_{r,1,1} r_1) = 0.00000,\ J_{\alpha^{(0)}_{\theta,1}}(\alpha^{(0)}_{r,1,1} r_1) = +1.00000$

$\text{AROM}(1,2) \equiv (\alpha^{(0)}_{r,1,2} r_1) = 3.83171,\ J_{\alpha^{(0)}_{\theta,1}}(\alpha^{(0)}_{r,1,2} r_1) = -0.40276$

$\text{AROM}(1,3) \equiv (\alpha^{(0)}_{r,1,3} r_1) = 7.01559,\ J_{\alpha^{(0)}_{\theta,1}}(\alpha^{(0)}_{r,1,3} r_1) = +0.30012$

$\text{ATOM}(2) \equiv \alpha^{(0)}_{\theta,2} = 1.00$

$\text{AROM}(2,1) \equiv (\alpha^{(0)}_{r,2,1} r_1) = 1.84118,\ J_{\alpha^{(0)}_{\theta,2}}(\alpha^{(0)}_{r,2,1} r_1) = +0.58187$

.
.
.

RI5353 - INPUT GENERATION PROGRAM -r INTEGRATION

This program is used to calculate the integrals of products of Bessel functions of different orders and to create a file of integrals for use by the main program.

a. Input: Lines 1120, 1150, 1170, 1190: From File RN5353

MTOVMX $\equiv (m_\theta)_{max} \equiv$ # terms, main chamber θ series expansion

MROVMX $\equiv (m_r)_{max} \equiv$ # terms, main chamber r series expansion

NTUVMX $\equiv (n_\theta)_{max} \equiv$ # terms, baffle compartment θ series expansion

NRUVMX $\equiv (n_r)_{max} \equiv$ # terms, baffle compartment r series expansion

MINGRL $\equiv (m)_{max} \equiv$ # terms, r integral series approximation

EPSSER $\equiv \epsilon \equiv$ term value, r integral series approximation cutoff

IPRDET $\equiv$ Inactive

ATOM(MTOD) $\equiv \alpha^{(0)}_{\theta,m_\theta}$

AROM(MTOD,MROD) $\equiv \alpha^{(0)}_{r,m_\theta,m_r} r_1$

BESSOM(MTOD,MROD) $\equiv J_{\alpha^{(0)}_{\theta,m_\theta}}(\alpha^{(0)}_{r,m_\theta,m_r} r_1)$

ATUM(NTUD) $\equiv \alpha^{(\mu)}_{\theta,n_\theta}$

ARUM(NTUD,NRUD) $\equiv \alpha^{(\mu)}_{r,n_\theta,n_r} r_1$

BESSUM(NTUD,NRUD) $\equiv J_{\alpha^{(\mu)}_{\theta,n_\theta}}(\alpha^{(\mu)}_{r,n_\theta,n_r} r_1)$

b. Perform r Integration: Lines 1210-1780 + Subroutines

$$\text{FINTEM(MTOD,MROD,NTUD,NRUD)} = I_R^{(\mu)}\begin{pmatrix} m_\theta, m_r \\ n_\theta, n_r \end{pmatrix} \quad : \text{(Eqn. D-11)}$$

SUBRØUTINE SERIEF - Calculates series approximation to the r integral*

$$\int_0^{r_1} J_\mu(ar)J_\nu(br)rdr = \left\{ \frac{r^2\left(\frac{ar}{2}\right)^\mu \left(\frac{br}{2}\right)^\nu}{\Gamma(\nu+1)} \sum_{m=0} \frac{(-1)^m\left(\frac{ar}{2}\right)^{2m} {}_2F_1(-m,-\mu-m;\nu+1;b^2/a^2)}{(2+\mu+\nu+2m)m!\,\Gamma(\mu+m+1)} \right\}\Bigg|_0^{r_1}$$

where

Γ is the Gamma Function - SUBRØUTINE GAMMAF

and

$${}_2F_1(\alpha,\beta;\rho;z) \equiv \sum_{n=0}^{\infty} \frac{(\alpha)_n(\beta)_n}{n!(\rho)_n} z^n \; ; \qquad (\alpha)_n \equiv \alpha(\alpha+1)(\alpha+2)\ldots(\alpha+n-1), \quad (\alpha)_0 \equiv 1$$

is a Hypergeometric function† that is evaluated by SUBRØUTINE HYPERF

c. Output: Lines 1790, 1810

FINTEM filed in RT5353

MTERMX = $(m)_{max}$ = # terms actually used in series approx. } printed

EPSSER = ϵ }

*Watson, G. N., A Treatise on the Theory of Bessel Functions, Cambridge University Press, London, 1962, pg. 148.

†Ibid, p. 100

TIT355 - INPUT GENERATION PROGRAM

This program is used to generate a file of theta integrals needed by the main program.

a. Input: Line 1040

THTO = θ_0

MUBAR = $\bar{\mu}$

MTOVMX = $(m_\theta)_{max}$ = # terms, main chamber θ series expansion

MTUVMX = $(n_\theta)_{max}$ = # terms, baffle compartment θ series expansion

b. Perform θ Integration: Lines 1050-1470: (Eqn. D-11)

FINTTM(MUD,MTOD,NTUD) = $I_\theta^{(0_\mu)}_{(^m_{n_\theta})}$

c. Output: Lines 1480-1510

FINTTM filed in TØT355

THTO
MUBAR
MTOVMX
NTUVMX
} printed

B3D353 - MAIN PROGRAM

This program is used to obtain the eigenvalue (frequency and damping coefficient) as well as the series expansion coefficients for the interface pressures and axial velocities for a particular three-dimensional baffled chamber with gain/loss end-wall boundary conditions. Complex quantities are noted. A full sample calculation is given at the end of this Appendix.

Input Files Needed

RN5353 - Bessel Function Data

RT5353 - r Integrals $I_R^{(0_\mu)}{}_{(m_\theta,m_r)}{}_{(n_\theta,n_r)}$ (Eqn. D-11)

TØT355 - Integrals $I_\theta^{(0_\mu)}{}_{(m_\theta)}{}_{m_r}$ (Eqn. D-11)

a. Input: Lines 1290, 1300-1310, 1320-1330, 1340, 1350

MTOVMX ≡ $(m_\theta)_{max}$ ≡ # terms, main chamber θ series expansion

MROVMX ≡ $(m_r)_{max}$ ≡ # terms, main chamber r series expansion

NTUVMX ≡ $(n_\theta)_{max}$ ≡ #terms, baffle compartment θ series expansion

NRUVMX ≡ $(n_r)_{max}$ ≡ # terms, baffle compartment r series expansion

} In Input Data Files

IDJM1
DUM1
IDJM2

} Inactive (dummy variables)

ATOM(MTOD) ≡ $\alpha^{(0)}_{\theta,m_\theta}$

AROM(MTOD,MROD) ≡ $\alpha^{(0)}_{r,m_\theta,m_r}r_1$

BESSOM(MTOD,MROD) ≡ $J_{\alpha^{(0)}_{\theta,m_\theta}}(\alpha^{(0)}_{r,m_\theta,m_r}r_1)$

ATUM(MTUD) ≡ $\alpha^{(\mu)}_{\theta,n_\theta}$

ARUM(MTUD,MRUD) ≡ $\alpha^{(\mu)}_{r,n_\theta,n_r}r_1$

BESSUM(MTUD,MRUD) ≡ $J_{\alpha^{(\mu)}_{\theta,n_\theta}}(\alpha^{(\mu)}_{r,n_\theta,n_r}r_1)$

b. Input 1: Line 1370

MUBAR = $\overline{\mu}$

R1 = r_1

Z0 = z_o

Z1 = z_1

Z2 = z_2

BETA0P = $\beta_{z_{o+}}$ (Complex)

BETA2L = $\beta_{z_{2-}}$ (Complex)

c. Definition: Lines 1400-1420

BSUM01 = $b_{0,0}^{(1)(0)} = +0.5$

BSUM02 = $b_{0,0}^{(2)(0)} = -1.0$

BSUM03 = $b_{0,0}^{(2)(0)} = +0.5$

} initial pressure distribution (other coefficients are zero)

d. Input 3: Line 1440

MTOVMC = # θ terms retained, main chamber series

MROVMC = # r terms retained, main chamber series

NTUVMC = # θ terms retained, baffle compartment series

NRUVMC = # r terms retained, baffle compartment series

JIT = number of iterations performed

e. Input 4: Line 1460

ITYPE = { 0 for step calculation of characteristic function
1 for root finding calculation of characteristic function

f. Input 5: Line 1500 (ITYPE = 0)

EIR1ST = kr_1 initial guess (Complex)

EIR1SP = kr_1 increment (Complex)

NEIR1S = number of calculations

IDETAL = { 0 for simple printout of characteristic function
1 for detailed printout of series expansion coefficients, pressure and velocity profiles

g. Input: Line 1530: (ITYPE = 0)(IDETAL = 1)

IPBSUM, IPVBUM, IPASOM, IPVAOM = { 0 for no print / 1 for printout } of {
BSUM(MUD,NTUD,NRUD) = $b^{(\mu)(\ell)}_{n_\theta,n_r}$
VBUM(MUD,NTUD,NRUD) = $b^{(\mu)(\ell)}_{n_\theta,n_r}\left|_{\overline{R}}\right|^{(\mu)}_{n_\theta,n_r}(z_1)$
ASOM(MTOD,MROD) = $a^{(0)(\ell)}_{m_\theta,m_r}$
VAOM(MTOD,MROD) = $a^{(0)(\ell)}_{m_\theta,m_r}\left|_{\overline{L}}\right|^{(0)}_{m_\theta,m_r}(z_1)$ }

h. Input: Line 1550: (ITYPE = 0)(IDETAL = 1)

MPBSUM, MPVBUM, MPASOM, MPVAOM = { 0 for no print / 1 for printout } of {
$p^{(\mu)(\ell)}(r,\theta,z_1)$
$\partial p^{(\mu)(\ell)}(r,\theta,z_1)/\partial z$
$p^{(0)(\ell)}(r,\theta,z_1)$
$\partial p^{(0)(\ell)}(r,\theta,z_1)/\partial z$ }

f'. Input 6: Line 1580: (ITYPE = 1)

EIR1ST = kr_1 initial guess (Complex)

EIR1FD = kr_1 finite difference (Complex)

NEIR1M = number of calculations

CHFNTL = tolerance-final characteristic function value

i. Definition: Lines 1700-2110 (Eqns. D-7a,b,c,d; D-14a,b; D-15a,b; D-16a,b)

JI	$= 0$	(Complex)
AZOV	$= \alpha^{(0)}_{z,m_\theta,m_r}$	(Complex)
DELLOV	$= \delta^{(0)}_{L_{z,m_\theta,m_r}}$	(Complex)
HLOM(MTOD,MROD)	$= \Gamma^{(0)}_{L_{m_\theta,m_r}}(z_l)$	(Complex)
AZUV	$= \alpha^{(\mu)}_{z,n_\theta,n_r}$	(Complex)
DELLUV	$= \delta^{(\mu)}_{R_{z,n_\theta,n_r}}$	(Complex)
HRUM(NTUD,NRUD)	$= H^{(\mu)}_{R_{n_\theta,n_r}}(z_l)$	(Complex)
BSUM(MUD,NTUD,NRUD)	$= b^{(\mu)(0)}_{n_\theta,n_r}$	(Complex)

j. Calculation - Iteration Dependent Variables: Lines 2140-2380 (Eqns. D-17, D-18)

VBUM(MUD,NTUD,NRUD)	$= b^{(\mu)(\ell)}_{n_\theta,n_r}\Gamma^{(\mu)}_{R_{n_\theta,n_r}}(z_l)$	(Complex)
BLOM(MTOD,MROD)	$= B^{(0)(\ell)}_{m_\theta,m_r}$	(Complex)
VAOM(MTOD,MROD)	$= a^{(0)(\ell)}_{m_\theta,m_r}$	(Complex)
ASOM(MTOD,MROD)	$= a^{(0)(\ell)}_{m_\theta,m_r}\Gamma^{(0)}_{L_{m_\theta,m_r}}(z_l)$	(Complex)

k. Perform Iteration: Lines 2390-2590: (JI < JIT): (Eqn. D-18e)

JI = JI + 1

BSUM(MUD,NTUD,NRUD)	$= b^{(\mu)(\ell+1)}_{n_\theta,n_r}$	(Complex)

l. Compute Characteristic Function: Lines 2620-2850: (Eqn. D-19)

$$\text{SUM1} = \sum_{m_\theta=1} \sum_{m_r=1} \left(\left[a^{(0)(\ell)}_{m_\theta, m_r} \right]^2 H^{(0)}_{L m_\theta, m_r}(z_1) \right) \qquad \text{(Complex)}$$

$$\text{SUM2} = \sum_{\mu=1}^{\bar{\mu}} \left\{ \sum_{n_\theta=1} \sum_{n_r=1} \left(\left[b^{(\mu)(\ell)}_{n_\theta, n_r} \right]^2 H^{(\mu)}_{R n_\theta, n_r}(z_1) \right) \right\} \qquad \text{(Complex)}$$

$$\text{CHARFN} = \text{SUM1} - \text{SUM2} \qquad \text{(Complex)}$$

m. General Printout: Line 2890

$\text{EIGNR1} = kr_1$ (Complex)

SUM1 (Complex)

CHARFN (Complex)

SUM2 (Complex)

n. Detailed Printout: Lines 2920-3140: (IDETAL = 1)
(According to inputs g, h)

Calls SUBROUTINES $\begin{pmatrix} \text{PV3DBC} \\ \text{PV3DMC} \end{pmatrix}$ for interface pressure/axial-velocity profiles

o. Increment Eigenvalue: Lines 3160-3480

ITYPE = 0 $\Longrightarrow$ EIGNR1 = EIGNR1 + EIR1SP (Complex)

ITYPE = 1 $\Longrightarrow$ $\text{EIGNR1} = \text{EIGNR1} - \dfrac{\text{CHARFN}}{\dfrac{d(\text{CHARFN})}{d(\text{EIGNR1})}}$

p. Return Options: Lines 3500-3540

IGØTØ = 1 Input 1
IGØTØ = 3 Input 3
IGØTØ = 4 Input 4
IGØTØ = 5 Input 5
IGØTØ = 6 Input 6

SUBROUTINES CALLED BY MAIN PROGRAM

PV3DBC - Baffle Compartment Interface Pressure/Axial Velocity Profiles

This program takes coefficients of pressure/axial-velocity series expressions and generates the appropriate radial and tangential profiles at the interface on the baffle compartment side.

a. Input: Line 5300

NRPNT ≡ number of equally spaced r printout points
TVAL ≡ θ value for r profile
NTPNT ≡ number of equally spaced θ printout points
RVAL ≡ r value for θ profile
TSTØP ≡ last θ value printed
(NRPNT ≡ NTPNT ≡ 0 for return to main program)

b. Output: Line 5520: (Eqn. D-6a)

Value of pressure/axial velocity at r location
r location

c. Output: Line 5970: (Eqn. D-6a)

Value of pressure/axial velocity at θ location
θ location

PV3DMC - Main Chamber Interface Pressure/Axial Velocity Profiles

This program takes coefficients of pressure/axial velocity series expressions and generates the appropriate radial and tangential profiles at the interface on the main chamber side.

a. Input: Line 6280

NRPNT = number of equally spaced r printout points
TVAL = θ value for r profile
NTPNT = number of equally spaced θ printout points
RVAL = r value for θ profile
TSTØP = last θ value printed
(NRPNT = NTPNT = 0 for return to main program)

b. Output: Line 6530: (Eqn. D-6b)

Value of pressure/axial velocity at r location
r location

c. Output: Line 6860: (Eqn. D-6b)

Value of pressure/axial velocity at θ location
θ location

AUXILIARY SUBRØUTINES

BESFNP - Bessel Function Calculation Program

This program takes the order and argument from the variable list and, for Bessel functions of integer or half-integer order, returns the value of the Bessel function using standard recursion formulae.

a. Input: Line 7000 (Variable List)

ØRDER ≡ order of Bessel function (integer or half integer)
ARGMNT ≡ argument of Bessel function

b. Output: Line 7000 (Variable List)

BESFNV ≡ value of Bessel function $J_{\text{ØRDER}}(\text{ARGMNT})$

BESSOP - Zero Order Bessel Function Evaluation

This program takes the argument from the variable list, upon call by BESFNP, and returns the value of the zero order Bessel function of that argument.

a. Input: Line 8000 (Variable List)

ARGMNT ≡ argument of Bessel function

b. Output: Line 8000 (Variable List)

BESSOV ≡ value of zero order Bessel function $J_o(\text{ARGMNT})$

BESSIP - Order One Bessel Function Evaluation

This program takes the argument from the variable list, upon call by BESFNP, and returns the value of the order one Bessel function of that argument.

a. Input: Line 9000 (Variable Test)

ARGMNT ≡ argument of Bessel function

b. Output: Line 9000 (Variable List)

BESSIV ≡ value of order one Bessel function J_1(ARGMNT)

RN5353

```
0100      5     3     5     3
0200     80    1.0E-25     0
1010   0.00
1011           0.00000 +1.00000
1012           3.83171 -0.40276
1013           7.01559 +0.30012
1020   1.00
1021           1.84118 +0.58187
1022           5.33144 -0.34613
1023           8.53632 +0.27330
1030   2.00
1031           3.05424 +0.48650
1032           6.70613 -0.31353
1033           9.96947 +0.25474
1040   3.00
1041           4.20119 +0.43439
1042           8.01524 -0.29116
1043          11.34592 +0.24074
1050   4.00
1051           5.31755 +0.39965
1052           9.28240 -0.27438
1053          12.68191 +0.22959
2010   0.00
2011           0.00000 +1.00000
2012           3.83171 -0.40276
2013           7.01559 +0.30012
2020   1.50
2021           2.46054 +0.52534
2022           6.02929 -0.32806
2023           9.26140 +0.26330
2030   3.00
2031           4.20119 +0.43439
2032           8.01524 -0.29116
2033          11.34592 +0.24074
2040   4.50
2041           5.86842 +0.38601
2042           9.90431 -0.26739
2043          13.33793 +0.22479
2050   6.00
2051           7.50127 +0.35414
2052          11.73494 -0.25017
2053          15.26818 +0.21261
```

RI5353

```
1000 DIMENSION ATOM(5),AROM(5,3),BESSOM(5,3)
1010& ,ATUM(5),ARUM(5,3),BESSUM(5,3)
1020& ,FINTEM(5,3,5,3)
1030 COMMON ATOV,AROV,ATUV,ARUV,AROV02,ARUV02,ATOVP1,ATUVP1,RARAR2
1040&,MINGRL,EPSSER,IPRDET,MTERM,RM,SERIEV,HYPERV
1050 DATA MTOVST,MROVST,NTUVST,NRUVST/1,1,1,1/
1060 CALL OPENF(1,"RN5353")
1070 CALL OPENF(2,"RT5353")
1080 2 FORMAT(4I5)
1090 4 FORMAT(I5,E10.2,I5)
1100 6 FORMAT(F5.2,3(/5X,2F9.5))
1110 12 FORMAT(1X,1P5E12.6)
1120 READ(1,2) MTOVMX,MROVMX,NTUVMX,NRUVMX
1130 PRINT,"MTOVMX=",MTOVMX,"  MROVMX=",MROVMX
1140 PRINT,"NTUVMX=",NTUVMX,"  NRUVMX=",NRUVMX
1150 READ(1,4) MINGRL,EPSSER,IPRDET
1160 PRINT,"MINGRL=",MINGRL,"  EPSSER=",EPSSER
1170 READ(1,6) (ATOM(MT),(AROM(MT,MR),BESSOM(MT,MR),MR=1,MROVMX),
1180&MT=1,MTOVMX)
1190 READ(1,6) (ATUM(NT),(ARUM(NT,NR),BESSUM(NT,NR),NR=1,NRUVMX),
1200&NT=1,NTUVMX)
1210 MTOVND=MTOVMX
1220 MROVND=MROVMX
1230 NTUVND=NTUVMX
1240 NRUVND=NRUVMX
1250 MTERMX=0
1260 DO 90 MTOV=MTOVST,MTOVND
1270  DO 80 MROV=MROVST,MROVND
1280   DO 70 NTUV=NTUVST,NTUVND
1290    DO 60 NRUV=NRUVST,NRUVND
1300   ATOV=ATOM(MTOV)
1310   ATOVP1=ATOV+1.0
1320   AROV=AROM(MTOV,MROV)
1330   AROV02=AROV/2.0
1340   ATUV=ATUM(NTUV)
1350   ATUVP1=ATUV+1.0
1360   ARUV=ARUM(NTUV,NRUV)
1370   ARUV02=ARUV/2.0
1380 IF ((AROV.EQ.0.0).OR.(ARUV.EQ.0.0))  GO TO 10
1390 AROATO=AROV02**ATOV
1400 RATARO=(ATOV/AROV)**2
1410 ARUATU=ARUV02**ATUV
1420 RATARU=(ATUV/ARUV)**2
1430 RARAR2=(ARUV/AROV)**2
1440 GO TO 40
1450 10 IF ((AROV.EQ.0.0).AND.(ARUV.EQ.0.0))  GO TO 30
1460 IF (ARUV.EQ.0.0)  GO TO 20
1470 ATOV=ATUV
1480 ATOVP1=ATUVP1
1490 ATUV=0.0
```

RI5353 CØNTINUED

```
1500 ATUVP1=1.0
1510 AROV=ARUV
1520 AROV02=ARUV02
1530 ARUV=0.0
1540 ARUV02=0.0
1550 20 AROATO=AROV02**ATOV
1560 RATARO=(ATOV/AROV)**2
1570 ARUATU=1.0
1580 RATARU=0.0
1590 RARAR2=0.0
1600 GØ TØ 40
1610 30 AROATO=1.0
1620 RATARO=0.0
1630 ARUATU=1.0
1640 RATARU=0.0
1650 RARAR2=1.0
1660 40 CØNTINUE
1670 CALL SERIEF
1680 CALL GAMMAF(ATUVP1,ATUVFT)
1690 FINTEV=(AROATO*ARUATU*SERIEV)/ATUVFT
1700    BESSOV=BESSOM(MTOV,MROV)
1710    BESSUV=BESSUM(NTUV,NRUV)
1720    REFERV=0.5*SQRT((1.0-RATARO)*(1.0-RATARU))*ABS(BESSOV*BESSUV)
1730    FINTEM(MTOV,MROV,NTUV,NRUV)=FINTEV/REFERV
1740    IF(MTERM.GT.MTERMX)  MTERMX=MTERM
1750    60 CØNTINUE
1760   70 CØNTINUE
1770  80 CØNTINUE
1780 90 CØNTINUE
1790 WRITE(2,12) FINTEM
1800 CALL CLØSEF(2)
1810 PRINT,↑2,"MINGRL=",MTERMX,"  EPSSER=",EPSSER
1820 STØP
1830 END
```

SERIEF

```
2000 SUBRØUTINE SERIEF
2010 CØMMØN ATOV,AROV,ATUV,ARUV,AROVØ2,ARUVØ2,ATOVP1,ATUVP1,RARAR2
2020&,MINGRL,EPSSER,IPRDET,MTERM,RM,SERIEV,HYPERV
2030 ARØØ22=AROVØ2**2
2040 ATPAT=ATOV+ATUV
2050 CALL GAMMAF(ATOVP1,ATOVFT)
2060 MTERM=0
2070 TM=1.0/((ATPAT+2.0)*ATOVFT)
2080 CALL HYPERF
2090 SERIEV=TM*HYPERV
2100 RM=0.0
2110 DØ 10 MTERM=1,MINGRL
2120 RM=RM+1.0
2130 RMT2P=2.0*RM+ATPAT
2140 TM=-(ARØØ22/(RM*(RM+ATOV)))*(RMT2P/(RMT2P+2.0))*TM
2150 CALL HYPERF
2160 SERIEV=SERIEV+TM*HYPERV
2170 IF (ABS(TM*HYPERV).LT.EPSSER) RETURN
2180 10 CØNTINUE
2190 RETURN
2200 END
```

HYPERF

```
3000 SUBRØUTINE HYPERF
3010 CØMMØN ATOV,AROV,ATUV,ARUV,AROV02,ARUV02,ATOVP1,ATUVP1,RARAR2
3020&,MINGRL,EPSSER,IPRDET,MTERM,RM,SERIEV,HYPERV
3030 RMP1=RM+1.0
3040 TN=1.0
3050 HYPERV=TN
3060 IF (MTERM.EQ.0)  RETURN
3070 RN=0.0
3080 DØ 10 N=1,MTERM
3090 RN=RN+1.0
3100 RMP1LR=RMP1-RN
3110 TN=((RMP1LR*(RMP1LR+ATOV))/(RN*(RN+ATUV)))*(RARAR2*TN)
3120 10 HYPERV=HYPERV+TN
3130 RETURN
3140 END
```

GAMMAF

```
4000 SUBRØUTINE GAMMAF(VIN,VØUT)
4010 DVIN=VIN-1.0
4020 IN=DVIN
4030 DVINT=IN
4040 IF ((DVIN-DVINT).GT.0.1)  GØ TØ 20
4050 VØUT=1.0
4060 10 IF (DVIN.LT.1.1)  RETURN
4070 VØUT=DVIN*VØUT
4080 DVIN=DVIN-1.0
4090 GØ TØ 10
4100 20 VØUT=1.7724539
4110 25 IF (DVIN.LT.0.4)  RETURN
4120 VØUT=DVIN*VØUT
4130 DVIN=DVIN-1.0
4140 GØ TØ 25
4150 END
```

```
READY
EDIT WEAVE RI5353,SERIEF,HYPERF,GAMMAF

READY
0001$NDM

RUN

RI5353    20:03  NAR  JAN. 12,1971


MTOVMX=          5  MROVMX=          3
NTUVMX=          5  NRUVMX=          3
MINGRL=         80  EPSSER=    1.000000000E-25


MINGRL=         47  EPSSER=    1.000000000E-25
STØP

RUNNING TIME:    56.2 SECS    I/Ø TIME :     1.2 SECS
```

generate RI5353

RT5353

```
00001   1.00000E+00 9.67313E-01 9.22928E-01 8.83553E-01 8.49802E-01
00002  -2.10339E-06 2.11320E-01 3.05500E-01 3.56611E-01 3.87206E-01
00003   9.49233E-07 1.00415E-01 1.59612E-01 1.98336E-01 2.25312E-01
00004   9.44745E-01 9.96511E-01 9.97657E-01 9.84623E-01 9.67039E-01
00005  -3.27231E-01-8.20215E-02 6.59354E-02 1.64999E-01 2.35210E-01
00006  -1.71789E-02-1.30458E-02 1.56329E-02 4.90277E-02 8.11803E-02
00007   8.83553E-01 9.67401E-01 9.94150E-01 1.00002E+00 9.96421E-01
00008  -4.62054E-01-2.52876E-01-1.07963E-01-1.40526E-06 8.33344E-02
00009   7.64672E-02 1.34842E-02-3.72199E-03-1.47468E-06 1.35717E-02
00010   8.34738E-01 9.32908E-01 9.74331E-01 9.92687E-01 9.99329E-01
00011  -5.24798E-01-3.52624E-01-2.23533E-01-1.20578E-01-3.64610E-02
00012   1.64850E-01 7.22143E-02 2.57870E-02 5.01536E-03-7.47042E-04
00013   7.95438E-01 9.00522E-01 9.50839E-01 9.77617E-01 9.91701E-01
00014  -5.55671E-01-4.13531E-01-3.01520E-01-2.07817E-01-1.28013E-01
00015   2.34142E-01 1.31372E-01 6.93630E-02 3.24678E-02 1.19165E-02
00016  -2.10339E-06-2.50142E-01-3.84780E-01-4.62054E-01-5.08659E-01
00017   9.99997E-01 8.84508E-01 7.13454E-01 5.60109E-01 4.32444E-01
00018  -4.61341E-07 2.99353E-01 4.03202E-01 4.27188E-01 4.15870E-01
00019   2.66278E-01 7.89033E-02-6.76728E-02-1.74684E-01-2.53002E-01
00020   7.98422E-01 9.85139E-01 9.89372E-01 9.28085E-01 8.44564E-01
00021  -5.37175E-01-1.47291E-01 1.19312E-01 2.90780E-01 3.96792E-01
00022   3.56611E-01 2.29840E-01 1.04664E-01-1.40736E-06-8.46711E-02
00023   5.60109E-01 8.54296E-01 9.71726E-01 1.00000E+00 9.81608E-01
00024  -7.32880E-01-4.66097E-01-2.10314E-01 1.46999E-05 1.62905E-01
00025   3.97926E-01 3.14024E-01 2.12267E-01 1.18118E-01 3.62867E-02
00026   3.77426E-01 6.99101E-01 8.74342E-01 9.62348E-01 9.96461E-01
00027  -7.62856E-01-6.25355E-01-4.34598E-01-2.44656E-01-7.51745E-02
00028   4.19145E-01 3.65685E-01 2.84323E-01 2.02210E-01 1.26580E-01
00029   2.41269E-01 5.59126E-01 7.60339E-01 8.84344E-01 9.55530E-01
00030  -7.24129E-01-6.86021E-01-5.65383E-01-4.16711E-01-2.65940E-01
00031   9.49233E-07-3.73455E-02 1.17572E-02 7.64672E-02 1.37432E-01
00032  -4.70261E-07-4.04626E-01-6.30548E-01-7.32880E-01-7.63758E-01
00033   9.99972E-01 8.17943E-01 5.25268E-01 2.61456E-01 5.19486E-02
00034   1.33416E-01 2.27360E-02-8.36204E-03 1.19396E-03 2.84210E-02
00035   3.65832E-01 1.36086E-01-1.26406E-01-3.33400E-01-4.78956E-01
00036   6.72104E-01 9.72363E-01 9.79017E-01 8.54416E-01 6.83296E-01
00037   1.98336E-01 8.61584E-02 2.37390E-02-1.25647E-06-2.65251E-04
00038   4.27188E-01 3.74899E-01 1.94447E-01 6.78837E-06-1.71199E-01
00039   2.61464E-01 7.17394E-01 9.40930E-01 1.00003E+00 9.58858E-01
00040   2.35841E-01 1.36730E-01 6.40396E-02 2.22356E-02 3.31560E-03
00041   4.03560E-01 4.67158E-01 3.74879E-01 2.28593E-01 7.37166E-02
00042  -3.30600E-02 4.16991E-01 7.34236E-01 9.16220E-01 9.89849E-01
00043   2.59524E-01 1.75743E-01 1.02068E-01 5.12379E-02 2.04375E-02
00044   3.55163E-01 4.89015E-01 4.68126E-01 3.74572E-01 2.51720E-01
00045  -2.22725E-01 1.62892E-01 4.97724E-01 7.43713E-01 8.93815E-01
```

TIT355

```
1000 DIMENSIØN FINTTM(3,5,5)
1010 CALL ØPENF(1,"TØT355")
1020 2 FØRMAT(1X,1P3E15.8)
1030 PRINT,"   INPUT:THTO,MUBAR,MTOVMX,NTUVMX"
1040 INPUT,THTO,MUBAR,MTOVMX,NTUVMX
1050 PI=3.1415926536
1060 FMUBAR=FLØAT(MUBAR)
1070 THTDIF=2.0*PI/FMUBAR
1080 PTHTDF=PI*THTDIF
1090 DØ 1000 MUD=1,MUBAR
1100 FMUD=FLØAT(MUD)
1110 THTU=THTDIF*(FMUD-1.0)
1120 THTUP1=THTDIF*FMUD
1130 THTUPO=THTUP1-THTO
1140 THTUO=THTU-THTO
1150 FINTTM(MUD,1,1)=1.0/SQRT(FMUBAR)
1160 DØ 10 NTUD=2,NTUVMX
1170 10 FINTTM(MUD,1,NTUD)=0.0
1180 DØ 20 MTOD=2,MTOVMX
1190 FMTOD=FLØAT(MTOD)
1200 ATOV=FMTOD-1.0
1210 ARGUP1=ATOV*THTUPO
1220 ARGU=ATOV*THTUO
1230 C=SQRT(FMUBAR/2.0)/(ATOV*PI)
1240 FVALUE=C*(SIN(ARGUP1)-SIN(ARGU))
1250 IF((ABS(FVALUE)).LT.(1.0E-6))  FVALUE=0.0
1260 20 FINTTM(MUD,MTOD,1)=FVALUE
1270 DØ 40 MTOD=2,MTOVMX
1280 FMTOD=FLØAT(MTOD)
1290 ATOV=FMTOD-1.0
1300 ARGUP1=ATOV*THTUPO
1310 ARGU=ATOV*THTUO
1320 DØ 40 NTUD=2,NTUVMX
1330 FNTUD=FLØAT(NTUD)
1340 ATUV=((FNTUD-1.0)*FMUBAR)/2.0
1350 IF (ATOV.EQ.ATUV)  GØ TØ 30
1360 C=(ATOV/(ATOV**2-ATUV**2))/SQRT((PI**2)/FMUBAR)
1370 AC=(FNTUD-1.0)*PI
1380 FVALUE=C*(CØS(AC)*SIN(ARGUP1)-SIN(ARGU))
1390 IF((ABS(FVALUE)).LT.(1.0E-6))  FVALUE=0.0
1400 FINTTM(MUD,MTOD,NTUD)=FVALUE
1410 GØ TØ 40
1420 30 C=1.0/SQRT(FMUBAR)
1430 FVALUE=C*CØS(ARGU)
1440 IF((ABS(FVALUE)).LT.(1.0E-6))  FVALUE=0.0
1450 FINTTM(MUD,MTOD,NTUD)=FVALUE
1460 40 CØNTINUE
1470 1000 CØNTINUE
1480 WRITE(1,2) FINTTM,THTO
1490 CALL CLØSEF(1)
```

TIT355 CØNTINUED

```
1500 PRINT,"   THTO=",THTO,",     MUBAR=",MUBAR
1510 PRINT,"MTOVMX=",MTOVMX,",  NTUVMX=",NTUVMX
1520 STØP
1530 END
```

```
READY
ØLD:TIT355

READY
0001$NDM

RUN

TIT355     19:46   NAR   JAN. 12,1971


   INPUT:THTO,MUBAR,MTOVMX,NTUVMX
 ?0.00,3,5,5

  THTO=    0.000000000E+00,    MUBAR=          3
MTOVMX=          5, NTUVMX=          5
STØP

RUNNING TIME:     2.3 SECS    I/Ø TIME :      .7 SECS
```

generate TØT355

T6T355

00001	5.7735027E-01	5.7735027E-01	5.7735027E-01
00002	3.3761862E-01	-6.7523724E-01	3.3761862E-01
00003	-1.6880931E-01	3.3761862E-01	-1.6880931E-01
00004	0.0000000E+00	0.0000000E+00	0.0000000E+00
00005	8.4404655E-02	-1.6880931E-01	8.4404655E-02
00006	0.0000000E+00	0.0000000E+00	0.0000000E+00
00007	3.8197186E-01	0.0000000E+00	-3.8197186E-01
00008	5.4567409E-01	0.0000000E+00	-5.4567409E-01
00009	0.0000000E+00	0.0000000E+00	0.0000000E+00
00010	-1.3889886E-01	0.0000000E+00	1.3889886E-01
00011	0.0000000E+00	0.0000000E+00	0.0000000E+00
00012	-5.9683104E-02	1.1936620E-01	-5.9683104E-02
00013	1.9098593E-01	-3.8197186E-01	1.9098593E-01
00014	5.7735027E-01	5.7735027E-01	5.7735027E-01
00015	2.7283705E-01	-5.4567409E-01	2.7283705E-01
00016	0.0000000E+00	0.0000000E+00	0.0000000E+00
00017	2.4803368E-02	0.0000000E+00	-2.4803368E-02
00018	-5.8764902E-02	0.0000000E+00	5.8764902E-02
00019	0.0000000E+00	0.0000000E+00	0.0000000E+00
00020	4.4937866E-01	0.0000000E+00	-4.4937866E-01
00021	0.0000000E+00	0.0000000E+00	0.0000000E+00
00022	-1.3641852E-02	2.7283705E-02	-1.3641852E-02
00023	2.9841552E-02	-5.9683104E-02	2.9841552E-02
00024	0.0000000E+00	0.0000000E+00	0.0000000E+00
00025	-9.5492966E-02	1.9098593E-01	-9.5492966E-02
00026	0.0000000E+00		

B3D353

```
0100C THREE-DIMENSIONAL BAFFLED CHAMBER MAIN PROGRAM
1000 DIMENSION FINTRM(5,3,5,3),FINTTM(3,5,5)
1010&  ,ATOM(5),AROM(5,3),BESSOM(5,3),ATUM(5),ARUM(5,3),BESSUM(5,3)
1020&  ,HLOM(5,3),HRUM(5,3)
1030&  ,ASOM(5,3),VAOM(5,3),BSUM(3,5,3),VBUM(3,5,3)
1040&  ,BLOM(5,3)
1050 COMMON MUBAR,R1,ATOM,AROM,BESSOM,ATUM,ARUM,BESSUM
1060&  ,NRPNT,TVAL,NTPNT,RVAL
1070 COMPLEX BETAOP,BETA2L,EIR1ST,EIR1SP,EIR1FD,EIGNR1,EIR12
1080&  ,AZOV,ARGO,RTARGO,DELLOV,CTANO,AZUV,ARGU,RTARGU,DELRUV,CTANU
1090&  ,HLOM,HLOV,HRUM,HRUV
1100&  ,ASOM,ASOV,VAOM,BSUM,BSUV,BLOM,BLOV,VBUM
1110&  ,TM,SERSUM,SUM1,SUM2,CHARFN,CHARFO,CHARFL,CHARFU
1120 CALL OPENF(1,"RN5353")
1130 CALL OPENF(2,"RT5353")
1140 CALL OPENF(3,"TOT355")
1150 2 FORMAT(4I5/I5,E10.2,I5)
1160 6 FORMAT(F5.2,3(/5X,2F9.5))
1170 8 FORMAT(1X,5E12.5)
1180 10 FORMAT(1X,3E15.7)
1190 11 FORMAT(//"THREE-DIMENSIONAL BAFFLED CHAMBER")
1200 12 FORMAT(//T2,"MUBAR=",I2/
1210&T6,"R1=",F5.2,T21,"ZO=",F5.2,T36,"Z1=",F5.2,T51,"Z2=",F5.2/
1220&T11,"BETAOP=",2F5.2,T31,"BETA2L=",2F5.2)
1230 14 FORMAT(/T2,"TANGENTIAL MODE NUMBER",I3)
1240 16 FORMAT(/T2,"MTOVMC=",I2,T16,"MROVMC=",I2/
1250&T2,"NTUVMC=",I2,T16,"NRUVMC=",I2//T2,"JIT=",I2)
1260 18 FORMAT(//T16,"EIGNR1",T52,"SUM1"/T16,"CHARFN",T52,"SUM2")
1270 19 FORMAT(T10,1PE16.10,",",1PE17.10)
1280 20 FORMAT(2(1PE16.10,",",1PE16.10," :",1PE16.10,",",1PE16.10/))
1290 READ(1,2) MTOVMX,MROVMX,NTUVMX,NRUVMX,IDUM1,DUM1,IDUM2
1300 READ(1,6) (ATOM(MT),(AROM(MT,MR),BESSOM(MT,MR),MR=1,MROVMX),
1310&MT=1,MTOVMX)
1320 READ(1,6) (ATUM(NT),(ARUM(NT,NR),BESSUM(NT,NR),NR=1,NRUVMX),
1330&NT=1,NTUVMX)
1340 READ(2,8) FINTRM
1350 READ(3,10) FINTTM,PHEOOP
1360 1001 PRINT," 1 INPUT:MUBAR,R1,ZO,Z1,Z2,BETAOP,BETA2L"
1370 INPUT,MUBAR,R1,ZO,Z1,Z2,BETAOP,BETA2L
1380 1002 CONTINUE
1390 NMODE=1
1400 BSUMO1=+0.5
1410 BSUMO2=-1.0
1420 BSUMO3=+0.5
1430 1003 PRINT," 3 INPUT:MTOVMC,MROVMC,NTUVMC,NRUVMC,JIT"
1440 INPUT,MTOVMC,MROVMC,NTUVMC,NRUVMC,JIT
1450 1004 PRINT," 4 INPUT:ITYPE"
1460 INPUT,ITYPE
1470 IDETAL=0
1480 IF(ITYPE)  1008,1005,1006
```

B3D353 CONTINUED

```
1490 1005 PRINT,'' 5 INPUT:EIR1ST,EIR1SP,NEIR1S,IDETAL''
1500 INPUT,EIR1ST,EIR1SP,NEIR1S,IDETAL
1510 IF(IDETAL.NE.1)  GØ TØ 1007
1520 PRINT,''   INPUT:IPBSUM,IPVBUM,IPASOM,IPVAOM''
1530 INPUT,IPBSUM,IPVBUM,IPASOM,IPVAOM
1540 PRINT,''   INPUT:MPBSUM,MPVBUM,MPASOM,MPVAOM''
1550 INPUT,MPBSUM,MPVBUM,MPASOM,MPVAOM
1560 GØ TØ 1007
1570 1006 PRINT,'' 6 INPUT:EIR1ST,EIR1FD,NEIR1M,CHFNTL''
1580 INPUT,EIR1ST,EIR1FD,NEIR1M,CHFNTL
1590 1007 CØNTINUE
1600 PRINT 11
1610 PRINT 12,MUBAR,R1,Z0,Z1,Z2,BETAOP,BETA2L
1620 PRINT 14,NMØDE
1630 PRINT 16,MTOVMC,MROVMC,NTUVMC,NRUVMC,JIT
1640 PRINT 18
1650 NEIR1D=0
1660 NCNTRL=-2
1670 EIGNR1=EIR1ST
1680 1 CØNTINUE
1690C
1700C DEFINTITIØNS
1710C
1720 JI=0
1730 EIR12=EIGNR1**2
1740 DØ 30 MTOD=1,MTOVMC
1750 DØ 29 MROD=1,MROVMC
1760 IF((MTOD.EQ.1).AND.(MROD.EQ.1))  GØ TØ 29
1770 AROV=AROM(MTOD,MROD)
1780 AROV2=AROV**2
1790 RTARGO=EIR12-AROV2
1800 AZOV=CSQRT(RTARGO)
1810 ARGO=AZOV*(Z1-Z0)/R1
1820 DELLOV=(0.0,1.0)*EIGNR1*BETAOP/AZOV
1830 CTANO=CSIN(ARGO)/CCØS(ARGO)
1840 HLOV=-AZOV*(CTANO+DELLOV)/(1.0-DELLOV*CTANO)
1850 HLOM(MTOD,MROD)=HLOV/R1
1860 29 CØNTINUE
1870 30 CØNTINUE
1880 HLOM(1,1)=0.0
1890 DØ 40 NTUD=1,NTUVMC
1900 DØ 39 NRUD=1,NRUVMC
1910 ARUV=ARUM(NTUD,NRUD)
1920 ARUV2=ARUV**2
1930 RTARGU=EIR12-ARUV2
1940 AZUV=CSQRT(RTARGU)
1950 ARGU=AZUV*(Z2-Z1)/R1
1960 DELRUV=(0.0,1.0)*EIGNR1*BETA2L/AZUV
1970 CTANU=CSIN(ARGU)/CCØS(ARGU)
1980 HRUV=+AZUV*(CTANU+DELRUV)/(1.0-DELRUV*CTANU)
```

B3D353 CONTINUED

```
1990 HRUM(NTUD,NRUD)=HRUV/R1
2000 39 CONTINUE
2010 40 CONTINUE
2020 DO 43 MUD=1,MUBAR
2030 DO 42 NTUD=1,NTUVMC
2040 DO 41 NRUD=1,NRUVMC
2050 BSUM(MUD,NTUD,NRUD)=0.0
2060 41 CONTINUE
2070 42 CONTINUE
2080 43 CONTINUE
2090 BSUM(1,1,1)=BSUM01
2100 BSUM(2,1,1)=BSUM02
2110 BSUM(3,1,1)=BSUM03
2120 45 CONTINUE
2130C
2140C BLOM CALCULATION
2150C
2160 DO 90 MTOD=1,MTOVMC
2170 DO 80 MROD=1,MROVMC
2180 IF((MTOD.EQ.1).AND.(MROD.EQ.1))  GO TO 80
2190 SERSUM=0.0
2200 DO 70 MUD=1,MUBAR
2210 DO 60 NTUD=1,NTUVMC
2220 DO 50 NRUD=1,NRUVMC
2230 TM=BSUM(MUD,NTUD,NRUD)*HRUM(NTUD,NRUD)
2240 VBUM(MUD,NTUD,NRUD)=TM
2250 TM=TM*FINTRM(MTOD,MROD,NTUD,NRUD)*FINTTM(MUD,MTOD,NTUD)
2260 SERSUM=SERSUM+TM
2270 50 CONTINUE
2280 60 CONTINUE
2290 70 CONTINUE
2300 BLOM(MTOD,MROD)=SERSUM
2310 VAOM(MTOD,MROD)=SERSUM
2320 ASOM(MTOD,MROD)=SERSUM/HLOM(MTOD,MROD)
2330 80 CONTINUE
2340 90 CONTINUE
2350 BLOM(1,1)=0.0
2360 VAOM(1,1)=0.0
2370 ASOM(1,1)=0.0
2380 IF(JI.GE.JIT)  GO TO 150
2390 JI=JI+1
2400C
2410C ITERATION EQUATION CALCULATION
2420C
2430 DO 140 MUD=1,MUBAR
2440 DO 130 NTUD=1,NTUVMC
2450 DO 120 NRUD=1,NRUVMC
2460 SERSUM=0.0
2470 DO 110 MTOD=1,MTOVMC
2480 DO 100 MROD=1,MROVMC
```

```
B3D353 CONTINUED

2490 IF((MTOD.EQ.1).AND.(MROD.EQ.1))  GO TO 100
2500 TM=ASOM(MTOD,MROD)
2510 TM=TM*FINTRM(MTOD,MROD,NTUD,NRUD)*FINTTM(MUD,MTOD,NTUD)
2520 SERSUM=SERSUM+TM
2530 100 CONTINUE
2540 110 CONTINUE
2550 BSUM(MUD,NTUD,NRUD)=SERSUM
2560 120 CONTINUE
2570 130 CONTINUE
2580 140 CONTINUE
2590 GO TO 45
2600 150 CONTINUE
2610C
2620C CHARACTERISTIC EQUATION CALCULATION
2630C
2640 SERSUM=0.0
2650 DO 170 MTOD=1,MTOVMC
2660 DO 160 MROD=1,MROVMC
2670 IF((MTOD.EQ.1).AND.(MROD.EQ.1))  GO TO 160
2680 ASOV=ASOM(MTOD,MROD)
2690 TM=(ASOV**2)*HLOM(MTOD,MROD)
2700 SERSUM=SERSUM+TM
2710 160 CONTINUE
2720 170 CONTINUE
2730 SUM1=SERSUM
2740 SERSUM=0.0
2750 DO 200 MUD=1,MUBAR
2760 DO 190 NTUD=1,NTUVMC
2770 DO 180 NRUD=1,NRUVMC
2780 BSUV=BSUM(MUD,NTUD,NRUD)
2790 TM=(BSUV**2)*HRUM(NTUD,NRUD)
2800 SERSUM=SERSUM+TM
2810 180 CONTINUE
2820 190 CONTINUE
2830 200 CONTINUE
2840 SUM2=SERSUM
2850 CHARFN=SUM1-SUM2
2860C
2870C GENERAL PRINTOUT
2880C
2890 IF(NCNTRL.EQ.-2)  PRINT 20,EIGNR1,SUM1,CHARFN,SUM2
2900 IF(IDETAL.NE.1)  GO TO 260
2910C
2920C DETAILED PRINTOUT--BSUM,VBUM,ASOM,VAOM
2930C
2940 IF((IPBSUM+MPBSUM).NE.0)  PRINT,↑2,"BSUM",↑
2950 IF(IPBSUM.NE.1)  GO TO 241
2960 PRINT 19,(((BSUM(MD,NT,NR),MD=1,MUBAR),NT=1,NTUVMC),NR=1,NRUVMC)
2970 241 CONTINUE
2980 IF(MPBSUM.EQ.1)  CALL PV3DBC(BSUM,NTUVMC,NRUVMC)
```

B3D353 CØNTINUED

```
2990 IF((IPVBUM+MPVBUM).NE.0)  PRINT,↑2,"VBUM",↑
3000 IF(IPVBUM.NE.1)  GØ TØ 243
3010 PRINT 19,(((VBUM(MD,NT,NR),MD=1,MUBAR),NT=1,NTUVMC),NR=1,NRUVMC)
3020 243 CØNTINUE
3030 IF(MPVBUM.EQ.1)  CALL PV3DBC(VBUM,NTUVMC,NRUVMC)
3040 IF((IPASOM+MPASOM).NE.0)  PRINT,↑2,"ASOM",↑
3050 IF(IPASOM.NE.1)  GØ TØ 245
3060 PRINT 19,((ASOM(MT,MR),MT=1,MTOVMC),MR=1,MROVMC)
3070 245 CØNTINUE
3080 IF(MPASOM.EQ.1)  CALL PV3DMC(ASOM,MTOVMC,MROVMC,PHEØØP)
3090 IF((IPVAOM+MPVAOM).NE.0)  PRINT,↑2,"VAOM",↑
3100 IF(IPVAOM.NE.1)  GØ TØ 247
3110 PRINT 19,((VAOM(MT,MR),MT=1,MTOVMC),MR=1,MROVMC)
3120 247 CØNTINUE
3130 IF(MPVAOM.EQ.1)  CALL PV3DMC(VAOM,MTOVMC,MROVMC,PHEØØP)
3140 260 CØNTINUE
3150C
3160C CHANGE EIGNR1--STEP CHANGE ØR RØØT FINDER
3170C
3180 NEIR1D=NEIR1D+1
3190 IF(ITYPE.EQ.1)  GØ TØ 300
3200 EIGNR1=EIGNR1+EIR1SP
3210 IF(NEIR1D.LT.NEIR1S)  GØ TØ 1
3220 GØ TØ 1008
3230 300 CØNTINUE
3240 EIR1FR=EIR1FD
3250 EIR1FI=-(0.0,1.0)*EIR1FD
3260 IF(ABS(EIR1FR).GT.(1.0E-10))  GØ TØ 301
3270 CHARFI=-(0.0,1.0)*CHARFN
3280 CHARFN=+(0.0,1.0)*CHARFI
3290 GØ TØ 302
3300 301 CØNTINUE
3310 IF(ABS(EIR1FI).GT.(1.0E-10))  GØ TØ 302
3320 CHARFR=CHARFN
3330 CHARFN=CHARFR
3340 302 CØNTINUE
3350 NCNTRL=NCNTRL+1
3360 IF(NCNTRL)  310,320,330
3370 310 CHARFØ=CHARFN
3380 IF((CABS(CHARFØ).LT.CHFNTL).ØR.(NEIR1D.GT.NEIR1M))  GØ TØ 1008
3390 EIGNR1=EIGNR1-EIR1FD/2.0
3400 GØ TØ 1
3410 320 CHARFL=CHARFN
3420 EIGNR1=EIGNR1+EIR1FD
3430 GØ TØ 1
3440 330 CHARFU=CHARFN
3450 EIGNR1=EIGNR1-EIR1FD/2.0-CHARFØ*EIR1FD/(CHARFU-CHARFL)
3460 NCNTRL=-2
3470 GØ TØ 1
3480 1008 PRINT,↑2,↑2
```

B3D353 CØNTINUED

```
3490C
3500C WHERE T0 G0?
3510C
3520 PRINT,"    INPUT:IGØTØ"
3530 INPUT,IGØTØ
3540 GØ TØ (1001,1002,1003,1004,1005,1006,9999),IGØTØ
3550 9999 STØP
3560 END
```

PV3DBC

```
5000 SUBRØUTINE PV3DBC(CØEF,NTUVMC,NRUVMC)
5010 DIMENSIØN CØEF(3,5,3),REFERM(5,3),BESRVM(5,3),PVVAL(50),RTVAL(50)
5020& ,ATOM(5),AROM(5,3),BESSOM(5,3),ATUM(5),ARUM(5,3),BESSUM(5,3)
5030& ,CØSFN(5),MUDM(50)
5040 CØMMØN MUBAR,R1,ATOM,AROM,BESSOM,ATUM,ARUM,BESSUM
5050& ,NRPNT,TVAL,NTPNT,RVAL
5060 CØMPLEX CØEF
5070 5 FØRMAT(/5X,"R-VARIATIØN CØMPARTMENT",I3,5X,"TVAL=",F10.4,"*PI"/)

5080 10 FØRMAT(2X,1P2E17.10)
5090 15 FØRMAT(/5X,"THETA-VARIATIØN",5X,"RVAL=",1PE17.10/)
5100 20 FØRMAT(2X,1PE17.10,0PF10.4,"*PI",I10)
5110 PI=3.1415926536
5120 PIT2=2.0*PI
5130 FMUBAR=FLØAT(MUBAR)
5140 PIØFMU=PI/FMUBAR
5150 PIT2ØF=PIT2/FMUBAR
5160 R1202=(R1**2)/2.0
5170 DØ 110 NTUD=1,NTUVMC
5180 DØ 100 NRUD=1,NRUVMC
5190 EPSV=PIØFMU
5200 IF(NTUD.EQ.1)  EPSV=PIT2ØF
5210 ATUV2=(ATUM(NTUD))**2
5220 ARUV2=(ARUM(NTUD,NRUD))**2
5230 REFRV2=EPSV*R1202*(1.0-(ATUV2/ARUV2))
5240 BESUV2=(BESSUM(NTUD,NRUD))**2
5250 REFERM(NTUD,NRUD)=SQRT(REFRV2*BESUV2)
5260 100 CØNTINUE
5270 110 CØNTINUE
5280 REFERM(1,1)=SQRT(PIT2ØF*R1202)
5290 1 PRINT,↑2,↑,"          INPUT:NRPNT,TVAL,NTPNT,RVAL,TSTØP",↑*
5300 INPUT,NRPNT,TVAL,NTPNT,RVAL,TSTØP
5310 IF((NRPNT.EQ.0).AND.(NTPNT.EQ.0))  RETURN
5320 IF(NRPNT.EQ.0)  GØ TØ 1000
5330 TVALØP=TVAL
5340 TVAL=TVAL*PI
5350 IF((TVAL.GT.0.0).AND.(TVAL.LT.PIT2ØF))  MUD=1
5360 IF((TVAL.GT.PIT2ØF).AND.(TVAL.LT.(2.0*PIT2ØF)))  MUD=2
5370 IF((TVAL.GT.(2.0*PIT2ØF)).AND.(TVAL.LT.(3.0*PIT2ØF)))  MUD=3
5380 FMUD=FLØAT(MUD)
5390 DØ 200 NTUD=1,NTUVMC
5400 CØSFN(NTUD)=CØS(ATUM(NTUD)*(TVAL-(FMUD-1.0)*PIT2ØF))
5410 200 CØNTINUE
5420 RINC=R1/NRPNT
5430 NRPNT1=NRPNT+1
5440 RPØS=0.0
5450 DØ 500 NRD=1,NRPNT1
5460 RTVAL(NRD)=RPØS
5470 SUM=0.0
5480 DØ 410 NTUD=1,NTUVMC
5490 DØ 400 NRUD=1,NRUVMC
```

PV3DBC CONTINUED

```
5500 RPOSER=ARUM(NTUD,NRUD)*RPOS/R1
5510 CALL BESFNP(ATUM(NTUD),RPOSER,BESSFN)
5520 SUM=SUM+COEF(MUD,NTUD,NRUD)*COSFN(NTUD)*BESSFN/REFERM(NTUD,NRUD)
5530 400 CONTINUE
5540 410 CONTINUE
5550 PVVAL(NRD)=SUM
5560 RPOS=RPOS+RINC
5570 500 CONTINUE
5580 PRINT 5,MUD,TVALOP
5590 PRINT 10,(PVVAL(NRD),RTVAL(NRD),NRD=1,NRPNT1)
5600 1000 CONTINUE
5610 IF(NTPNT.EQ.0)  GO TO 1
5620 DO 1110 NTUD=1,NTUVMC
5630 DO 1100 NRUD=1,NRUVMC
5640 RPOSER=ARUM(NTUD,NRUD)*RVAL/R1
5650 CALL BESFNP(ATUM(NTUD),RPOSER,BESSFN)
5660 BESRVM(NTUD,NRUD)=BESSFN/REFERM(NTUD,NRUD)
5670 1100 CONTINUE
5680 1110 CONTINUE
5690 TINC=PIT2/NTPNT
5700 TINCOP=2.0/NTPNT
5710 NTPNT1=NTPNT+1
5720 TPOS=1.0E-10
5730 TPOSOP=0.0
5740 TSTOP=TPOS+TSTOP*PI
5750 DO 1500 NTD=1,NTPNT1
5760 RTVAL(NTD)=TPOSOP
5770 IF((TPOS.GT.0.0).AND.(TPOS.LT.PIT20F))  MUD=1
5780 IF((TPOS.GT.PIT20F).AND.(TPOS.LT.(2.0*PIT20F)))  MUD=2
5790 IF((TPOS.GT.(2.0*PIT20F)).AND.(TPOS.LT.(3.0*PIT20F)))  MUD=3
5800 MUDM(NTD)=MUD
5810 FMUD=FLOAT(MUD)
5820 SUM=0.0
5830 DO 1410 NTUD=1,NTUVMC
5840 DO 1400 NRUD=1,NRUVMC
5850 TM=BESRVM(NTUD,NRUD)*COS(ATUM(NTUD)*(TPOS-(FMUD-1.0)*PIT20F))
5860 SUM=SUM+TM*COEF(MUD,NTUD,NRUD)
5870 1400 CONTINUE
5880 1410 CONTINUE
5890 PVVAL(NTD)=SUM
5900 NTMAX=NTD
5910 IF(TPOS.GT.TSTOP)  GO TO 1600
5920 TPOS=TPOS+TINC
5930 TPOSOP=TPOSOP+TINCOP
5940 1500 CONTINUE
5950 1600 CONTINUE
5960 PRINT 15,RVAL
5970 PRINT 20,(PVVAL(NTD),RTVAL(NTD),MUDM(NTD),NTD=1,NTMAX)
5980 GO TO 1
5990 END
```

PV3DMC

```
6000 SUBRØUTINE PV3DMC(CØEF,MTOVMC,MROVMC,PHEØØP)
6010 DIMENSIØN CØEF(5,3),REFERM(5,3),BESRVM(5,3),PVVAL(50),RTVAL(50)
6020& ,ATOM(5),AROM(5,3),BESSOM(5,3),ATUM(5),ARUM(5,3),BESSUM(5,3)
6030& ,CØSFN(5)
6040 CØMMØN MUBAR,R1,ATOM,AROM,BESSOM,ATUM,ARUM,BESSUM
6050& ,NRPNT,TVAL,NTPNT,RVAL
6060 CØMPLEX CØEF
6070 5 FØRMAT(/5X,"R-VARIATIØN MAIN CHAMBER",7X,"TVAL=",F10.4,"*PI"/)
6080 10 FØRMAT(2X,1P2E17.10)
6090 15 FØRMAT(/5X,"THETA-VARIATIØN",5X,"RVAL=",1PE17.10/)
6100 20 FØRMAT(2X,1PE17.10,0PF10.4,"*PI")
6110 PI=3.1415926536
6120 PIT2=2.0*PI
6130 R1202=(R1**2)/2.0
6140 DØ 110 MTOD=1,MTOVMC
6150 DØ 100 MROD=1,MROVMC
6160 EPSV=PI
6170 IF(MTOD.EQ.1)  EPSV=PIT2
6180 ATOV2=(ATOM(MTOD))**2
6190 AROV2=(AROM(MTOD,MROD))**2
6200 REFRV2=EPSV*R1202*(1.0-(ATOV2/AROV2))
6210 BESOV2=(BESSOM(MTOD,MROD))**2
6220 REFERM(MTOD,MROD)=SQRT(REFRV2*BESOV2)
6230 100 CØNTINUE
6240 110 CØNTINUE
6250 REFERM(1,1)=SQRT(PIT2*R1202)
6260 PHEEO=PHEØØP*PI
6270 1 PRINT,↑2,↑,"           INPUT:NRPNT,TVAL,NTPNT,RVAL,TSTØP",↑*
6280 INPUT,NRPNT,TVAL,NTPNT,RVAL,TSTØP
6290 IF((NRPNT.EQ.0).AND.(NTPNT.EQ.0))  RETURN
6300 IF(NRPNT.EQ.0)  GØ TØ 1000
6310 TVALØP=TVAL
6320 TVAL=TVAL*PI
6330 DØ 200 MTOD=1,MTOVMC
6340 CØSFN(MTOD)=CØS(ATOM(MTOD)*(TVAL-PHEEO))
6350 200 CØNTINUE
6360 RINC=R1/NRPNT
6370 NRPNT1=NRPNT+1
6380 RPØS=0.0
6390 DØ 500 NRD=1,NRPNT1
6400 RTVAL(NRD)=RPØS
6410 SUM=0.0
6420 DØ 410 MTOD=1,MTOVMC
6430 DØ 400 MROD=1,MROVMC
6440 RPØSER=AROM(MTOD,MROD)*RPØS/R1
6450 CALL BESFNP(ATOM(MTOD),RPØSER,BESSFN)
6460 SUM=SUM+CØEF(MTOD,MROD)*CØSFN(MTOD)*BESSFN/REFERM(MTOD,MROD)
6470 400 CØNTINUE
6480 410 CØNTINUE
6490 PVVAL(NRD)=SUM
```

PV3DMC CONTINUED

```
6500 RP0S=RP0S+RINC
6510 500 CONTINUE
6520 PRINT 5,TVAL0P
6530 PRINT 10,(PVVAL(NRD),RTVAL(NRD),NRD=1,NRPNT1)
6540 1000 CONTINUE
6550 IF(NTPNT.EQ.0)  G0 T0 1
6560 D0 1110 MTOD=1,MTOVMC
6570 D0 1100 MROD=1,MROVMC
6580 RP0SER=AROM(MTOD,MROD)*RVAL/R1
6590 CALL BESFNP(ATOM(MTOD),RP0SER,BESSFN)
6600 BESRVM(MTOD,MROD)=BESSFN/REFERM(MTOD,MROD)
6610 1100 CONTINUE
6620 1110 CONTINUE
6630 TINC=PIT2/NTPNT
6640 TINC0P=2.0/NTPNT
6650 NTPNT1=NTPNT+1
6660 TP0S=1.0E-10
6670 TP0S0P=0.0
6680 TST0P=TP0S+TST0P*PI
6690 D0 1500 NTD=1,NTPNT1
6700 RTVAL(NTD)=TP0S0P
6710 SUM=0.0
6720 D0 1410 MTOD=1,MTOVMC
6730 D0 1400 MROD=1,MROVMC
6740 TM=BESRVM(MTOD,MROD)*C0S(ATOM(MTOD)*(TP0S-PHEE0))
6750 SUM=SUM+TM*C0EF(MTOD,MROD)
6760 1400 CONTINUE
6770 1410 CONTINUE
6780 PVVAL(NTD)=SUM
6790 NTMAX=NTD
6800 IF(TP0S.GT.TST0P)  G0 T0 1600
6810 TP0S=TP0S+TINC
6820 TP0S0P=TP0S0P+TINC0P
6830 1500 CONTINUE
6840 1600 CONTINUE
6850 PRINT 15,RVAL
6860 PRINT 20,(PVVAL(NTD),RTVAL(NTD),NTD=1,NTMAX)
6870 G0 T0 1
6880 END
```

BESFNP

```
7000 SUBRØUTINE BESFNP(ØRDER,ARGMNT,BESFNV)
7010 IØRDER=IFIX(ØRDER)
7020 ØRDDIF=ØRDER-FLØAT(IØRDER)
7030 IF(ØRDDIF.GT.(1.0E-8))  GØ TØ 1000
7040C INTEGER ØRDER BESSEL FUNCTIØNS
7050 IF(IØRDER.EQ.0)  BESFNV=1.0
7060 IF(IØRDER.NE.0)  BESFNV=0.0
7070 IF(ARGMNT.LT.(1.0E-8))  RETURN
7080 CALL BESSOP(ARGMNT,BESSOV)
7090 IF(IØRDER.GT.0)  GØ TØ 100
7100 BESFNV=BESSOV
7110 RETURN
7120 100 CØNTINUE
7130 CALL BESS1P(ARGMNT,BESS1V)
7140 IF(IØRDER.GT.1)  GØ TØ 200
7150 BESFNV=BESS1V
7160 RETURN
7170 200 CØNTINUE
7180 BESL1=BESSOV
7190 BESO=BESS1V
7200 IØRD=1
7210 300 CØNTINUE
7220 ØRDT2=2.0*FLØAT(IØRD)
7230 BESFNV=(ØRDT2/ARGMNT)*BESO-BESL1
7240 IØRD=IØRD+1
7250 IF(IØRD.EQ.IØRDER)  RETURN
7260 BESL1=BESO
7270 BESO=BESFNV
7280 GØ TØ 300
7290C HALF-INTEGER BESSEL FUNCTIØNS
7300 1000 CØNTINUE
7310 PI=3.1415926536
7320 BESFNV=0.0
7330 IF(ARGMNT.LT.(1.0E-8))  RETURN
7340 CHALF=SQRT(2.0/(PI*ARGMNT))
7350 BESM12=CØS(ARGMNT)
7360 BESP12=SIN(ARGMNT)
7370 IF(IØRDER.GT.0)  GØ TØ 1100
7380 BESFNV=CHALF*BESP12
7390 RETURN
7400 1100 CØNTINUE
7410 BESL1=BESM12
7420 BESO=BESP12
7430 IØRD=1
7440 1200 CØNTINUE
7450 ØRDT2=2.0*(FLØAT(IØRD)-0.50)
7460 BESFNV=(ØRDT2/ARGMNT)*BESO-BESL1
7470 IF(IØRD.NE.IØRDER)  GØ TØ 1300
7480 BESFNV=CHALF*BESFNV
7490 RETURN
```

BESFNP CØNTINUED

```
7500 1300 CØNTINUE
7510 IØRD=IØRD+1
7520 BESL1=BESO
7530 BESO=BESFNV
7540 GØ TØ 1200
7550 END
```

BESSOF

```
6000  SUBROUTINE BESSOF(ARGMNT,BESSOV)
6010  DIMENSION CB0(7),CF0(7),CT0(8)
6020  DATA CB0/1.0,-2.2499997,1.2656208,-0.3163866,4.44479E-2
6030& ,-3.9444E-3,2.1E-4/,CF0/7.9788456E-1,-7.7E-7,-5.5274E-3
6040& ,-9.512E-5,1.37237E-3,-7.2605E-4,1.4476E-4/,CT0/3.0,-0.7853982
6050& ,-4.166397E-2,-3.954E-5,2.62573E-3,-5.4125E-4,-2.9333E-4
6060& ,1.3558E-4/
6070  IF(ARGMNT.GT.3.0)  GO TO 1000
6080C ARGMNT LESS THAN OR EQUAL TO 3.0
6090  X=ARGMNT/3.0
6100  SUM=0.0
6110  DO 100 J=1,7
6120  K=2*(J-1)
6130  SUM=SUM+CB0(J)*(X**K)
6140  100 CONTINUE
6150  BESSOV=SUM
6160  RETURN
6170C ARGMNT GREATER THAN 3.0
6180  1000 CONTINUE
6190  X=3.0/ARGMNT
6200  SUM=0.0
6210  DO 1100 J=1,7
6220  K=J-1
6230  SUM=SUM+CF0(J)*(X**K)
6240  1100 CONTINUE
6250  F0=SUM
6260  SUM=0.0
6270  DO 1200 J=1,8
6280  K=J-1
6290  SUM=SUM+CT0(J)*(X**K)
6300  1200 CONTINUE
6310  T0=SUM/X
6320  BESSOV=(F0*COS(T0))/SQRT(ARGMNT)
6330  RETURN
6340  END
```

BESS1P

```
9000 SUBRØUTINE BESS1P(ARGMNT,BESS1V)
9010 DIMENSIØN CB1(7),CF1(7),CT1(8)
9020 DATA CB1/5.0E-1,-5.6249985E-1,2.1093573E-1,-3.954289E-2
9030& ,4.43319E-3,-3.1761E-4,1.109E-5/,CF1/7.9788456E-1,1.56E-6
9040& ,1.659667E-2,1.7105E-4,-2.49511E-3,1.13653E-3,-2.0033E-4
9050& /,CT1/3.0,-2.35619449,1.2499612E-1,5.65E-5,-6.37879E-3
9060& ,7.4348E-4,7.9824E-4,-2.9166E-4/
9070 IF(ARGMNT.GT.3.0)  GØ TØ 1000
9080C ARGMNT LESS THAN ØR EQUAL TØ 3.0
9090 X=ARGMNT/3.0
9100 SUM=0.0
9110 DØ 100 J=1,7
9120 K=2*(J-1)
9130 SUM=SUM+CB1(J)*(X**K)
9140 100 CØNTINUE
9150 BESS1V=ARGMNT*SUM
9160 RETURN
9170C ARGMNT GREATER THAN 3.0
9180 1000 CØNTINUE
9190 X=3.0/ARGMNT
9200 SUM=0.0
9210 DØ 1100 J=1,7
9220 K=J-1
9230 SUM=SUM+CF1(J)*(X**K)
9240 1100 CØNTINUE
9250 F1=SUM
9260 SUM=0.0
9270 DØ 1200 J=1,8
9280 K=J-1
9290 SUM=SUM+CT1(J)*(X**K)
9300 1200 CØNTINUE
9310 T1=SUM/X
9320 BESS1V=(F1*CØS(T1))/SQRT(ARGMNT)
9330 RETURN
9340 END
```

```
B3D353     22:22  NAR  JAN. 12,1971


 1 INPUT:MUBAR,R1,Z0,Z1,Z2,BETA0P,BETA2L
 ?3,1.0,0.0,2.1,2.8,0.0,0.0,0.0,0.0

 3 INPUT:MTOVMC,MROVMC,NTUVMC,NRUVMC,JIT
 ?5,3,5,3,10

 4 INPUT:ITYPE
 ?0

 5 INPUT:EIR1ST,EIR1SP,NEIR1S,IDETAL
 ?1.10,0.00,0.10,0.00,5,0


THREE-DIMENSIØNAL BAFFLED CHAMBER


 MUBAR= 3
     R1= 1.00        Z0= 0.00        Z1= 2.10        Z2= 2.80
          BETA0P= 0.00 0.00    BETA2L= 0.00 0.00

 TANGENTIAL MØDE NUMBER  1

 MTOVMC= 5      MROVMC= 3
 NTUVMC= 5      NRUVMC= 3

 JIT=10


                EIGNR1                                          SUM1
                CHARFN                                          SUM2
 1.100000000E+00, 0.000000000E+00 : 2.943477660E-03, 6.146290016E-15
 6.138665321E-03, 1.407650197E-14 :-3.195187661E-03,-7.930211954E-15

 1.200000000E+00, 0.000000000E+00 : 3.886428437E-03,-5.570740690E-15
 8.103408722E-03,-9.681394213E-15 :-4.216980286E-03, 4.110653523E-15

 1.300000000E+00, 0.000000000E+00 : 5.012276134E-03,-1.841705356E-14
 1.041393414E-02,-5.366821725E-14 :-5.401658013E-03, 3.525116370E-14

 1.400000000E+00, 0.000000000E+00 : 1.020821592E-01, 4.942021580E-11
-6.230056143E-03,-7.275944016E-12 : 1.083122153E-01, 5.669615981E-11

 1.500000000E+00, 0.000000000E+00 : 8.850854586E+02, 4.203559133E-07
 1.910474609E+02, 1.065998027E-07 : 6.940379977E+02, 3.137561106E-07



   INPUT:IGØTØ
 ?4
```

typical run

a. find region of root

```
4 INPUT:ITYPE
?1

6 INPUT:EIGLST,EIGIFD,NEIGIM,CHFNTL
?1.45,0.00,1.0E-5,0.00,20,1.0E-6
```

b. find root precisely

```
THREE-DIMENSIONAL BAFFLED CHAMBER


MUBAR= 3
     R1= 1.00        Z0= 0.00        Z1= 2.10        Z2= 2.80
         BETAUP= 0.00 0.00   BETA2L= 0.00 0.00

TANGENTIAL MODE NUMBER  1

MTUVMC= 5       MRUVMC= 3
NTUVMC= 5       NRUVMC= 3

JIT=10

                EIGNR1                                  SUM1
                CHARFN                                  SUM2
1.450000000E+00, 0.000000000E+00 : 8.748537560E+00, 4.321623299E-09
2.466632698E-01, 3.172635014E-10 : 8.501874290E+00, 4.004359798E-09

1.445704103E+00, 0.000000000E+00 : 5.922080494E+00, 2.934867061E-09
6.519954227E-02, 1.652005972E-10 : 5.856880952E+00, 2.769666464E-09

1.443500406E+00, 0.000000000E+00 : 4.849426205E+00, 2.407140180E-09
1.073479987E-02, 1.140781782E-10 : 4.838691405E+00, 2.293062002E-09

1.442971456E+00, 0.000000000E+00 : 4.622473622E+00, 2.295354934E-09
4.958661100E-04, 1.038518176E-10 : 4.621977736E+00, 2.191503117E-09

1.442944566E+00, 0.000000000E+00 : 4.611225931E+00, 2.289813620E-09
1.220032572E-06, 1.033508791E-10 : 4.611224711E+00, 2.186462741E-09

1.442944499E+00, 0.000000000E+00 : 4.611198152E+00, 2.289799934E-09
2.910383046E-11, 1.033496426E-10 : 4.611198152E+00, 2.186450291E-09


  INPUT:IGOTO
?4
```

```
 4 INPUT:ITYPE
 ?0

 5 INPUT:EIR1ST,EIR1SP,NEIR1S,IDETAL
 ?1.442944499,0.00,0.00,0.00,1,1

   INPUT:IPBSUM,IPVBUM,IPASOM,IPVAOM
 ?0,0,0,0

   INPUT:MPBSUM,MPVBUM,MPASOM,MPVAOM
 ?1,0,1,0


THREE-DIMENSIØNAL BAFFLED CHAMBER


 MUBAR= 3
     R1= 1.00        Z0= 0.00        Z1= 2.10        Z2= 2.80
          BETAOP= 0.00 0.00   BETA2L= 0.00 0.00

 TANGENTIAL MØDE NUMBER  1

 MTOVMC= 5      MROVMC= 3
 NTUVMC= 5      NRUVMC= 3

 JIT=10


                EIGNR1                                    SUM1
                CHARFN                                    SUM2
 1.442944499E+00, 0.000000000E+00 : 4.611197980E+00, 2.289799849E-09
-7.683411241E-09, 1.033496348E-10 : 4.611197988E+00, 2.186450214E-09
```

c. check pressure match

```
INPUT:NRPNT,TVAL,NTPNT,RVAL,TSTØP    ?20,1.0E-8,40,1.0,1.05

 R-VARIATIØN CØMPARTMENT  1      TVAL=     0.0000*PI
                        r
 3.208488334E-01   0.000000000E+00
 3.680667881E-01   5.000000000E-02
 4.522753703E-01   1.000000000E-01
 5.514674265E-01   1.500000000E-01
 6.542467119E-01   2.000000000E-01
 7.538401985E-01   2.500000000E-01
 8.461021757E-01   3.000000000E-01
 9.281785572E-01   3.500000000E-01
 9.980206354E-01   4.000000000E-01
 1.054651052E+00   4.500000000E-01
 1.098659082E+00   5.000000000E-01
 1.132332955E+00   5.500000000E-01
 1.159115810E+00   6.000000000E-01
 1.182539420E+00   6.500000000E-01
 1.205118913E+00   7.000000000E-01
 1.227716042E+00   7.500000000E-01
 1.249607361E+00   8.000000000E-01
 1.269115144E+00   8.500000000E-01
 1.284408367E+00   9.000000000E-01
 1.294086334E+00   9.500000000E-01
 1.297383316E+00   1.000000000E+00

 THETA-VARIATIØN      RVAL=  1.000000000E+00
                        θ
 1.297383316E+00     0.0000*PI          1
 1.282450983E+00     0.0500*PI          1
 1.230228410E+00     0.1000*PI          1
 1.132538265E+00     0.1500*PI          1
 1.006710187E+00     0.2000*PI          1
 9.013995673E-01     0.2500*PI          1
 8.654279342E-01     0.3000*PI          1
 8.991267796E-01     0.3500*PI          1
 9.313336833E-01     0.4000*PI          1
 8.524209203E-01     0.4500*PI          1
 5.907519324E-01     0.5000*PI          1
 1.802798582E-01     0.5500*PI          1
-2.351890570E-01     0.6000*PI          1
-4.741978769E-01     0.6500*PI          1
-8.673475164E-01     0.7000*PI          2
-1.144832867E+00     0.7500*PI          2
-1.496333494E+00     0.8000*PI          2
-1.747986765E+00     0.8500*PI          2
-1.827863061E+00     0.9000*PI          2
-1.795720557E+00     0.9500*PI          2
-1.766357359E+00     1.0000*PI          2
-1.795720557E+00     1.0500*PI          2
-1.827863061E+00     1.1000*PI          2

INPUT:NRPNT,TVAL,NTPNT,RVAL,TSTØP    ?0,0.0,0,0.0,0.0
```

$p^{(\mu)(\ell)}(r,0.0,z_1)$

$p^{(\mu)(\ell)}(1.0,\theta,z_1)$

INPUT:NRPNT,TVAL,NTPNT,RVAL,TSTOP ?20,1.0E-8,40,1.0,1.0

R-VARIATION MAIN CHAMBER TVAL= 0.0000*PI

	r
1.372336022E-12	0.000000000E+00
2.191124735E-01	5.000000000E-02
4.061566657E-01	1.000000000E-01
5.602279405E-01	1.500000000E-01
6.852978267E-01	2.000000000E-01
7.877967025E-01	2.500000000E-01
8.740810181E-01	3.000000000E-01
9.486298404E-01	3.500000000E-01
1.013455921E+00	4.000000000E-01
1.068715921E+00	4.500000000E-01
1.114050809E+00	5.000000000E-01
1.149953014E+00	5.500000000E-01
1.178513601E+00	6.000000000E-01
1.203214786E+00	6.500000000E-01
1.227866780E+00	7.000000000E-01
1.255163092E+00	7.500000000E-01
1.285498165E+00	8.000000000E-01
1.316589078E+00	8.500000000E-01
1.344115076E+00	9.000000000E-01
1.363169324E+00	9.500000000E-01
1.369977185E+00	1.000000000E+00

$p^{(0)(\ell)}(r,0.0,z_1)$

THETA-VARIATION RVAL= 1.000000000E+00

	θ
1.369977185E+00	0.0000*PI
1.343437119E+00	0.0500*PI
1.272900338E+00	0.1000*PI
1.181709996E+00	0.1500*PI
1.097296205E+00	0.2000*PI
1.038785843E+00	0.2500*PI
1.007379760E+00	0.3000*PI
9.834884356E-01	0.3500*PI
9.320658475E-01	0.4000*PI
8.144435752E-01	0.4500*PI
6.024415387E-01	0.5000*PI
2.895868696E-01	0.5500*PI
-1.047238489E-01	0.6000*PI
-5.397050468E-01	0.6500*PI
-9.647114272E-01	0.7000*PI
-1.333643618E+00	0.7500*PI
-1.617054440E+00	0.8000*PI
-1.807725512E+00	0.8500*PI
-1.918010210E+00	0.9000*PI
-1.970377663E+00	0.9500*PI
-1.985144713E+00	1.0000*PI
-1.970377663E+00	1.0500*PI
-1.918010210E+00	1.1000*PI

$p^{(0)(\ell)}(1.0,\theta,z_1)$

INPUT:NRPNT,TVAL,NTPNT,RVAL,TSTOP ?0,0.0,0,0.0,0.0

NOMENCLATURE FOR APPENDICES C AND D

$A \equiv$ series expansion coefficient - pressure gradient

$a \equiv$ series expansion coefficient - pressure

$B \equiv$ series expansion coefficient - pressure gradient

$b \equiv$ series expansion coefficient - pressure

$c \equiv$ sound speed

$F \equiv$ axial Green's function term

$G \equiv$ Green's function

$H \equiv$ axial influence coefficient

$I \equiv$ integral coefficient

$J \equiv$ Bessel function

$k \equiv$ eigenvalue

$m \equiv$ summation index

$n \equiv$ summation index

$p \equiv$ pressure

$r \equiv$ radial coordinate - 3D chamber

$x \equiv$ axial coordinate - 2D chamber

$y \equiv$ transverse coordinate - 2D chamber

$z \equiv$ axial coordinate - 3D chamber

$\alpha \equiv$ rigid wall eigenvalue

$\beta \equiv$ specific acoustic admittance

$\Gamma \equiv$ Gamma function

$\delta \equiv$ phase angle

$\theta \equiv$ angular coordinate - 3D chamber

$\Lambda \equiv$ normalization parameter

$\psi \equiv$ eigenfunction

Subscripts

0 ≡ nozzle end

1 ≡ interface

2 ≡ injector end

L ≡ left

m ≡ summation index

n ≡ summation index

R ≡ right

r ≡ radial component (3D)

x ≡ axial component (3D)

y ≡ transverse component (3D)

z ≡ axial component (3D)

μ ≡ compartment number

$\bar{\mu}$ ≡ number of compartments

Superscripts

(0) ≡ main chamber

(μ) ≡ μ th compartment

(ℓ) ≡ iteration number

EQUIVALENCE OF SYMBOLS USED IN MAIN TEST AND APPENDICES C AND D

MAIN TEXT	APPENDICES
c	c
G	G
k	k
k_q	$\alpha^{(\mu)}_{x,n_y}$
k_m	$\alpha^{(0)}_{x,m_y}$
ℓ	$x_2-x_1,\ z_2-z_1$
L	$x_1-x_o,\ z_1-z_o$
zero	$x_o,\ z_o$
m	m_y-1
$m\pi/W$	$\frac{1}{2}\alpha^{(0)}_{y,m_y}$
p_a	$p^{(0)}$
$p_{b\mu}$	$p^{(\mu)}$
q	n_y-1
$q\bar{n}/w$	$\alpha^{(\mu)}_{y,n_y}$

MAIN TEXT	APPENDICES
R	r_1
w	$y_{\mu+1}-y_\mu$
W	$y_{\bar{\mu}}-y_o$
zero	y_o
y_I	$\beta_{x_{2-}}$
y_N	$\beta_{x_{o+}}$

DISTRIBUTION LIST

Dr. R. J. Priem MS 500-209
NASA Lewis Research Center
21000 Brookpark Road
Cleveland, Ohio 44135 (2)

Norman T. Musial
NASA Lewis Research Center
21000 Brookpark Road
Cleveland, Ohio 44135

Library
NASA Lewis Research Center
21000 Brookpark Road
Cleveland, Ohio 44135 (2)

Report Control Office
NASA Lewis Research Center
21000 Brookpark Road
Cleveland, Ohio 44135

Brooklyn Polytechnic Institute
Attn: V. D. Agosta
Long Island Graduate Center
Route 110
Farmingdale, New York 11735

Chemical Propulsion Information Agency
Johns Hopkins University/APL
Attn: T. W. Christian
8621 Georgia Avenue
Silver Spring, Maryland 20910

NASA
Lewis Research Center
Attn: E. W. Conrad, MS 500-204
21000 Brookpark Road
Cleveland, Ohio 44135

North American Rockwell Corporation
Rocketdyne Division
Attn: T. A. Coultas, D/578 BA28
6633 Canoga Avenue
Canoga Park, California 91304

National Technical Information Service
Springfield, Virginia 22151
(40 Copies)

NASA Representative
NASA Scientific and Technical
Information Facility
P.O. Box 33
College Park, Maryland 20740
(2 Copies with Document Release Authorization Form)

Aerospace Corporation
Attn: O. W. Dykema
Post Office Box 95085
Los Angeles, California 90045

Ohio State University
Department of Aeronautical and
Astronautical Engineering
Attn: R. Edse
Columbus, Ohio 43210

TRW Systems
Attn: G. W. Elverum
One Space Park
Redondo Beach, California 90278

Bell Aerospace Company
Attn: T. F. Ferger
Post Office Box 1
Mail Zone J-81
Buffalo, New York 14205

Pratt & Whitney Aircraft
Florida Research & Development Center
Attn: G. D. Garrison
Post Office Box 710
West Palm Beach, Florida 33402

NASA
Lewis Research Center
Attn: L. Gordon, MS 500-209
21000 Brookpark Road
Cleveland, Ohio 44135

Purdue University
School of Mechanical Engineering
Attn: R. Goulard
Lafayette, Indiana 47907

Air Force Office of Scientific Research
Chief Propulsion Division
Attn: Lt. Col. R. W. Haffner (NAE)
1400 Wilson Boulevard
Arlington, Virginia 22209

Pennsylvania State University
Mechanical Engineering Department
Attn: G. M. Faeth
207 Mechanical Engineering Bldg.
University Park, Pennsylvania 16802

University of Illinois
Aeronautics/Astronautic Engineering
Department
Attn: R. A. Strehlow
Transportation Building, Room 101
Urbana, Illinois 61801

NASA
Manned Spacecraft Center
Attn: J. G. Thibadaux
Houston, Texas 77058

Massachusetts Institute of Technology
Department of Mechanical Engineering
Attn: T. Y. Toong
17 Massachusetts Avenue
Cambridge, Massachusetts 02139

Illinois Institute of Technology
Attn: T. P. Torda
Room 200 M. H.
3300 S. Federal Street
Chicago, Illinois 60616

AFRPL
Attn: R. R. Weiss
Edwards, California 93523

U.S. Army Missile Command
AMSMI-RKL, Attn: W. W. Wharton
Redstone Arsenal, Alabama 35808

University of California
Aerospace Engineering Department
Attn: F. A. Williams
Post Office Box 109
LaJolla, California 92037

Georgia Institute of Technology
Aerospace School
Attn: B. T. Zinn
Atlanta, Georgia 30332

Marshall Industries
Dynamic Science Division
Attn: L. Zung
2400 Michelson Drive
Irvine, California 92664

Mr. Donald H. Dahlene
U.S. Army Missile Command
Research, Development, Engineering
and Missile Systems Laboratory
Attn: AMSMI-RK
Redstone Arsenal, Alabama 35809

TISIA
Defense Documentation Center
Cameron Station
Building 5
5010 Duke Street
Alexandria, Virginia 22314

Office of Assistant Director
(Chemical Technician)
Office of the Director of Defense
Research and Engineering
Washington, D.C. 20301

D. E. Mock
Advanced Research Projects Agency
Washington, D.C. 20525

Dr. H. K. Doetsch
Arnold Engineering Development Center
Air Force Systems Command
Tullahoma, Tennessee 37389

Library
Air Force Rocket Propulsion Laboratory
(RPR)
Edwards, California

Library
Bureau of Naval Weapons
Department of the Navy
Washington, D.C.

Library
Director (Code 6180)
U.S. Naval Research Laboratory
Washington, D.C. 20390

APRP (Library)
Air Force Aero Propulsion Laboratory
Research and Technology Division
Air Force Systems Command
United States Air Force
Wright-Patterson AFB, Ohio 45433

Technical Information Department
Aeronutronic Division of Philco Ford
Corporation
Ford Road
Newport Beach, California 92663

Library-Documents
Aerospace Corporation
2400 E. El Segundo Boulevard
Los Angeles, California 90045

Princeton University
James Forrestal Campus Library
Attn: D. Harrje
Post Office Box 710
Princeton, New Jersey 08540

U.S. Naval Weapons Center
Attn: T. Inouye, Code 4581
China Lake, California 93555

Office of Naval Research
Navy Department
Attn: R. D. Jackel, 473
Washington, D.C. 20360

Air Force Aero Propulsion Laboratory
Attn: APTC Lt. M. Johnson
Wright Patterson AFB, Ohio 45433

Naval Underwater Systems Center
Energy Conversion Department
Attn: Dr. R. S. Lazar, Code TB 131
Newport, Rhode Island 02840

NASA
Langley Research Center
Attn: R. S. Levine, MS 213
Hampton, Virginia 23365

Aerojet General Corporation
Attn: J. M. McBride
Post Office Box 15847
Sacramento, California 95809

Colorado State University
Mechanical Engineering Department
Attn: C. E. Mitchell
Fort Collins, Colorado 80521

University of Wisconsin
Mechanical Engineering Department
Attn: P. S. Myers
1513 University Avenue
Madison, Wisconsin 53706

North American Rockwell Corporation
Rocketdyne Division
Attn: J. A. Nestlerode
AC46 D/596-124
6633 Canoga Avenue
Canoga Park, California 91304

University of Michigan
Aerospace Engineering
Attn: J. A. Nicholls
Ann Arbor, Michigan 48104

Tulane University
Attn: J. C. O'Hara
6823 St. Charles Avenue
New Orleans, Louisiana 70118

University of California
Department of Chemical Engineering
Attn: A. K. Oppenheim
6161 Etcheverry Hall
Berkeley, California 94720

Army Ballistics Laboratories
Attn: J. R. Osborn
Aberdeen Proving Ground, Maryland 21005

Sacramento State College
School of Engineering
Attn: F. H. Reardon
6000 J. Street
Sacramento, California 95819

Purdue University
School of Mechanical Engineering
Attn: B. A. Reese
Lafayette, Indiana 47907

NASA
George C. Marshall Space Flight Center
Attn: R. J. Richmond, SNE-ASTN-PP
Huntsville, Alabama 35812

Jet Propulsion Laboratory
California Institute of Technology
Attn: J. H. Rupe
4800 Oak Grove Drive
Pasadena, California 91103

University of California
Mechanical Engineering Thermal Systems
Attn: Prof. R. Sawyer
Berkeley, California 94720

ARL (ARC)
Attn: K. Scheller
Wright Patterson AFB, Ohio 45433

Library
Bell Aerosystems, Inc.
Box 1
Buffalo, New York 14205

Report Library, Room 6A
Battelle Memorial Institute
505 King Avenue
Columbus, Ohio 43201

D. Suichu
General Electric Company
Flight Propulsion Laboratory Department
Cincinnati, Ohio 45215

Library
Ling-Temco-Vought Corporation
Post Office Box 5907
Dallas, Texas 75222

Marquardt Corporation
16555 Saticoy Street
Box 2013 - South Annex
Van Nuys, California 91409

P. F. Winternitz
New York University
University Heights
New York, New York

I. Forsten
Picatinny Arsenal
Dover, New Jersey 07801

R. Stiff
Propulsion Division
Aerojet-General Corporation
Post Office Box 15847
Sacramento, California 95803

Library, Department 596-306
Rocketdyne Division of Rockwell
North American Rockwell Inc.
6633 Canoga Avenue
Canoga Park, California 91304

Library
Stanford Research Institute
333 Ravenswood Avenue
Menlo Park, California 94025

Library
Susquehanna Corporation
Atlantic Research Division
Shirley Highway and Edsall Road
Alexandria, Virginia 22314

STL Tech. Lib. Doc. Acquisitions
TRW System Group
1 Space Park
Redondo Beach, California 90278

Dr. David Altman
United Aircraft Corporation
United Technology Center
Post Office Box 358
Sunnyvale, California 94088

Library
United Aircraft Corporation
Pratt and Whitney Division
Florida Research and Development Center
Post Office Box 2691
West Palm Beach, Florida 33402

Library
Air Force Rocket Propulsion
Laboratory (RPM)
Edwards, California 93523

Allan Hribar, Assistant Professor
Post Office Box 5014
Tennessee Technological University
Cookeville, Tennessee 38501

NASA
Lewis Research Center
Attn: E. O. Bourke MS 500-209
21000 Brookpark Road
Cleveland, Ohio 44135

NASA
Lewis Research Center
Attn: D. L. Nored 500-203
21000 Brookpark Road
Cleveland, Ohio 44135

NASA
Lewis Research Center
Attn: Contracting Officer, 500-313
21000 Brookpark Road
Cleveland, Ohio 44135